

Winter 2006

Tropical forest structure: Ground measurements of coarse necromass and satellite observations of crown geometry

Michael W. Palace

University of New Hampshire, Durham

Follow this and additional works at: <https://scholars.unh.edu/dissertation>

Recommended Citation

Palace, Michael W., "Tropical forest structure: Ground measurements of coarse necromass and satellite observations of crown geometry" (2006). *Doctoral Dissertations*. 357.
<https://scholars.unh.edu/dissertation/357>

This Dissertation is brought to you for free and open access by the Student Scholarship at University of New Hampshire Scholars' Repository. It has been accepted for inclusion in Doctoral Dissertations by an authorized administrator of University of New Hampshire Scholars' Repository. For more information, please contact nicole.hentz@unh.edu.

**TROPICAL FOREST STRUCTURE: GROUND MEASUREMENTS OF COARSE
NECROMASS AND SATELLITE OBSERVATIONS OF CROWN GEOMETRY**

BY

MICHAEL W. PALACE

BA, University of Virginia, 1992

MS, University of Virginia, 1995

DISSERTATION

Submitted to the University of New Hampshire

in Partial Fulfillment of

the Requirements for the Degree of

Doctor of Philosophy

in

Natural Resources and Earth System Sciences

December, 2006

UMI Number: 3241648

INFORMATION TO USERS

The quality of this reproduction is dependent upon the quality of the copy submitted. Broken or indistinct print, colored or poor quality illustrations and photographs, print bleed-through, substandard margins, and improper alignment can adversely affect reproduction.

In the unlikely event that the author did not send a complete manuscript and there are missing pages, these will be noted. Also, if unauthorized copyright material had to be removed, a note will indicate the deletion.

UMI[®]

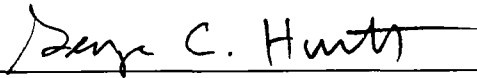
UMI Microform 3241648

Copyright 2007 by ProQuest Information and Learning Company.

All rights reserved. This microform edition is protected against unauthorized copying under Title 17, United States Code.

ProQuest Information and Learning Company
300 North Zeeb Road
P.O. Box 1346
Ann Arbor, MI 48106-1346

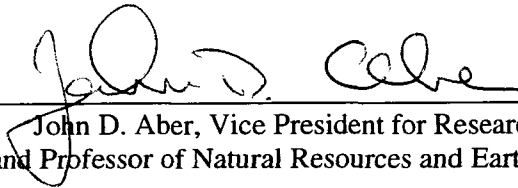
This dissertation has been examined and approved.



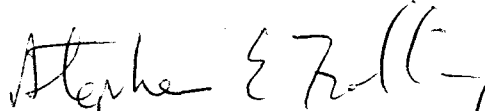
Dissertation Director, George C. Hurtt, Assistant Professor
of Natural Resources and Earth, Oceans, and Space



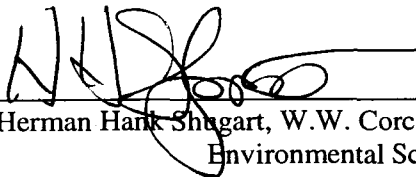
Michael M. Keller, Affiliate Professor
of Natural Resources



John D. Aber, Vice President for Research and Public Service
and Professor of Natural Resources and Earth, Oceans, and Space



Stephen E. Frolking, Research Associate Professor
of Earth Sciences and Earth, Oceans, and Space



Herman Hank Shugart, W.W. Corcoran Professor, Department of
Environmental Sciences, University of Virginia

12/7/06

Date

ACKNOWLEDGEMENTS

The research conducted herein was funded through the NASA Large Scale Biosphere Atmosphere Experiment in Amazonia. Support for this research was provided by the NASA Terrestrial Ecology Program (NCC5-225 and NCC5-357), the NASA New Millennium Program (NCC5-481), the NASA LBA Program (LC-13), the NASA New Investigator Program (NAG5-8709), EMBRAPA, the USDA Forest Service, and USAID. I would like to thank Dr. Michael Keller for guidance, encouragement, and the chance to spend time in tropical forests in Amazonia. I would also like to thank Steve Hagen and Rob Braswell for helping both in the field and in the office. I would also like to thank my committee members; Dr. Steve Frolking, Dr. George Hurtt, Dr. John Aber, Dr. Hank Shugart. I would also like to thank Greg Asner. This would not have been possible without the help of administrative staff at the Complex System Research Center (Karen Bushold, Faith Sheridan, Gary DesJardins, Linda Tibbets, Bindy Camire, Jennifer Parsons, and others) and the LBA office in Santarem, Para, Brazil. As fieldwork was a large piece of this work and over 5 years in length, there are many people to thank, E Gandini, Daniela Pauletto, Farid P.A. Massih, Hudson Silva and Jadson Dias, F. Ferreira Filho, A. Warner, T. Harris, J. Hicke, M. Hunter, J. Zweede and the staff of the Fundação Floresta Tropical, CIKEL Brasil Verde S.A. IBAMA for access to the Tapajós National Forest. Finally thanks to my family and my wife Shannon Poulin for support, discussion on my research, and allowing me to look at trees, twigs and logs.

TABLE OF CONTENTS

ACKNOWLEDGEMENTS.....	iii
LIST OF TABLES.....	vii
LIST OF FIGURES.....	ix
ABSTRACT.....	xi

CHAPTER	PAGE
I. INTRODUCTION.....	1
1.1 Chapter 2.....	5
1.2 Chapter 3.....	6
1.3 Chapter 4.....	7
1.4 Chapter 5.....	9

II. AMAZON FOREST STRUCTURE FROM IKONOS SATELLITE	
DATA AND AUTOMATED CROWN DELINEATION.....	11
2.1 Introduction.....	11
2.2 Methods.....	13
2.3 Results.....	20
2.4 Discussion.....	28
2.5 Conclusions.....	31
III. NECROMASS IN UNDISTURBED AND LOGGED FORESTS IN	
THE BRAZILIAN AMAZON.....	32
3.1 Introduction.....	32
3.2 Methods.....	34
3.3 Results.....	43
3.4 Discussion.....	47
3.5 Conclusions.....	56
IV. NECROMASS PRODUCTION IN AN AMAZON FOREST:	
EXAMINATION OF UNDISTURBED AND LOGGED FOREST	
SITES.....	58
4.1 Introduction.....	58
4.2 Methods.....	62
4.3 Results.....	68
4.4 Discussion.....	74
4.5 Conclusions.....	84

V. A REVIEW OF ABOVE GROUND COARSE NECROMASS IN TROPICAL FORESTS.....	86
5.1 Introduction.....	86
5.2 Methods.....	87
5.3 Discussion.....	118
5.4 Conclusions.....	128
REFERENCES.....	129

LIST OF TABLES

2.1. Center coordinates of each 1x1 km IKONOS image subset used in the analysis.....	14
2.2. (a) Crown characteristics from the automated crown detection algorithm for Cauaxi and Tapajos.....	22
2.2. (b) DBH estimates from the automated crown detection algorithm.....	22
2.3. Remotely sensed estimates and field data of stand density and biomass from Cauaxi and Tapajos in the Brazilian Amazon.....	23
2.4. Results from automated algorithm run on IKONOS image data at different LBA-ECO sites throughout the Brazilian Amazon.....	26
2.5. Comparisons of crown detection algorithm results	27
3.1. Comparison of density and void space by site and decay class.....	44
3.2. Comparison between treatments and sites for necromass pool components.....	45
3.3. Comparison of site and treatments for average site densities generated from total site volume and total site mass.....	51
3.4. Estimation of pools and fluxes of necromass for an undisturbed forest assuming steady state.....	54
4.1. Production of Necromass over a four year period at Tapajos National Forest, Para, Brazil.....	68
4.2. Necromass Pools at Tapajos from two sample periods (2001 and 2004).....	72
4.3. Sources of Necromass for Production and Pool Estimates.....	72

4.4. A simple model to estimate pools and fluxes of necromass in an undisturbed forest assuming steady state.....	73
4.5. Production and mortality estimates of coarse necromass in an undisturbed forest assuming steady state.....	73
4.7. Examination of standing dead.....	74
5.1. Reviewed literature for tropical necromass, field measurements of CWD, biomass, fallen and standing pools, and production and decomposition rates.....	89
5.2. Reviewed literature for tropical necromass, necromass to biomass ratio, field measurements of production and decomposition rates compared with estimate production and decomposition rates.....	93
5.3. Literature reviewed with methods presented.....	97
5.4. Decay class explanation.....	101
5.5. Density and decay class estimates for tropical forest.....	103

LIST OF FIGURES

2.1(a). Digital number data used for termination of an ordinate (8 pixels).....	15
2.1(b). Digital number data used for termination of an ordinate (20 pixels).....	15
2.2. An example of ordinal transects.....	16
2.3. Sample output from crown detection algorithm at Fazenda Cauaxi (eastern Amazon).....	17
2.4 IKONOS image of the 64 ha area on the Fazenda Cauaxi (eastern Amazon).....	19
2.5. IKONOS image of the 64 ha area at the Tapajos National Forest (central Amazon).....	20
2.6(a). Cumulative frequency distribution for field observed canopy diameters and automated crown estimate at Cauaxi	24
2.6(b). Comparison of DBH size class distribution for field observed and automated estimates at Cauaxi	24
2.6(c). Comparison of field measured and observed and automated estimation of DBH size class distribution at Tapajos	24
3.1. Fallen vs. standing necromass for sites and treatments.....	46
4.1. Flux of newly fallen necromass shown for RIL (closed circles) and UF (open circles) treatments for nine sampling periods.....	69
4.2. A compartmental model of coarse necromass component measured and estimated.....	83
5.1. A simple model solved for many values in parameters.....	117

5.2a. Biomass and Necromass field measured values in undisturbed and disturbed tropical forests.....	122
5.2b. Biomass and Necromass field measured values in undisturbed tropical forests showing areas of high and low disturbance.....	123
5.3. Fallen vs. standing necromass for sites and treatments. Error bars represent standard errors (from Palace <i>et al.</i> in press).....	124
5.4. Fallen necromass and standing dead field measured values in undisturbed and disturbed tropical forests.....	124
5.5. A comparison of estimated decay rates ((biomass *0.2 y ⁻¹) / necromass stock) and field measured CWD stocks.....	127

ABSTRACT

TROPICAL FOREST STRUCTURE: GROUND MEASUREMENTS OF COARSE NECROMASS AND SATELLITE OBSERVATIONS OF CROWN GEOMETRY

by

Michael W. Palace

University of New Hampshire, December, 2006

Forests are structurally diverse, but these structures derive from the same processes of disturbance and growth. Understanding forest structure can help unlock the history, function, and future of a forested ecosystem. Components of forest structure include tree size distributions, foliage distributions and variation in canopy density, and coarse woody debris (coarse necromass). Tropical rainforests are structurally the most complex of all ecosystems. In addition to having high biological diversity, Amazon forests are marked by complex vegetation dynamics and a diverse forest stand structures, which play an important role in the interactions of water and carbon between the biosphere and atmosphere. Two aspects of forest structure in Amazonia are examined in this thesis, canopy geometry and coarse necromass. A crown delineation algorithm was developed that uses high resolution satellite image data. This algorithm was applied to two forests with field based data on forest structure and then applied at seven locations across the Amazon basin. The algorithm provided forest structure based on crown geometry across

vast areas where field based studies would be prohibitive due to cost and time. Coarse necromass dynamics were studied through a combination of field work using novel techniques that measured necromass density, volume, and calculated mass for fallen and standing coarse necromass stocks at two tropical forested sites. For both sites, the effect that reduced impact logging (RIL) had on coarse necromass pools was found to generate 50% more coarse necromass. Density and void space estimates were found to not be significantly different between sites. Standing dead and fallen coarse necromass were found to be proportionally related across sites and forest types. The production of necromass at one site, Tapajos, was examined over a 4.5 year period, providing an estimate of necromass cycling. RIL and undisturbed forests were found to have similar coarse necromass production. Mortality rates used to estimate coarse necromass production tend to underestimate the amount by about 55%. Finally a review of current literature dealing with coarse necromass dynamics in tropical forests was conducted.

CHAPTER I

INTRODUCTION

Forests play important roles in the ecosystem functioning and biological diversity throughout the world (Spies 1998). The complexity of forest floristics and structure are results of autecological properties of species and the responses of these species to patterns in space and time (Watts 1947). Spatial and temporal variation in disturbances and growth influence forest types and their unique assemblages of species, but the physical, chemical, and biological processes that these forest types function in are similar (Tansley 1935, Whitmore 1982). The history, function, and future tracks of a forested ecosystem are understood by examination and understanding the forest structure (Spies 1998). Components of forest structure to name a few include canopy geometry and tree architecture, size distributions of trees, species diversity, and even the dead and decay material from trees, termed necromass (Spies 1998).

Tropical rainforests are structurally the most complex of all ecosystems (Whitmore 1982). Terborgh *et al.* (1996) wrote that tropical forests are not “it would be better to argue that tropical forests are not qualitatively different from temperate forests, only more complex.” Flying over the Amazon forest gives the viewer the impression of a vast carpet of smooth simple green vegetation. However this can not be further from the

truth. The Amazonian forest is made up of heterogeneous canopies and forest types with unique assemblages of tree species, complex vegetation dynamics and history, and high biodiversity (Brown *et al.* 1995, Chave *et al.* 2001, Houghton *et al.* 2001, Salati and Vose, 1984, Terborgh *et al.* 1996, Terborgh 1992).

The Amazonian forest is the largest continuous tropical forest in the world and accounts for 40% of this remaining ecotype (Melillo *et al.* 1993). The biodiversity of this forest is immense, providing haven to 30% of all plant species and 40% of all bird species (Silva *et al.* 2005). Compilations indicate that within Amazonia there are 40,000 plant species, 30,000 fish species, and 427 mammals, 1294 birds, 378 reptiles, 427 amphibians (Silva *et al.* 2005).

The Amazonian forest plays an important role in the interactions of water and carbon between the biosphere and the atmosphere (Melillo *et al.* 1993). The forest is a huge reservoir for carbon due to biomass and necromass stocks and highly productive due to photosynthesis, both approximately 10% of the global total (Melillo *et al.* 1993). With ongoing deforestation and logging, regional and global climate change, and the influence that these have on the carbon cycle the Amazon forest has become the focus of much scientific research and debate (Keller *et al.* 2004b, Nobre *et al.* 1991, Werth and Avissar 2002).

The historical sequence of forest degradation and loss has accelerated in the Brazilian Amazon (Keller *et al.* 2004b, Davidson and Artaxo 2004). This is primarily due to the

immense natural resources that this region contains. Factors driving these changes are selective logging, land clearing for agriculture and pasture for cattle, mining, hydroelectric power, and road and infrastructure (Keller *et al.* 2004b, Davidson and Artaxo 2004).

Selective logging affects 15,000 to 20,000 km² y⁻¹ in the Brazilian Amazon (Asner *et al.* 2005), changing the storage and cycling of carbon in the necromass pools (Keller *et al.*, 2004a, Gerwing 2002, Palace *et al.* in press). Selective logging impacts vary with the intensity of extraction (Asner *et al.* 2004). Forests are revisited many times when loggers return to harvest additional trees as the markets develop (Matricardi *et al.* 2001). Conventional selective harvesting practices involved the creation of roads, patios, and skid trails to extract selective tree species. There tends to be little planning and much damage is done to the canopy. As much as 6 additional trees may be killed for each tree harvested and ground damage can be 8.9-11.2% (Matricardi *et al.* 2001, Pereira *et al.* 2002).

Reduced impact logging (RIL) is a method of selective logging that attempts to minimize the damage due to logging. Methods employed include tree surveys, cutting of vines, road planning, protective devices on treads, and planned directional felling (Pereira *et al.* 2002). Though RIL is increasing in use, the majority of logging in the Brazilian Amazon is not done with RIL practices (personal communication).

Three major question that the scientific community are exploring are; (1) what is the

Amazon carbon stock? (2) how is it changing? and (3) what are the rates of carbon cycling? This thesis explores these three questions by examining the forest structure of Amazonia forests through the analysis of crown geometry and necromass stocks and fluxes. This was done using field measurements of coarse woody debris and satellite observations of crown geometry using high resolution image data. For the purpose of this thesis, tree geometry is defined as crown width, area, depth, and shape. Necromass is defined as all organic dead material. Necromass that is greater than 2 cm in diameter, from tree trunks, vines, and branches is termed coarse necromass or coarse woody debris (CWD).

This thesis has four main components. First, an automated algorithm that detects crown structure in forests using high resolution image data was developed. An examination of 51 (1 km²) areas from seven (NASA Large Scale Biosphere Atmosphere Experiment in Amazonia LBA) sites located throughout the Amazon using this algorithm was conducted. Second, the measurement of coarse necromass and its role in the carbon budget was done through a combination of field work using novel techniques that measured coarse necromass density, volume, and calculated mass for fallen and standing necromass stocks at two tropical forested sites. For both sites, the effect reduced impact logging had on the coarse necromass pool was examined. Third, the production of necromass at one site was examined over a 4.5 year period, providing an estimate of necromass cycling. Finally, a literature review of above ground coarse necromass in tropical forests was conducted.

Chapter 2: Amazon Forest Structure from IKONOS Satellite Data and Automated Crown Delineation

The height and architectural complexity of the canopy, along with the logistical challenges of tropical field research and methodologies, limit studies of tropical forest structure. Remote sensing can supplement traditional ecological studies by providing observations of large areas (Roughgarden *et al.* 1991, Shugart *et al.* 2001). In this chapter we developed a new automated tree crown detection algorithm with 1-m panchromatic IKONOS satellite images to examine forest canopy structure in the Brazilian Amazon. The algorithm was calibrated with tree geometry and forest stand data at the Fazenda Cauaxi (3.75° S, 48.37° W) in the eastern Amazon, and then compared with field data at Tapajos National Forest (3.08° S, 54.94° W) in the central Amazon. We used the remote sensing algorithm to estimate crown dimensions and aboveground biomass in 51 forest stands (1 km²) throughout the Brazilian Amazon.

This remote sensing method is a first step toward automated analysis of crown width distributions and stem frequency using high spatial resolution panchromatic imagery from IKONOS over remote tropical forest ecosystems. Using allometric relations, we estimated DBH distributions and biomass of these forests. We found that the remotely sensed crown width and DBH distributions tended to overlook small trees and overestimate the size and frequency of large trees. These errors are probably caused by the merging of smaller tree crowns, division of larger tree crowns, and the inability to

view smaller understory trees with optical remote sensing data. High spatial resolution satellite data are increasingly available. With such data, it is possible to randomly sample large areas and develop estimates of forest structure for regions such as the Amazon basin, where ground based information is severely limited.

Chapter 3: Necromass in Undisturbed and Logged Forests in the Brazilian Amazon

In this chapter we estimated volume, density, and mass of fallen and standing coarse necromass in undisturbed and selectively logged forests at Juruena, Mato Grosso, Brazil (10.48° S, 58.47° W). We also measured standing dead trees at the Tapajos National Forest, Para, Brazil (3.08° S, 54.94° W) complementing our earlier study there on fallen coarse necromass. We compared forest that was selectively logged using reduced-impact logging methods and undisturbed forest. We estimated coarse necromass density accounting for void volume for necromass greater than 10 cm diameter at Juruena for five decay classes that ranged from freshly fallen to highly decayed material.

Coarse necromass represents about 19-26% of the aboveground carbon for undisturbed forests at these sites. With RIL harvest management, logged forests had approximately 1.5 times as much total coarse necromass as undisturbed forests. Density and void space estimates for decay classes were similar at the two sites, indicating that these measurements may be usefully applied for necromass studies conducted in similar forest types in Amazonia. Proportions of standing dead and fallen small, medium, and large coarse necromass size classes were similar across sites within treatments (RIL vs. UF).

Decay class proportions were also similar across sites within treatments. RIL treatments showed a proportionate increase in both fallen and standing coarse necromass across sites compared to UF. Small and medium size classes make up about 12-21% percent of total coarse fallen necromass. Standing dead made up 12-17% of the total coarse necromass. Comprehensive studies of necromass in tropical forests need to include both standing dead and smaller size class measurements (< 10 cm diameter) because collectively these contribute a large proportion of the overall coarse necromass pool. A simple compartment model with the assumption of steady state for undisturbed forests indicates that coarse necromass at our two study sites has a residence time of about 7 y in the forests studied. The rapid decay of this necromass suggests that the flux of carbon dioxide from necromass may account for approximately 15% of the gross CO₂ efflux from these undisturbed forests.

Chapter 4: Necromass Production in an Amazon Forest: Examination of Undisturbed and Logged Forest Sites

In this chapter we developed methodology to examine the production of coarse necromass in tropical forests. We examined production of fallen coarse necromass over four and a half years using repeated surveys in forest areas that had been subjected to reduced impact logging and in an undisturbed forest at the Tapajos National Forest, Belterra, Brazil (3.08° S, 54.94° W). We also estimated fallen coarse necromass and standing dead stocks at two times during our study. For both production and stock estimates of fallen necromass, we identified the source of each piece of necromass as either trunk, branch, or unidentifiable. We grouped fallen necromass into three diameter

size classes; large (>10 cm), medium (5-10 cm) and small (2-5 cm) for both production and stock estimates. Decay class densities were used to determine mass from volume measurements.

Findings indicate that select logging in the form of RIL alters the stock of fallen necromass, but not the standing dead stock. RIL also has no influence on production dynamics in the few years following logging. We found that the production and decay of necromass are approximately 12% of the total above ground respiration. Necromass accounts for 14% of the total above ground biomass in an undisturbed forest. Smaller diameter necromass decays more quickly than larger necromass and account for 30% of the fallen necromass created. Standing dead necromass accounts for up to 15% of the total necromass. Based on these findings, we encourage the tally of standing dead and fallen necromass into distinct size classes. We also suggest that production estimates may prove useful and better than the use of mortality rates in understanding necromass dynamics. Finally, a better knowledge of necromass dynamics in tropical forests will aid in regional and carbon ecosystem models.

Coarse necromass production was 55% greater than an estimate based on mortality rate of 0.015 y^{-1} and a biomass estimate of 282 Mg ha^{-1} . Use of mortality alone ignores branchfall and differential mortality rates of biomass components such as vines, small trees, and shrubs that also generate coarse necromass. For carbon cycling studies, we believe that direct measurement of the production of coarse necromass is preferable to the estimation of necromass production from mortality statistics.

Chapter 5: A review of above ground coarse necromass in tropical forests

We reviewed and analyzed current literature pertaining to coarse necromass dynamics in tropical forests in this last chapter. We examined literature pertaining to stocks or pools of above ground coarse necromass, the disturbance and the episodic production of coarse necromass, and the slower process of decomposition in tropical forests. We present a set of definitions and a review of current literature pertaining to coarse necromass and we examine methodologies and tools that aid coarse necromass study. Data was compiled from existing studies and pools and fluxes were compared among tropical forest sites.

We compiled data from existing studies and compared pools and fluxes of coarse necromass among tropical forest sites. General relationships among coarse necromass components were explored such as necromass to biomass proportions and fallen to standing dead necromass. Methodology was comparable across the literature for necromass production and stock estimates. Coarse fallen stock was almost two times more frequently measured than standing dead. We calculated production and decomposition rate estimates through the use of a simple model when these values are not available. General relations and proportions between necromass components were explored and were found to vary greatly. No definitive relations were found among necromass components across sites. In undisturbed forests there appears to be a peak in the coarse necromass with middle values of the biomass distribution. Beyond that peak as biomass increases the proportion of coarse necromass decreases. The ratio of coarse necromass to biomass ranged from 0.4 % in an undisturbed forest to 304% in a disturbed

forest. Standing dead necromass accounts for a large proportion of the total coarse necromass stock, up to 66% in an undisturbed forest and 98% at a heavily disturbed site, and should be included in further field estimates. We found that localized variability is high and complicates or hinders the development of general relationships of coarse necromass components across the tropics. Many of the studies (42%) only examined only one component of coarse necromass dynamics. We stress the importance of measuring multiple coarse necromass components and ideally conducting these measurements over years or even decades in order to improve our knowledge of necromass dynamics in tropical forests.

CHAPTER II

AMAZON FOREST STRUCTURE FROM IKONOS SATELLITE DATA AND AUTOMATED CROWN DELINEATION¹

Introduction

Amazon forests are marked by high biological diversity and complex vegetation dynamics that result in a spatially diverse array of forest stand structures (Richards 1952, Denslow 1980, Salati and Vose 1984, Terborgh 1992, Terborgh *et al.* 1996, Ozanne *et al.* 2004). Knowledge of the forest structure in the region is vital for estimation of carbon stocks and fluxes (Houghton *et al.* 2000; Houghton *et al.* 2001), habitat and faunal distributions (Schwarzkoft and Rylands 1989), and interactions between the biosphere and atmosphere (Keller *et al.* 2004b). However, the height and architectural complexity of the canopy, along with the logistical challenges of tropical field research and methodologies, limit studies of tropical forest structure. Remote sensing can supplement traditional ecological studies by providing observations of large areas (Roughgarden *et al.* 1991, Shugart *et al.* 2001).

A series of Landsat sensors have provided the data most often used in remote sensing studies of land cover in the humid tropics (Roberts *et al.* 2003). The spatial resolution (~

¹ This chapter is based on and contains material from a manuscript that will be submitted for publication in 2006. M. Palace, M. Keller, G.P. Asner, S. Hagen, B. Braswell. Amazon Forest Structure from IKONOS Satellite Data and Automated Crown Delineation. Soon to be submitted to *Biotropica*.

30 m) and spectral coverage (7 bands) of Landsat data allow identification of broad land-cover features and changes such as deforestation (e.g., Skole and Tucker 1993). More subtle changes resulting from logging can be discerned in spectral mixture model analysis of Landsat and similar data (Asner *et al.* 2005, Souza *et al.* 2003). However, extraction of tropical forest structural properties from Landsat data is challenging because the image resolution is comparable to the size of the largest tree crowns (Moran *et al.* 1994; Steininger 1996, Scarth and Phinn 2000). Higher spatial resolution imagery with a pixel size much smaller than the average crown width is thus desirable for examining forest structure (Culvenor 2002, Pouliot *et al.* 2002, Read *et al.* 2003, Leckie *et al.* 2003).

Crown delineation from satellite images can be performed using visual interpretation or automated methods (Wulder *et al.* 2000, Culvenor 2002, Pouliot *et al.* 2002). Visual interpretation approaches are resource intensive and difficult to implement consistently (Asner *et al.* 2002), whereas existing automated routines can be readily replicated but also may be inaccurate (Culvenor 2002). Three sources of high resolution imagery that have been used in crown geometric analysis are aerial photographs, videography, and satellite images. Due to its high spatial resolution, photographic imagery has primarily been used for the estimation of stand density and crown width (Dawkins 1962, Bolduc *et al.* 1999, Fensham *et al.* 2002). Videography has also been used along transects to analyze forest structural components, including individual crowns (Culvenor 2002, Brown *et al.* 2005). Newer satellite instruments, such as IKONOS and Quickbird, provide relatively inexpensive high-resolution images for remote areas. These high resolution satellite image data have been used to estimate the number of trees per area,

individual crowns widths, and gap structure in tropical forests (Asner *et al.* 2002, Read *et al.* 2003, Clark *et al.* 2004). However, previous studies have covered small geographic areas ($< 10 \text{ km}^2$) because only labor-intensive manual methods were used. Moreover, the high-resolution satellite methods have not examined site variation of biomass in tropical forests.

We developed an automated detection technique to estimate crown sizes from IKONOS satellite images collected over tropical forests in Brazil. We compared the remotely sensed crown measurements to field surveys at two forest sites in the central and eastern Amazon, and used allometric equations to extend the remote sensing estimates to biomass. We then applied and evaluated the detection algorithm and allometric equations to 51 forest stands from IKONOS images spread throughout the Brazilian Amazon to estimate crown dimensions and biomass across a range of mature forest conditions.

Methods

Satellite Imagery

We used seven IKONOS satellite images (Space Imaging Inc., Thorton, CO, USA) collected throughout the Brazilian Amazon. The 1-m panchromatic data were acquired through the Large-Scale Biosphere-Atmosphere Experiment in Amazonia (LBA) project (Hurt *et al.* 2003, Keller *et al.* 2004b; <http://eos-webster.sr.unh.edu/home.jsp>). The IKONOS images were subset to 51 one km^2 areas containing intact, closed-canopy forest for subsequent analysis using our crown detection and analysis algorithm (Table 2.1). Two of these areas, Cauaxi and Tapajos were used to develop our automated crown

detection algorithm, through comparisons with field data. No cross validation was conducted because we only collected field data for Cauaxi that included crown widths. Geographical coordinates for all of the IKONOS areas analyzed are presented in Table 2.1.

Table 2.1. Center coordinates of each 1x1 km IKONOS image subset used in the analysis.

Image/Site	Longitude	Latitude	Site	Longitude	Latitude
Cauaxi	-48.315	-3.745	Alta Floresta	-55.955	-9.575
Cauaxi	-48.315	-3.765	Alta Floresta	-55.955	-9.595
Cauaxi	-48.315	-3.775	Alta Floresta	-55.955	-9.605
Cauaxi	-48.315	-3.785	Alta Floresta	-55.945	-9.595
Cauaxi	-48.305	-3.725	Alta Floresta	-55.945	-9.605
Cauaxi	-48.305	-3.735	Alta Floresta	-55.925	-9.605
Cauaxi	-48.305	-3.755	Alta Floresta	-55.925	-9.615
Cauaxi	-48.305	-3.775	Alta Floresta	-55.915	-9.605
Cauaxi	-48.295	-3.725	Alta Floresta	-55.915	-9.615
Cauaxi	-48.295	-3.735	Alta Floresta	-55.915	-9.625
Cauaxi	-48.295	-3.755	Santarem km 67	-54.975	-2.835
Cauaxi	-48.295	-3.775	Santarem km 67	-54.975	-2.875
Cauaxi	-48.275	-3.735	Santarem km 67	-54.965	-2.865
Cauaxi	-48.275	-3.745	Santarem km 67	-54.965	-2.875
Caxiuana	-51.455	-1.745	Santarem km 67	-54.955	-2.875
Jaru	-61.945	-10.075	Santarem km 67	-54.945	-2.855
Jaru	-61.935	-10.055	Santarem km 67	-54.945	-2.865
Manaus	-60.225	-2.615	Santarem km 67	-54.945	-2.875
Manaus	-60.225	-2.625	Santarem km 67	-54.935	-2.865
Manaus	-60.215	-2.605	Santarem km 67	-54.935	-2.875
Manaus	-60.215	-2.615	Santarem km 83	-54.985	-3.055
Manaus	-60.205	-2.585	Santarem km 83	-54.975	-3.055
Manaus	-60.205	-2.635	Santarem km 83	-54.965	-3.065
Manaus	-60.195	-2.615	Santarem km 83	-54.955	-3.065
Manaus	-60.195	-2.635	Santarem km 83	-54.945	-3.065
Manaus	-60.185	-2.585			

Crown Detection and Analysis

We developed an automated crown detection algorithm for use with high spatial resolution remote sensing data from IKONOS and similar spaceborne sensors, based on spatial analysis of the brightness patterns in the image (visible reflectance, DN). There are two preprocessing steps. First, the modal, maximum and minimum brightness value of each IKONOS image is calculated. These statistics are used to set the dynamic range of an iterative, local-maximum finding step, as explained later. Second, a 3 x 3 pixel

moving window averaging filter is used to smooth the image.

After preprocessing, local maximum brightness values are identified by searching the entire image for the highest brightness value. After a local maximum is selected, image brightness values are analyzed in 360 directions (ordinates) from each local maximum or nodal pixel. Each individual ordinal transect is terminated when the digital number (DN) difference between a pixel and the next pixel along is greater than a threshold value (the derivative threshold) (Figure 2.1). The ordinate length is limited to 40 m based on maximum crown dimensions observed in field studies and knowledge that an ordinate can cascade down adjacent canopies, thus not detecting the crown edge.

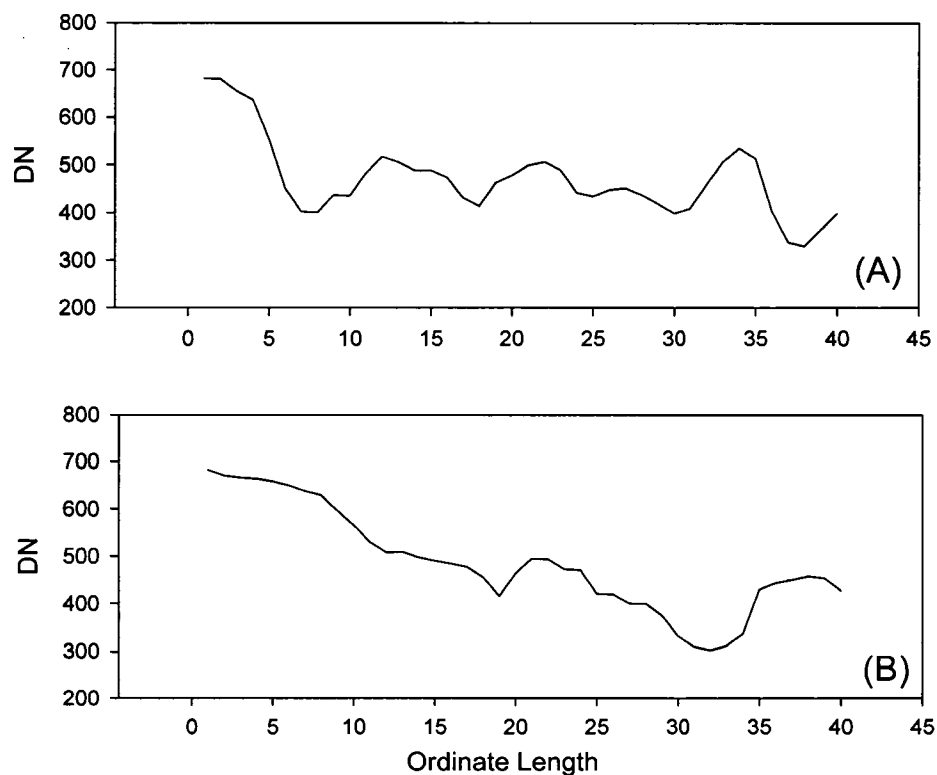
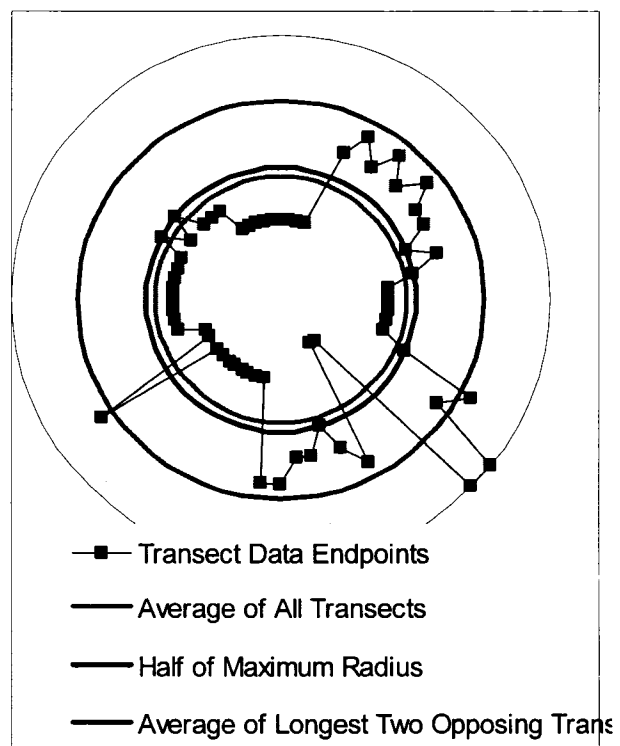


Figure 2.1. Digital number data used for termination of an ordinate. (a) The crown edge is estimated to be 8 pixels from the local maxima. (b) The crown edge is estimated to be 20 pixels from local maxima.

For simplicity, tree crowns are approximated as circles centered on the local maximum, based on the assumption that an undamaged tree has branches that radiate evenly out from the central stem or trunk (Brandtberg and Walker 1998). The estimated crown is centered at the local maximum and has a radius of half the sum of the two longest opposing ordinal transects (Figure 2.2). After a crown is located and delineated, the pixels within the crown area are removed from further analysis. No new ordinal transects are extended into an existing crown, and local maxima are prohibited from being analyzed in the circular crown area. Crowns overlap when ordinal transects from a neighboring tree create a large enough crown width, and thus a large enough circular canopy, to create crown overlap (Figure 2.3). Once all local maxima of a specific brightness value are analyzed throughout an image, the algorithm proceeds to the next lower brightness value and begins finding local image pixel brightness maxima again.

Figure 2.2. An example of ordinal transects used in the automated crown detection algorithm. Length of ordinal transects are used to determine crown radius.



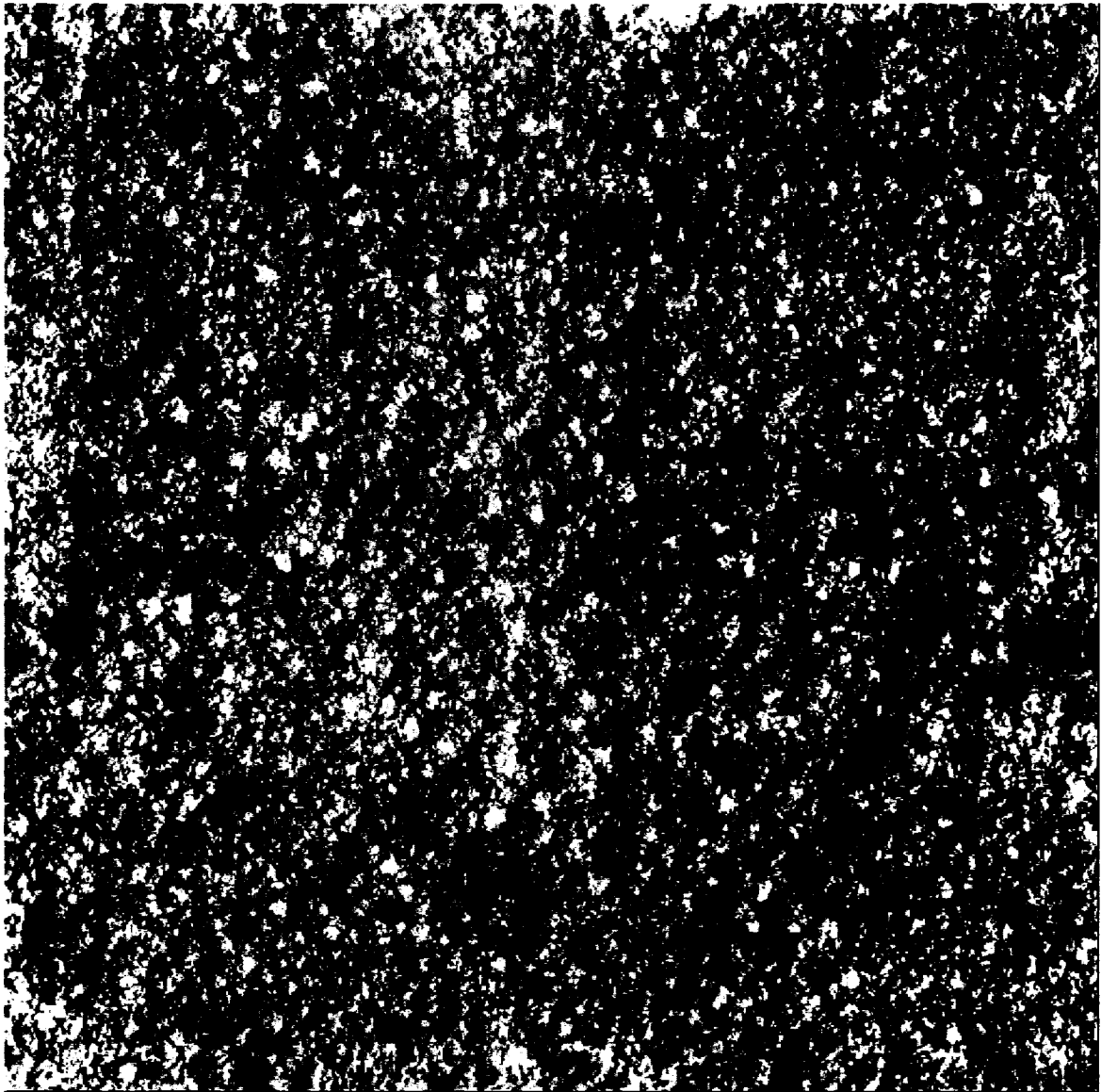


Figure 2.3. Sample output from crown detection algorithm. Green circles represent crown edge determined by the average of the two longest opposing transects. This is the 64 ha area on the Fazenda Cauaxi (eastern Amazon).

Field Data and Allometric Equations

Field data on crown dimensions are extremely sparse for Amazon forests; however, Asner *et al.* (2002) collected measurements of crown width, depth, tree height and diameter at breast height (DBH) for ~300 trees in a 50 ha stand on the Fazenda Cauaxi in the eastern Brazilian Amazon. We also measured the DBH and crown position

(understory or canopy) of over 2,700 trees as part of our stratified sampling methodology. We therefore relied on these measurements to test and calibrate our remote sensing algorithm. Additional stand data for the Tapajos National Forest in the central Brazilian Amazon were provided by Keller *et al.* (2001) and Rice *et al.* (2004) to test the algorithm in a second forest stand.

Most tree allometric equations utilize DBH, tree height, or both for estimating aboveground biomass and carbon stocks in tropical forests (e.g., Brown 1997, Chave *et al.* 2001). However, optical remote sensing data from IKONOS cannot be used to directly measure either height or DBH for trees in closed canopies, so other allometric equations based on crown diameter are needed. We developed a relation between crown width (m) and DBH (cm) from 300 individual trees measured using a stratified sampling method (Asner *et al.* 2002).

$$\text{DBH} = 0.038 * (\text{crown width})^2 + 2.33 * (\text{crown width}) + 15.58 \quad (1)$$

A commonly used allometric equation for tropical forests developed by Brown (1997) was then used to extend the remote sensing observations of crown width to biomass (kg dry matter) via DBH:

$$\text{Biomass} = (42.69 - 12.80 * \text{DBH} + 1.242 * \text{DBH}^2) / 1000 \quad (2)$$

Calibration at Cauaxi

A calibration of the algorithm was performed on the two parameters: (1) the derivative threshold and (2) the local maximum analysis range using data from 64 ha (800 by 800 m) of undisturbed forest at Cauaxi (Figure 2.4). Crown size distributions (binned in 2 m classes) from our automated crown delineation algorithm were compared with field measurements from Asner *et al.* (2002). We measured goodness of fit using the root mean squared error of crown width distribution to examine algorithm parameters that best simulated Cauaxi field data. Automated algorithm results were also compared to mean DBH (cm) and trees per unit area (frequency of trees; trees/ha) from the Cauaxi field data.

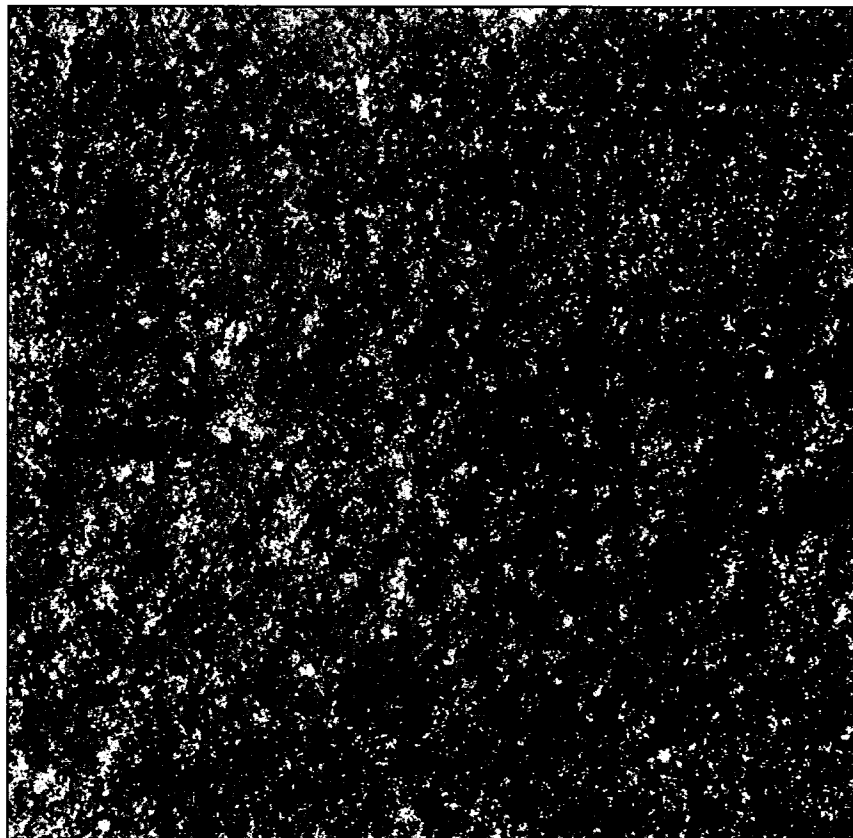


Figure 2.4. IKONOS image of the 64 ha area on the Fazenda Cauaxi (eastern Amazon) analyzed using the automated crown detection algorithm. Field data were collected at this site and first presented by Asner *et al.* (2002). This is the same area as Figure 2.3.

Analysis at Tapajos and 51 Other Locations

Following the Cauaxi calibration step, we ran the algorithm on an IKONOS image taken of the Tapajos National Forest in the central Brazilian Amazon (Figure 2.5). Only the local maximum analysis range, which is determined as the difference between the maximum and mode of DN values, was set to a different value during pre-processing of the Tapajos image. We then compared the results from the Tapajos image analysis to field data provided by Keller *et al.* (2001). To estimate differences in forest structure among a wider variety of forest sites, we examined 51 IKONOS image subsets listed in Table 2.1. Comparisons of the results from each site were done using an ANOVA with Tukey-Kramer HSD comparison ($\alpha = 0.05$).

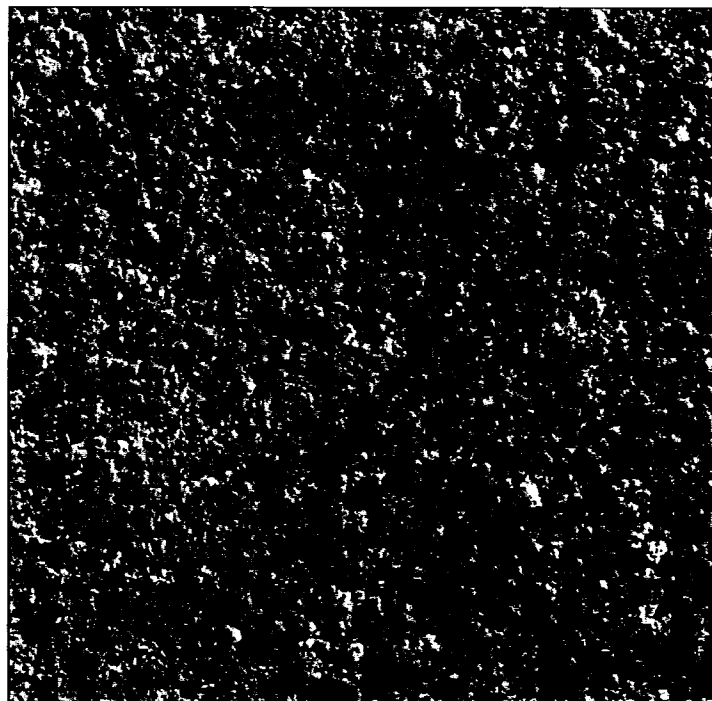


Figure 2.5. IKONOS image of the 64 ha area at the Tapajos National Forest (central Amazon) analyzed using the automated crown detection algorithm. Field data were collected at this site and presented by Keller *et al.* (2001).

Results

Calibration (Cauaxi)

Forest structural parameters for the Cauaxi image analysis are presented in Table 2.2. Average estimated crown width was 13 ± 6 m (mean \pm s.d.), with a minimum of 2 m and a maximum of 34 m. The distribution of crown widths (Figure 2.6a) was similar in magnitude and in overall pattern with the observed values, although a Kolmogorov-Smirnov test for difference between distributions indicated a significant difference ($\alpha=0.05$) between the field-measured tree crowns width distribution and the remotely sensed estimates. The frequency of trees for the automated algorithm was 76.6 trees/ha. Taking into account the allometric relation between crown width and DBH presented by Asner *et al.* (2002), DBH estimates from IKONOS were 54.0 ± 19 cm, with a distribution similar to that measured in the field (Figure 2.6b). Biomass estimated from the algorithm and eq. (2) was 262 Mg/ha. The tree areal frequency and biomass estimates compared well with field data (Tables 2.2-2.3). Significant differences were determined between mean field estimated crown width (for both all trees and no understory) and our automated mean crown estimate. These differences are due to large sample numbers which create an extremely small standard error of the mean. Our automated algorithm provided better estimates of the mean crown width and mean DBH than that of manual crown delineation from Asner *et al.* (2002) (Table 2.2a-b).

Table 2.2a. Crown characteristics derived from the automated crown detection algorithm for the Cauaxi and Tapajos forest stands.

Cauaxi				Tapajos			
Crown Width (m)	IKONOS	IKONOS	Field Data	Field Data	Crown Width (m)	IKONOS	Field Data
Quantiles	Automated	Manual*	No Understory*	All*	Quantiles	Automated	Derived from ***
maximum	34	40	41	41	maximum	38	30
upper quartile	16	20	15	15	upper quartile	18	15
median	12	16	11	11	median	12	13
lower quartile	8	10	8	8	lower quartile	8	11
minimum	2	3	1	1	minimum	2	6

Crown Width	IKONOS	IKONOS	Field Data	Field Data	Crown Width	IKONOS	Field Data
Moments	Automated	Manual*	No Understory*	All*	Moments	Automated	All
Mean	13	16	12	12	Mean	13	13
Std Dev	6	8	2	2	Std Dev	6	3
N	3972	1675	1370	2127	N	3963	5869

Table 2.2b. DBH estimates from automated crown detection algorithm.

Cauaxi				Tapajos			
DBH (cm)	IKONOS	Field Data	Field Data	DBH (cm)	IKONOS	Field Data	
Quantiles	Automated	No Understory*	All*	Quantiles	Automated	All**	
maximum	138.7	172.0	172.0	maximum	159.0	190.0	
upper quartile	66.1	53.0	53.0	upper quartile	69.7	59.6	
median	52.3	37.0	37.0	median	52.2	47.0	
lower quartile	39.6	26.0	26.0	lower quartile	39.6	39.6	
minimum	22.9	20.0	20.0	minimum	22.9	15.0	

DBH	IKONOS	Field Data	Field Data	DBH	IKONOS	Field Data
Moments	Automated	No Understory	All	Moments	Automated	All
Mean	54.0	43.1	43.1	Mean	55.8	51.9
Std Dev	19.0	3.6	3.6	Std Dev	22.1	16.9
N	3972	1370	2127	N	3963	5869

Table 2.3. Remotely sensed estimates and field data of stand density and biomass from Cauaxi and Tapajos in the Brazilian Amazon.

Source	Site	Size of Survey (ha)	Density (trees ha⁻¹)	Biomass (Mg ha⁻¹)
Keller et al. 2001	Tapajos km 83 (1997)	392	55.0 > 35 cm DBH	177 > 35 cm DBH
			168.0 > 15 cm DBH ²	224 > 15 cm DBH ²
Rice et al. 2004	Tapajos km 67 (2001)	4	496.0 > 10 cm DBH	311 > 10 cm DBH
	Tapajos km 67 (2001)	20	43.8 > 35 cm DBH	193 > 35 cm DBH
Field Data ¹	Cauaxi (2000)	15.8	137.3 >20 cm DBH	249 > 20 cm DBH
	Cauaxi (2000)	15.8	55.1 > 35 cm DBH	203 > 35 cm DBH
Automated Estimate	Cauaxi	51.8	76.6	262
Automated Estimate	Tapajos	51.8	76.4	290

¹ New data from Cauaxi based on original data presented by Asner et al. (2002)

² Estimates of DBH > 15 cm include smaller classes using de Liocourt quotient (Keller et al. 2001)

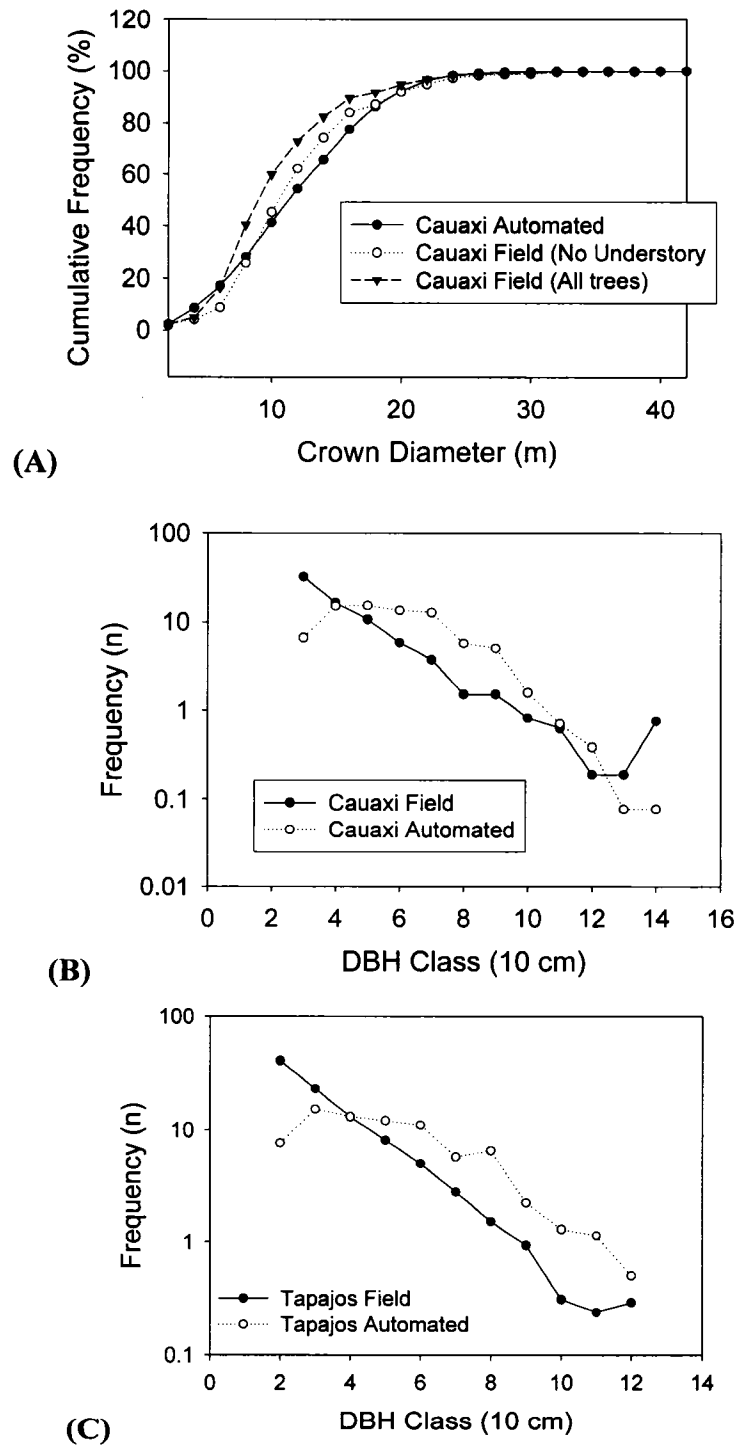


Figure 2.6. (a) Cumulative frequency distribution for field observed canopy diameters and automated crown estimate at Cauaxi. (b) Comparison of DBH size class distribution for field observed and automated estimates at Cauaxi. (c) Comparison of field measured and observed and automated estimation of DBH size class distribution at Tapajos. Observed DBH class 12 includes all DBH classes (10 cm DBH classes) summed ≥ 120 cm DBH.

Comparison with Tapajos

The automated algorithm estimated a mean crown width at Tapajos of 13 ± 6 m, with a minimum of 2 m and a maximum of 38 m (Table 2.2a). The estimated frequency of trees was 76.4 trees/ha, and the mean DBH was 56 ± 22 cm. The distribution of DBH size classes was determined using crown widths from the automated algorithm (Figure 2.6c). The automated estimate for above-ground biomass was 290 Mg/ha at Tapajos. Significant differences were determined between mean field estimated crown width (for both all trees and no understory trees) and our automated mean crown estimate. Once again this difference is likely due to large sample numbers (Table 2.2a-b). Though we lack actual field estimates of crown width at Tapajos, our automated algorithm compared well with field estimated mean DBH and mean crown width developed from Keller *et al.* 2001 and Eqn. (1) of this paper.

Multi-site Analysis

Estimates of crown width, frequency of trees, DBH, and biomass derived from the automated crown detection algorithm on 51 stands sub-set from seven IKONOS images in the Brazilian Amazon are presented in Table 2.4. The Jaru image had the largest estimated average crown width and DBH (16 m and 65 cm), whereas Manaus had the smallest of these two estimates (11 m and 49 cm). Manaus had the highest tree frequency (99 trees/ha) and Jaru had the lowest (53 trees/ha). Aboveground biomass was estimated to be lowest at Tapajos km 67 (258 Mg/ha), whereas Caxiuana and Jaru were remarkably similar (281 Mg/ha). Santarém km-83 and Alta Floresta also had similar biomass

estimates (275 Mg/ha). The algorithm indicated that aboveground biomass ranged between 258 and 281 Mg/ha across all sites. Biomass showed less variation between sites than crown width, tree frequency and DBH.

Manaus and Jaru had markedly different structural characteristics from all other sites (Table 2.5). There was an inverse relationship between mean crown width and the tree frequency. Alta Floresta showed a significant difference in estimated crown width and average DBH from Jaru and the two Tapajos sites. Biomass was found to be significantly different only between Santarem km-67 and Manaus, and Santarem km-67 and Alta Floresta.

Table 2.4. Results from automated algorithm run on IKONOS image data at different LBA-ECO sites throughout the Brazilian Amazon.

Site Name	IKONOS Tiles	Average Crown Width (m)		Average DBH (cm)		Biomass (Mg ha ⁻¹)		Areal Frequency (number ha ⁻¹)	
		Mean	Std Error	Mean	Std Error	Mean	Std Error	Mean	Std Error
Cauaxi	14	13.3	0.1	56	0.4	266	2	70	1
Caxiuana	1	12.3		53		281		83	
Jaru	2	15.6	0.2	65	0.5	281	5	53	2
Manaus	9	11.3	0.1	49	0.5	279	2	99	3
Alta Floresta	10	13.0	0.2	55	1.0	275	2	76	2
Santarem 67	10	13.8	0.1	58	0.5	258	3	65	2
Santarem 83	5	13.7	0.3	58	0.8	275	5	68	3

Table 2.5. Comparisons of crown detection algorithm results between different LBA forest sites using ANOVA. All comparison pairs use Tukey-Kramer HSD with an alpha value of 0.05. [+] indicates a significant difference between sites.

Crown Width

	Jaru	Santarem 83	Santarem 67	Cauaxi	Mato Grosso	Caxiuana	Manaus
Jaru	-	+	+	+	+	+	+
Santarem 83		-	-	-	+	+	+
Santarem 67			-	-	+	-	+
Cauaxi				-	-	-	+
Mato Grosso					-	-	+
Caxiuana						-	-
Manaus							-

DBH

	Jaru	Santarem 83	Santarem 67	Cauaxi	Mato Grosso	Caxiuana	Manaus
Jaru	-	+	+	+	+	+	+
Santarem 83		-	-	-	+	-	+
Santarem 67			-	-	+	+	+
Cauaxi				-	-	-	+
Mato Grosso					-	-	+
Caxiuana						-	-
Manaus							-

Density

	Manaus	Caxiuana	Mato Grosso	Cauaxi	Santarem 83	Santarem 67	Jaru
Manaus	-	-	+	+	+	+	+
Caxiuana		-	-	-	-	-	+
Mato Grosso			-	-	-	+	+
Cauaxi				-	-	-	+
Santarem 83					-	-	-
Santarem 67						-	-
Jaru							-

Biomass

	Caxiuana	Manaus	Mato Grosso	Jaru	Santarem 83	Cauaxi	Santarem 67
Caxiuana	-	-	-	-	-	-	-
Manaus		-	-	-	-	-	+
Mato Grosso			-	-	-	-	+
Jaru				-	-	-	-
Santarem 83					-	-	-
Cauaxi						-	-
Santarem 67							-

Discussion

Our algorithm for automated characterization of tropical forest canopy properties combines local maximum filtering and local minima value-finding methods, with analysis of ordinal transect data radiating outward from a crown apex (local maximum). Our method differs from an earlier approach (Pouliot *et al.* 2002) because we use a derivative threshold to end ordinal transect length instead of a regression analysis. Using the derivative threshold allowed us to account for crown overlap and varied crown shapes, sizes and spacing inherent in old-growth tropical forests. Iterative local maximum filtering allows for more of the canopy trees in an image to be examined, since some canopy trees with variation in color and brightness (due to leaf phenology and flowering) might overwhelm a single local maximum analysis.

Our algorithm estimated crown widths and areal frequency (trees/ha) from the IKONOS satellite imagery. Crown widths measured in the field for all trees at Cauaxi were generally smaller than automated estimates. Mean field-estimated crown width that excludes understory trees, matched more closely with automated crown detection algorithm (Table 2.2a) than with manual interpretation of the same IKONOS data (Asner *et al.* 2002). At both Cauaxi and Tapajos, the remotely sensed average crown widths were within 3 percent of the crown widths derived from field measurements (Table 2.2). Although, significant differences were determined at Cauaxi between mean field estimated crown width (for both all trees and no understory) and our automated mean crown estimate, our automated algorithm provided better estimates of the mean crown

width and mean DBH than that of manual crown delineation from Asner *et al.* (2002) (Table 2.2a-b). Considering the complexity of tropical forest structure and the inability to view understory trees in IKONOS image data, our algorithm compared well with field data (Table 2.3).

At Cauaxi, field-measured stem frequency was 55 trees/ha for trees greater than 35 cm DBH and 137 trees/ha for trees greater than 20 cm DBH. Our detection algorithm identified 77 trees/ha, whereas manual interpretation of the same IKONOS image (Asner *et al.* 2002) yielded 47 trees/ha. Field-measured stem frequency at Tapajos ranged from 44 to 55 trees/ha for trees greater than 35 cm DBH to 168 trees/ha for trees greater than 15 cm DBH (Table 2.2), whereas the automated crown detection algorithm counted 76 trees/ha at that site. Clearly, the automated crown detection algorithm is unable to count understory trees; the algorithm measured stem frequency with an apparent cut-off diameter near 28 cm.

We used allometric equations to estimate stand structural properties including the distribution of stem diameters (DBH) and stand biomass. Examination of the DBH distributions for Cauaxi indicated that the remote sensing underestimated the frequency of smaller trees (< 40 cm DBH) and overestimated the frequency of larger trees with DBHs > 120 cm (Figure 2.2a, Table 2.2). These errors are likely the result of the merging of smaller tree crowns, division of larger tree crowns, and the inability to view smaller understory trees with optical remote sensing data. At Tapajos, we compared the mean DBH for trees surveyed in the field (> 35 cm DBH) to the estimates from the

automated crown detection algorithm and found very similar results (field: 52 ± 17 cm; remote sensing: 53 ± 20 cm).

Aboveground biomass was estimated via two allometric equations: (1) crown width to DBH from field work done at Cauaxi; and (2) DBH to biomass (Brown 1997), and is thus subject to compounded errors. Nonetheless, field-estimated aboveground biomass at Cauaxi was 249 Mg/ha for trees greater than 20 cm DBH, whereas biomass estimated using automated crown detection algorithm was only 5 percent higher (Table 2.2).

An examination of 51 (1 km²) areas from seven LBA sites located throughout the Amazon differed considerably in estimates of crown width, DBH distribution, and stem frequency. Analysis of variance showed that crown widths at Jaru and Manaus differed from all other sites as well as with each other. Forest stands converged to similar biomass despite different structure parameters such as frequency and tree size (Table 2.3). The similarity of biomass across sites appears to result from a trade-off of stem frequency and maximum tree sizes. We note that we made no attempt to adjust our biomass estimates for wood density as has been suggested by recent studies (e.g., Baker *et al.* 2004), and we acknowledge the preliminary nature of these estimates.

Comprehensive validation data do not exist for most of the sites that we analyzed throughout the Amazon. Field forest structure data are rare across the Amazon.

However, we note that our estimates for Tapajos and Manaus show trends that are similar to field data collected by Viera *et al.* (2004). Our interest here was to develop baseline estimates that can guide future field measurements, and to exercise our algorithm as a

proof-of-concept for future analyses of forest structure over larger areas of remote tropical forests.

The frequency of gap-phase disturbance is a key regulator of forest dynamics in the lowland tropics (West *et al.* 1981, Denslow 1987, Brokaw 1985, 1987, Svenning 2000). Crown width is an important variable that we have examined using high resolution satellite imagery. Crown width distributions estimated by our automated crown detection algorithm may be a useful indicator for ecosystem disturbance regimes.

Conclusions

We developed and tested an automated forest tree crown detection algorithm that uses high spatial resolution imagery with a combination of techniques for crown size estimation. This remote sensing method is a first step toward automated analysis of crown width distributions and stem frequency using high spatial resolution panchromatic imagery from IKONOS over remote tropical forest ecosystems. Using allometric relations, we have estimated DBH distributions and biomass of these forests. We found that the remotely sensed crown width and DBH distributions tended to overlook small trees and overestimate the size and frequency of large trees. These errors are probably caused by the merging of smaller tree crowns, division of larger tree crowns, and the inability to view smaller understory trees with optical remote sensing data. High spatial resolution satellite data are increasingly available. With such data, it is possible to randomly sample large areas and develop estimates of forest structure for regions such as the Amazon basin, where ground based information is severely limited.

CHAPTER III

NECROMASS IN UNDISTURBED AND LOGGED FORESTS IN THE BRAZILIAN AMAZON²

Introduction

The death and subsequent decomposition of trees is an important component in forest ecosystem carbon cycling (Denslow, 1987; Harmon and Franklin, 1989). Dead trees or portions of dead trees are termed necromass. Necromass in tropical forests is rarely studied although it contributes a large proportion of the total carbon pool in tropical forests (Clark *et al.*, 2002; Chambers *et al.*, 2000; Keller *et al.*, 2004a). Necromass is important in nutrient cycling and it serves as habitat for some organisms (MacNally *et al.*, 2001; Norden and Paltto, 2001).

Necromass or coarse woody debris (CWD) is often divided into two categories: (1) fallen or downed necromass and (2) standing dead wood (snags) (Harmon *et al.*, 1986). In the Brazilian Amazon, previous estimates of CWD mass in undisturbed upland (*terra firme*) forests have ranged from 42.8 Mg C ha⁻¹ (Summers 1998 as cited by Rice *et al.*, 2004) to 15 Mg C ha⁻¹ (Brown *et al.*, 1995). Brown (1997) estimated that necromass accounts for 5% to 40% of the total carbon in a tropical forests, exclusive of soil carbon.

² This chapter is based on and contains material from an accepted manuscript. M. Palace, M. Keller, G.P. Asner, J. Silva, C. Passos. Necromass in Undisturbed and Logged Forests in the Brazilian Amazon. Accepted in *Forest Ecology and Management*.

In the Tapajós National Forest near Santarém, Brazil, the ratio of necromass to biomass ranged from 18% to 25% (Keller *et al.*, 2004a; Rice *et al.*, 2004). For tropical forested areas outside of the Brazilian Amazon, researchers have found CWD ranging from 3.8 to 6.0 Mg C ha⁻¹ in Jamaica (Tanner, 1980), 22.3 Mg C ha⁻¹ in Costa Rica (Clark *et al.*, 2002) and 22.5 Mg C ha⁻¹ in Malaysia (Yoda and Kira, 1982). Estimates of standing dead necromass are infrequent in tropical forests. Rice *et al.* (2004) found standing dead mass to be 8.6 Mg C ha⁻¹ or 18% of the total necromass, while Clark *et al.* (2002) found 3.1 Mg C ha⁻¹ or 12% of the total necromass.

The Amazon region contains the largest continuous expanse of tropical forest in the world and is important to carbon cycling on a global scale (Keller *et al.*, 2004b). Selective logging is a widespread practice in the Brazilian Amazon (Asner *et al.*, 2005). Although still uncommon in the Amazon region of Brazil, reduced impact logging (RIL) is a method of selective logging that limits the damage to the forest by use of tree surveys, vine cutting, road planning, articulated wheeled skidders, and planned directional felling (Pereira *et al.*, 2002). Canopy damage in RIL is about half that in conventional logging (Pereira *et al.*, 2002; Asner *et al.*, 2004). At the Fazenda Cauaxi in Pará State, Brazil, Keller *et al.* (2004a) estimated that conventional logging created 2.7 times more fallen necromass than that of RIL.

The mass of fallen CWD may be calculated from the product of measured volumes and estimates of CWD density (Keller *et al.*, 2004a). A difficulty in determining necromass density in tropical forests is the large number of tree species. Past studies in the tropics

have estimated CWD density using the average density of living trees or samples of decayed wood to estimate necromass density (Gerwing, 2002; Chambers *et al.*, 2000). Division of necromass into decay classes based on field inspection has been used to improve the quantification of CWD mass in forests (Harmon *et al.*, 1995, Eaton and Lawrence, 2006). Average density stratified by decay class facilitates the calculation of mass from necromass volume (Keller *et al.*, 2004a). Decay classes are easily recorded during measurements of volume and are critical for an accurate estimation of CWD mass because decayed logs have lower density than freshly fallen CWD (Harmon *et al.*, 1995). Void spaces in logs must be accounted for in density measurements either by using large pieces of necromass (e.g., Chambers *et al.*, 2000, Clark *et al.*, 2002) or by separately quantifying void space (Keller *et al.*, 2004a).

We measured fallen CWD volume and density at undisturbed and logged sites in Juruena, Mato Grosso, Brazil and compared these data to measurements from the Tapajos National Forest using identical methods (Keller *et al.*, 2004a). For this study, we measured the standing dead pool at both Juruena and Tapajos. For both sites, we examined the effect that reduced impact logging had on necromass pools. We include detailed error estimates for both densities and masses.

Methods

Sites

We measured density, void space, and volume of fallen and standing necromass at Juruena, Mato Grosso, Brazil (10.48° S, 58.47° W). We also measured standing

necromass at Juruena and Tapajos National Forest, Para, Brazil (3.08° S, 54.94° W). Biomass estimates were conducted in undisturbed forests (UF) at Juruena and compared with biomass estimates at Tapajos (Keller *et al.*, 2001). For the study of necromass we examined two forest types: areas that were selectively logged using RIL methods and undisturbed forest. A detailed site description for Tapajos is found in Keller *et al.* (2004a). A comprehensive description of the Juruena forest is presented in Feldpausch *et al.* (2005), although logging practices at our study sites were not identical to those described by Feldpausch *et al.* (2005).

Sample units at both sites were approximately 100 ha blocks with no historical clearing. The forest at Tapajos had suffered limited felling of *Manilkara huberi* for latex extraction about 25 years prior to our study. At Juruena, it is likely that some mahogany (*Swietenia macrophylla*) had been harvested in the last two decades. Logging took place about one year prior to our measurements. The amount of timber extracted, at Tapajos was between 20 and 30 m³ ha⁻¹, while only about 6.4 – 15.0 m³ ha⁻¹ were harvested at Juruena (Feldpausch *et al.*, 2005).

Measurements of CWD volume and subsequent mass estimates were compared between the new site, Juruena, and the Tapajos site (Keller *et al.*, 2004a). Density estimates for Tapajos were presented in Keller *et al.* (2004a) and are included in this paper for comparison with Juruena density estimates. Standing necromass results for Tapajos and Juruena are both presented for the first time in this paper.

Density and Void Space Estimation

Necromass density was determined using a plug extraction technique for large CWD (>10 cm diameter) in November 2003. This plug extraction method (Keller *et al.*, 2004a) uses a plug and tenon extractor attached to a portable power drill. Plugs were extracted every 5 cm from the center of a disk cut from a log in one of eight directions, 0°, 45°, 90°, 135°, 180°, 225°, 270°, and 315° selected randomly.

Each piece of CWD greater than 10 cm diameter (*large* CWD) was classified into one of five decay classes. These decay classes ranged from newly fallen necromass (Class 1) to highly decayed material that could be broken apart by hand (Class 5) (Harmon *et al.*, 1995; Keller *et al.*, 2004a). Decay class 1 material included newly fallen solid wood with leaves and/or fine twigs still attached. Necromass in decay class 2 was solid and had intact bark but no fine twigs or leaves. Decay class 3 necromass resembled class 2 except the bark was rotten or sloughing. Decay class 4 material was rotten and could be broken when kicked. Decay class 5 necromass was highly friable and rotten and it could be broken apart with bare hands. For pieces of CWD > 2 cm and < 10 cm, we did not assign decay classes. Sampling of these *small* (2-5 cm dia) and *medium* (5-10 cm dia) pieces was done either by plug extraction or by cutting with a knife. All necromass pieces were randomly selected along a transect with stratified probabilities to allow us to collect a sufficient sample number based on size, decay class, and treatment (RIL vs. UF).

For large fallen CWD, decay class, diameter, and other features such as large voids and the presence of termites or fungi were noted. We sketched each sample cross-section for

comparison to digital images (see below). We measured plug lengths and calculated volume for the cylindrical plugs. Plugs were stored in plastic bags and transported to the laboratory where they were dried at 60° C until reaching constant weight (up to 3 months). Plugs were then weighed and density was determined based on fresh volume and dry mass.

Void space was measured from digital images of each disk sampled for density. For each image we digitized the areas of wood and void. The smallest identified voids had diameters of ~ 5 mm. The proportion of void space was used to calculate the adjusted density for void space.

Fallen CWD Estimation

Line intercept sampling for fallen CWD volume was conducted at Juruena in November 2003 and in June 2004 (Brown, 1974; De Vries, 1986; Ringvall and Stahl, 1999). Most logged sites were sampled about six months following logging operations. CWD was separated into the same three diameter groups used in density estimation. Woody material with diameter < 2 cm was disregarded as it is normally included in litterfall studies. A tape was used to measure distance and then left on the ground to create the transect line. All wood pieces, with a diameter greater than 10 cm, intersecting the transect line, were recorded for diameter. Each transect was divided into 50 m segments. For each 50 m segment, a 10 m sub-sample was selected at random and the smaller classes (2-5 cm and 5-10 cm) were tallied. Large CWD was classified by decay class using identical criteria as those used in density estimates. A median diameter (3.5 cm for

small necromass pieces and 7.5 cm for medium necromass pieces) was used to calculate volume for the small and medium size classes. Use of median diameters for these two classes expedited estimates by allowing tallies of the numerous pieces on a line intersect transect using a go-no-go gauge (Brown, 1974).

Volume (V) ($\text{m}^3 \text{ha}^{-1}$) of CWD for an individual transect was determined using the following equation:

$$V = \frac{\pi^2 \sum (d_n)^2}{(8 * L)} \quad (1)$$

where d_n is the diameter of a piece of necromass at the line intercept and L is the length of the transect used in sampling. For each decay class, we determined the mean fallen CWD volume for each treatment that we sampled, with the contribution of each transect weighted based on its length (DeVries, 1986, p. 256; Keller *et al.*, 2004a). We sampled four forest blocks with three randomly located 1 km transects per block for a total of 12 km of line intercept sampling at Juruena.

Strip Plot Sampling (Snags)

Measurements of standing dead trees (snags) were conducted in July 2002 and June 2004 at Tapajos and Juruena, respectively. We measured standing dead trees along 10 m wide strip plots that followed the line transects for fallen CWD. We used the same five-group decay classification and the associated densities for each decay class for mass calculations. A laser ranger finder with built-in clinometer was used to measure the

heights of snags (Impulse-200LR, Laser Technology Inc., Englewood, Colorado). A tape was used to measure diameter at breast height (DBH, 1.3 m). If the snag was shorter than 1.3 m, the diameter was measured at the highest point. We estimated volume for snags by disk integration of a taper function around the vertical axis of the snag with height and diameter measurements. The taper function was

$$D_h = 1.59 * dbh * (h^{-0.091}) \quad (2)$$

where D_h is the diameter at a specific height based on the dbh (diameter at breast height = 1.3 m) and height (h) of the snag (Chambers *et al.*, 2000). Mass was calculated using the decay class density multiplied by snag-volume. Snags with buttresses were measured above the buttress whenever possible, otherwise we estimated diameter from two perpendicular positions.

The total area of strip plots sampled for standing dead was 11.1 ha for Tapajos and 12 ha for Juruena. At Tapajos, we sampled duplicate blocks of UF and RIL treatments with a transect sampling design similar to the one in Juruena (Keller *et al.*, 2004a). The areas of the strip plots were approximately evenly divided between UF and RIL treatments.

Biomass Plots

We estimated biomass at Juruena in undisturbed forests using the same strip plots used for standing necromass sampling. We sampled areas 5 meters on either side of the line intersect transects for all trees greater than 30 cm DBH. Every 50 meters along the strip,

a 10 meter section was chosen randomly for sampling trees greater than 10 cm DBH. Final biomass estimates were adjusted for area sampled. DBH was recorded for all trees sampled. We estimated biomass for each tree using the allometric relation for tropical moist forests developed by Brown (1997):

$$B = (42.69 - 12.80 * DBH + 1.242 * DBH^2) / 1000 \quad (3)$$

where B is the biomass (kg) for a given DBH (cm) for each individual tree measured in the field.

Mass Calculations and Estimation of Error

Fallen CWD mass and standing dead mass (M_i) were each determined from the product of the volume of material (V_i) and the respective density for the material class (ρ_i)

$$M_i = \rho_i \cdot V_i \quad (4).$$

Transect necromass mean estimates were weighted based on the length of each line intercept transect, as done in DeVries (1986). We calculated the standard error using weighted means from each block (Keller *et al.*, 2004a).

Statistical Analysis

Plug density and density adjusted for void space were compared by one-way analysis of variance (ANOVA) across seven classes of material (five decay classes for large material

and medium and small size classes). A Wilcoxon / Kruskal-Wallis Rank Sum test was conducted to examine void space at Juruena across the five decay classes. This non-parametric test was used because many of the necromass pieces had no void space and thus the data was not normally distributed nor could it be easily transformed. Because we performed multiple tests on density data, we conservatively selected the probability of $\alpha = 0.01$ as a threshold for significance for differences in density.

We examined plug density and adjusted density for void space using a two-way analysis of variance (ANOVA) with categories for decay/size class and site (Juruena and Tapajos). Void space was compared between sites for each decay class using a Wilcoxon / Kruskal-Wallis Rank Sum test.

CWD was sampled for density from a disk cut from a log along 8 radii (0° , 45° , 90° , 135° , 180° , 225° , 270° , and 315°) and then reduced to 5 different groups: top (0°), bottom (180°), B ($45^\circ + 315^\circ$), C ($90^\circ + 270^\circ$) and D ($135^\circ + 225^\circ$). We tested the effect of this radial position on a residual plug density with a one-way ANOVA. We defined the residual plug density as the density of a plug minus the average density of all plugs taken from the disk. A one-way ANOVA was also used to test the residual plug density based on the distance from the center of each sampled disk.

We conducted a series of two-way ANOVAs for the variables of volume and mass according to the categories of site (Juruena, Tapajos), treatment (UF, RIL), and site by treatment interaction for the pools that we measured (small, medium and large size

classes, total fallen CWD, standing dead, and total necromass). Mass and volume tests all used $\alpha = 0.05$ for indication of significant differences.

Overall density for both fallen and standing necromass for each site-treatment combination was calculated from total mass divided by total volume. Overall density was compared using two-way ANOVAs that examined site, treatment, and site by treatment interaction. We also examined the proportion of decay class 1-3 mass to total fallen mass, as well as small and medium size class mass to total fallen mass using two-way ANOVAs that examined site, treatment, and site by treatment interaction.

Orthogonal linear regression (JMP IN 5.1) was used to examine the relation between standing dead and fallen CWD for site and treatment. This regression uses an estimate of the ratio of variance of the two variables including analytical and sampling uncertainties (Tan and Iglewicz, 1999). The variance ratio is different for each sampled block. We tested the sensitivity of the orthogonal regression to variance ratio using maximum, mean, and minimum values.

Simple Model of Necromass

We used a simple compartment model for the necromass of undisturbed forests at Tapajos and Juruena. This model was parameterized using data from this study and from other research conducted at Tapajos and Juruena. The model uses estimates of biomass

and necromass pools, literature estimates for mortality (Rice *et al.*, 2004) and decay (Chambers *et al.*, 2000, 2001b), and the assumption of steady state (Table 3.4). The basic model is

$$dM/dt = -kM + F \quad (5)$$

where M is the necromass pool (Mg), F is the rate of necromass production (Mg y^{-1}), and k is the instantaneous decay rate (y^{-1}). By definition at steady state $kM = F$. The residence time (τ) for necromass at steady state is M/F .

Results

Density and Void Space

For necromass density and void space at Juruena we sampled 273 disks and removed 609 plugs. In addition, 113 small (2-5 cm dia) and 43 (5-10 cm dia) medium sized pieces of CWD were sampled for necromass density. Plug densities for large pieces of CWD at Juruena, were significantly different by decay class, with a decreasing density for increasing decay classes (ANOVA, $p < 0.001$) (Table 3.1). Void space was significantly different across decay classes with decay classes 1 and 2 having little void space and 4 and 5 having the most (Wilcoxon test, $p < 0.001$) (Table 3.1). We found no relation between the diameter of the larger CWD and density. On average small and medium size classes had densities similar to decay class 4, with densities of 0.52 g cm^{-3} for the small size class and 0.50 g cm^{-3} for the medium size class. We found no significant difference among relative densities based on the distance from the log center or among the radial directions.

Table 3.1. Comparison of density and void space by site and decay class. Tapajos DC 5 differs from Keller *et al.* (2004a) because some pieces of necromass in DC 5 were not included in this analysis. In Keller *et al.* (2004a) we sampled small highly friable pieces of CWD to examine if these differed from whole logs classified as DC 5. We excluded these small DC 5 pieces in this analysis to be consistent with our methods using at Juruena. Numbers in parenthesis are standard errors of the mean.

Site	Decay Class	Number Sampled	Plug Density (Mg m ⁻³)		Void Proportion (%)		Density Adjusted for Void (Mg m ⁻³)	
Juruena	1	31	0.72	(0.03) *	0.01	(0.00)	0.71	(0.02) *
	2	26	0.70	(0.04)	0.02	(0.01)	0.69	(0.04)
	3	24	0.66	(0.04)	0.08	(0.03)	0.60	(0.04)
	4	18	0.67	(0.07)	0.12	(0.04)	0.59	(0.06)
	5	18	0.44	(0.05)	0.20	(0.04)	0.33	(0.05)
	Small	113	0.52	(0.02) *	NA	NA	0.52	(0.02) *
	Medium	43	0.50	(0.04)	NA	NA	0.50	(0.04)
Tapajos	1	88	0.61	(0.02) *	0.02	(0.01)	0.60	(0.02) *
	2	35	0.71	(0.03)	0.02	(0.01)	0.70	(0.03)
	3	48	0.63	(0.02)	0.08	(0.02)	0.58	(0.03)
	4	52	0.58	(0.03)	0.21	(0.03)	0.45	(0.03)
	5	21	0.46	(0.05)	0.26	(0.04)	0.34	(0.05)
	Small	103	0.36	(0.01) *	NA	NA	0.36	(0.01) *
	Medium	86	0.45	(0.02)	NA	NA	0.45	(0.02)

* indicates significant difference between decay classes or size class between sites (t-test)

** indicates significant difference between decay classes or size class between sites (Wilcoxon / Kruskal-Wallis Test)

Comparison within decay classes between the two sites, Juruena and Tapajos, found that decay classes 1 had a significant difference between sites (ANOVA, $p < 0.0407$). The small size class also had a significantly different plug density (not adjusted for void space) between Tapajos and Juruena (ANOVA, $p < 0.0024$). No significant difference was found for void space within each decay class compared between sites. Adjusted density for void space was found to have a significant difference between decay class 1 (ANOVA, $p < 0.0024$) and the small size class between sites (ANOVA, $p < 0.001$).

Volume and Mass

We measured a total of 1093 snags at the two sites, 640 at Tapajos and 453 at Juruena. Standing dead volume estimates by block ranged from 9.3 m³ ha⁻¹ to 22.4 m³ ha⁻¹ and

standing dead mass ranged from 5.3 to 13.9 Mg ha⁻¹ for all blocks sampled at Juruena and Tapajos. Comparison of standing dead volume or mass yielded no significant differences for site or treatment although RIL treatments had a slightly greater standing dead mass (Table 3.2).

Table 3.2. Comparison between treatments and sites for necromass pool components. All estimates are in Mg ha⁻¹. Numbers in parenthesis are standard errors of the mean. Significant differences found by ANOVA are indicated by s – site, t – treatment, and t*s – treatment site interaction.

Site Treatment Measurement	Juruena RIL (Mg /ha)		Tapajos RIL (Mg /ha)		Juruena UF (Mg /ha)		Tapajos UF (Mg /ha)		Stats (s, t, t*s)
Standing Dead	8.8	(2.3)	12.9	(4.6)	5.3	(1.0)	7.7	(2.0)	
Total Fallen	67.0	(10.1)	72.6	(10.4)	44.9	(0.2)	50.7	(1.1)	t
Fallen Small	3.6	(1.0)	5.3	(1.4)	3.3	(0.3)	1.9	(0.4)	
Fallen Medium	5.0	(1.2)	10.0	(0.1)	3.7	(0.6)	4.0	(1.0)	s, t
Fallen Large	58.5	(7.9)	57.4	(9.0)	37.9	(0.6)	44.7	(0.4)	
Total All Necromass	75.9	(7.8)	85.5	(14.9)	50.2	(1.2)	58.4	(0.9)	t

At Juruena, we sampled a total of 2,650 pieces of necromass for volume estimation using line intercept sampling. Of these, 49% (n=1298) were in the large size class and 51% (n=1352) were in the small and medium size classes. Total fallen CWD volume estimates for Juruena were 90.6 (1.6) m³ ha⁻¹ for UF and 121.1 (19.5) m³ ha⁻¹ for RIL treatments. We found no significant difference for total fallen CWD volume for treatment, site or site x treatment interaction. Total fallen CWD mass was 44.9 (0.2) Mg ha⁻¹ for UF treatments at Juruena, and 67.0 (10.1) Mg ha⁻¹ for RIL. Total fallen CWD mass showed a significant difference by treatment, but no significant difference for site or site x treatment interaction (ANOVA, p < 0.0384) (Table 3.2). Total necromass combining fallen CWD and standing dead for UF treatments was 50.2 (1.2) Mg ha⁻¹ at Juruena and 58.4 (0.9) Mg ha⁻¹ at Tapajos (Table 3.2). We estimated total necromass at RIL treatments to be 75.9 (7.8) Mg ha⁻¹ for Juruena and 86.5 (14.9) Mg ha⁻¹ for Tapajos. Total necromass for all components showed a significant difference for treatment, but not

for site or site x treatment interaction (ANOVA, $p < 0.03854$). Fallen CWD and standing dead mass showed a clear proportional relation independent of site and treatment (Figure 3.1). The relation between fallen CWD and standing dead across sites and treatments was examined using orthogonal linear regression. Although the relation was not statistically significant, there was a high coefficient of determination ($r^2 = 0.84$, $p < 0.0862$). The orthogonal regression was not sensitive to the variance ratio when we used maximum, mean, and minimum values of variance.

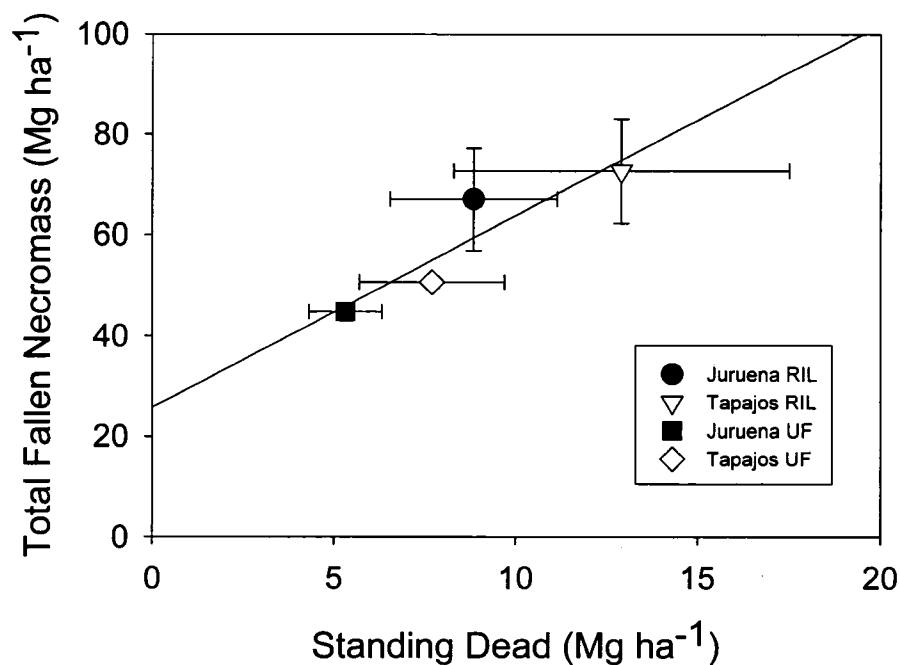


Figure 3.1. Fallen vs. standing necromass for sites and treatments. Error bars represent standard errors.

We estimated that aboveground biomass at Juruena was 281 (32) Mg ha⁻¹ for undisturbed forest for trees greater than 10 cm DBH, 263 (34) Mg ha⁻¹ for trees greater than 15 cm, and 186 (20) Mg ha⁻¹ for trees greater than 35 cm DBH. The number of trees greater than 35 cm DBH was 63 (10) ha⁻¹. Basal area for trees greater than 10 cm DBH was 25 (3)

$\text{m}^2 \text{ha}^{-1}$.

Total standing density of necromass, derived from standing dead mass divided by standing dead volume showed no significant difference between site, treatment, or site x treatment interaction. Total fallen necromass density showed a significant difference for site, treatment, and site x treatment interaction (ANOVA, $p < 0.0036$). Density for all necromass was also found to be significant for site, treatment and site x treatment interaction (ANOVA, $p < 0.0101$). The proportion of small and medium size classes to total fallen necromass was found to be only significantly different for site x treatment interaction (ANOVA, $p < 0.0263$).

Discussion

Density Sampling and Void Space Estimation

We found that plug density, void space, and density adjusted for void space decreased with higher decay classes and were significantly different between decay classes at Juruena. This finding agrees with results at Tapajos (Keller *et al.*, 2004a). In our sampling design, we randomized the radial position for extraction of plugs. Our previous study at Tapajos had shown that radial position had a significant influence on plug density (Keller *et al.*, 2004a). Interestingly, this was not the case in Juruena. We had observed in the field that wood soundness was highly variable within a fallen log. At Tapajos, there was a significant correlation between plug density and distance from the fallen log center (Keller *et al.*, 2004a), whereas we found no difference at Juruena.

The densities of necromass decay classes are quite similar for Juruena and Tapajos. Comparison across sites showed significant differences only for decay class 1. In the case of class 1, initial live tree density may be an important influence. Recent studies have discussed the importance of spatial variation in density to biomass estimates (Baker *et al.*, 2004; Nogueira *et al.*, 2005). We lack data for live biomass average density estimates for Tapajos and Juruena, but comparison with such data might aid in understanding the differences in the density of decay class 1 between our two study sites. All other decay classes show no significant difference between our two sites. Density for the small size class also differed significantly between sites. Because the small size class decays rapidly, the density of small material may vary seasonally.

Seasonal variability in decomposition is likely to be greatest for fine as opposed to coarse material because of its shorter lifetime, lower initial density, and easier decomposer access to interior portions of the wood. Variation in wood moisture content tends to be greater in small diameter size classes, likely influencing the rate of decomposition (Silva, M.S. Thesis, 2005). In the varzea forest in the Brazilian Amazon, the time that the wood falls influences its immediate and longer term decomposition (Martius, 1997). Juruena samples were collected at the beginning of the dry season. Fine litter decomposition in tropical moist forests is limited by moisture (Goulden *et al.*, 2004). We believe that the small and medium sized material collected at the beginning of the dry season had been exposed to a long period of optimal decay conditions and therefore tended to be less dense at Juruena than similar material collected at Tapajos.

The division of CWD into classes must bring some arbitrary divisions because decay is a continual process. However, as long as densities are matched with the decay classification at a given site, the classification will be useful for mass determination. The densities determined for Juruena are very similar to densities found at Tapajos. It is possible that our density estimates can be used in other areas of the Amazon with similar vegetation types although we caution that the necromass densities found in this study will not be applicable to all forest types in Amazonia. In particular, they would be inappropriate for secondary forests or forests of the western Amazon where the density of live wood is considerably less than in old growth forests of the eastern Amazon (Baker *et al.*, 2004).

Fallen and Standing Necromass

In the two undisturbed forests, the proportion of necromass to aboveground biomass (>15 cm DBH) is 26% at Tapajos and 19% at Juruena. This is similar to results from Rice *et al.* (2004), where necromass account for 25% of the aboveground estimate. We lack biomass measurements for the logged forest, but obviously the proportion of necromass would be higher, since the logging occurred less than one year prior to our field work.

Our estimates for fallen CWD created by logging in the Juruena RIL areas were greater than those reported by Feldpausch *et al.* (2005) for the same field site, although we conducted field work in areas that were logged during different years. Rohden Industria Ligna, the company that owns and manages the site, had been adopting RIL techniques

in preparation for FSC certification. Possibly, we encountered more damage because our measurements were made only at the beginning of the company's conversion from conventional to RIL practice prior to the study by Feldpausch *et al.* (2005). In addition, we note that we measured CWD and snag volume directly for entire logged blocks converting volume to biomass based on our intensive study of CWD densities.

Feldpausch *et al.* (2005) used an indirect method. They measured ground damage (decks, skids, and treefall gaps) by line intercept sampling. CWD production in treefall gaps was measured only for single tree gaps whereas we observed that multiple treefall gaps were common in the field. Necromass production in the damaged skid and deck areas was estimated based on average biomass calculated from belt transects. The total biomass loss estimate depended upon multiplication of these two factors. The approach taken by Feldpausch *et al.* (2005) necessarily compounds errors, and may have led to underestimation of total necromass production.

For fallen necromass, we found a significant difference between treatments, but no difference between sites and site x treatment interaction. There were no significant differences for standing dead mass or large fallen necromass. The total necromass component was different between treatments, but not for site or site x treatment interaction. Despite the lack of significance for standing dead, it still increases roughly in proportion with fallen necromass for all site-treatment combinations studied. While this may be a chance result, we think the lack of significance is simply an artifact of our sampling intensity. We measured five times as many pieces of fallen necromass as we did snags.

The proportion of necromass in decay classes 1, 2 and 3 is higher in RIL treatments than the undisturbed treatments, though not significantly different (Table 3.3). Immediately following logging, less decayed wood was present on the forest floor. The density of total fallen necromass and all necromass components were both significantly different for site, treatment, and site x treatment interaction. This indicates that fallen necromass decay classes are different between sites and treatments, and are likely to indicate different disturbance histories and possible difference in future decomposition rates.

Table 3.3. Comparison of site and treatments for average site densities generated from total site volume and total site mass. Proportions of necromass components are also compared. Numbers in parenthesis are standard errors of the mean. Significant differences found by ANOVA are indicated by s – site, t – treatment, and t*s – treatment site interaction.

Site Treatment	Juruena RIL		Tapajos RIL		Juruena UF		Tapajos UF		Stats (s, t, t*s)
Total Fallen Density	0.55	(0.01)	0.47	(0.01)	0.50	(0.01)	0.47	(0.00)	s, t, t*s
Standing Dead Density	0.61	(0.02)	0.56	(0.03)	0.56	(0.04)	0.57	(0.00)	s, t, t*s
Average Density All Necromass	0.56	(0.01)	0.48	(0.00)	0.50	(0.01)	0.48	(0.01)	
Proportion of Standing Dead vs. Total Fallen Necromass	0.14	(0.06)	0.17	(0.04)	0.12	(0.02)	0.15	(0.04)	
Proportion of Small and Medium Size Classes vs. Total Fallen Necromass	0.13	(0.01)	0.21	(0.01)	0.16	(0.02)	0.12	(0.03)	t*s
Proportion of DC 1-3 vs. Total Fallen Necromass	0.65	(0.16)	0.78	(0.02)	0.42	(0.03)	0.59	(0.02)	t

Reports of the mass of standing dead trees are rare in tropical forests. We found that standing dead made up 12-17% of the total necromass (Table 3.3). This estimate is similar to that found by Rice *et al.* (2004) and Clark *et al.* (2002). We did not measure attached dead wood or dead coarse roots. We are not aware of any measurements of these pools in tropical forests.

Small and medium size classes make up about 12-21% percent of total fallen necromass (Table 3.3). The portion of small and medium size classes to total fallen necromass were significantly different for site x treatment interaction and are likely related to the seasonal timing of sampling. Another study in the Amazon region estimated that smaller diameter (<10 cm) fallen necromass (<10 cm) to accounted for 12% of the total fallen necromass (Rice *et al.*, 2004). Our findings are slightly higher than other estimates in the literature and we stress the importance of including smaller necromass size classes in pool estimates.

Much small and medium sized material may not be accounted for if mortality alone is used to estimate necromass production. Many tree mortality studies only examine trees larger than 10 cm dbh, and thus do not include smaller stems that were an important component of coarse woody debris in our study. Contribution to the necromass pool by fallen branches may be an important component of necromass that is missed using mortality based estimates. Trees may lose branches through several processes that do not lead to whole tree mortality. For example, shaded lower branches may be shed and physical damage may result from crown interactions or animal activity. Chambers *et al.* (2001) considered limb-loss in a moist tropical forest outside Manaus. He estimated branch-fall to be $0.9 \text{ Mg ha}^{-1} \text{ y}^{-1}$ based upon a comparison of field measured allometries and an optimized model tree structure based on the hydraulic constraints to tree architecture.

Simple Model of Necromass

If we assume that the forest necromass pool is in steady state then we can estimate both the production and decay of necromass to evaluate its role in the forest carbon budget. The assumption of steady state for the necromass pool is reasonable for old growth forests when a large area is sampled except for the case of infrequent very large disturbances such as blow-downs (Nelson, 1994). Gap formation and other local perturbations will be averaged over a large sampling area. We used a DBH cutoff of 15 cm for live biomass to accommodate the data available at our two sites. Disregarding small trees in the live aboveground biomass pool creates a bias that tends to emphasize the role of necromass. Studies at other tropical sites suggest that trees less than 15 cm DBH and lianas contribute about 20% of the aboveground biomass (Keller *et al.*, 2001). We acknowledge this bias and attempt to capture only the general pattern of the necromass cycle for the ecosystems. Greater biomass estimates would result in greater modelled rates of necromass production and decay at steady state.

We calculated that necromass production (F) was 8.5 Mg ha⁻¹ y⁻¹ at Tapajos and 7.9 Mg ha⁻¹ y⁻¹ at Juruena (Table 3.4) using mortality rates of 0.03 (Silva *et al.*, 1995; Rice *et al.*, 2004). Although that mortality rate used is at the upper end of the range for old-growth tropical forests (Philips and Gentry, 1994), it yields results consistent with known decay rates for CWD. Decay rates (k) were estimated to be 0.14 y⁻¹ at Tapajos and 0.16 y⁻¹ at Juruena, with corresponding residence times (τ) of 6.9 y and 6.4 y (Table 3.4). If one uses an estimate of about 30 Mg C ha⁻¹ yr⁻¹ for total ecosystem respiration (Chambers *et*

al., 2004), our estimates of necromass decay are approximately 15% of the total ecosystem respiration (Chambers *et al.*, 2004). This estimate of necromass respiration is similar to those found in Chambers *et al.* (2004) and Rice *et al.* (2004).

Table 3.4. Estimation of pools and fluxes of necromass for an undisturbed forest assuming steady state. Bold numbers are estimated from the steady state model.

Site	Mortality Rate of 0.03		Mortality Rate of 0.01	
	Tapajos	Juruena	Tapajos	Juruena
Biomass*	282 ²	263 ¹	282 ²	263
Mortality (%)	0.03 ⁴	0.03 ⁴	0.01	0.01
Estimated Creation of CWD and Snags**	8.46	7.89	2.82	2.63
Standing Dead	7.7 ¹	5.3 ¹	7.7 ¹	5.3
Fallen CWD	50.7 ³	44.9 ¹	50.7 ³	44.9
Necromass Pool (fallen and snags)*	58.4 ¹	50.2 ¹	58.4 ¹	50.2
Estimated Decay Rate if at Steady State	0.14	0.16	0.05	0.05
Residence Time (y)	6.90	6.36	20.71	19.09
Estimate Creation if k = .13 and Steady State**	7.59 ⁵	6.53 ⁵	7.59 ⁵	6.53
Estimate Creation if k = .17 and Steady State**	9.93 ⁶	8.53 ⁶	9.93 ⁶	8.53

* all pool estimates in Mg ha⁻¹

** assuming decay amount equals creation amount

1 field data from this paper (>= 15cm DBH)

2 field data from Keller *et al.* (2001) (>= 15cm DBH)

3 field data from Keller *et al.* (2004)

4 field data from Rice *et al.* (2004)

5 field data from Chambers *et al.* (2000)

6 field data from Chambers *et al.* (2001)

Estimates for decay rates from our steady state model using a mortality rate of 0.01 were more common for old-growth forests in the Eastern Amazon, but were not consistent with literature values for CWD decay rates (Table 3.4). The mortality rate of 0.03 used in our simple model is at the high end of disturbances rates from the Amazon (Philips and Gentry, 1994), although it is derived from field data from Tapajos (Silva *et al.*, 1995; Rice *et al.*, 2004). A high mortality rate (0.03) partly compensates for the underestimation of biomass caused by exclusion of trees < 15 cm DBH, and the exclusion of other potential CWD inputs such as branchfall and partial tree disturbance. Estimates of decay rates using a 0.03 mortality rate are similar to field estimates by Chambers *et al.*

(2000 and 2001b) (Table 3.4).

Ideally field estimates of the necromass production would divide pools into small, medium and large size classes improving model accuracy and flux estimates. Chambers *et al.* (2000) showed that diameter influences decay rates. We lacked data for inputs or specific decay rates for individual size classes, therefore, for simplicity, we grouped small, medium and large diameter size classes into one necromass pool.

We can also examine necromass production using the necromass pool data and decay rate estimates. The estimates of CWD production and resulting residence time of necromass calculated from literature decay rates, and our necromass pool, are similar to our estimates of the model parameters when biomass and mortality rates are used in the modeling exercise (Table 3.4). This suggests that our assumptions of steady state, pool estimate, and use of mortality and decay rates are reasonable.

Disturbances that cause tree mortality and create necromass function on different temporal and spatial scales. An understanding of the mortality patterns and age structure of a forest and its variation in time and space can aid in estimation of the production of necromass. Although rainforest mortality is driven by many factors (includes large scale blowdowns), on the individual tree level mortality is influenced by competition, for nutrients and light (Prance, 1985; Martinez- Ramos *et al.*, 1998; Lieberman *et al.*, 1989). Field estimates of necromass production would provide an understanding of necromass carbon dynamics. Field measurements of necromass decay rates would also help us to

constrain carbon fluxes.

Our model does not include a separate standing dead necromass cycle and production of smaller necromass that may result from branch-fall rather than tree mortality. Standing dead material is likely to have a lower decay rate in moist tropical forest compared to large fallen CWD due to the lack of contact with the soil and periodic shortages of moisture. Contact with the soil allows fungi to transmit nutrients from the soil to the necromass promoting decomposition. Frey *et al.* (2003) found that fungal mycelia extended from the soil to CWD and translocated nutrients via the mycelia from soil to decaying wood. In addition, necromass on the forest floor is likely to have higher moisture content (Goulden *et al.*, 2004). Decay of smaller litter is rapid compared to larger CWD (Mackensen *et al.*, 2003). Small and medium size classes of necromass probably decay more quickly than larger fallen logs or snags and therefore contribute disproportionately to the carbon dioxide emission from the forest ecosystem. Smaller diameter necromass decay more quickly due to lower initial density,(Noguiera *et al.*, 2005) and easier access of decomposers to the interior wood (Mackensen *et al.*, 2003).

Conclusions

We examined necromass density, volume, and mass at two sites in the Brazilian Amazon. Necromass represents about 19-26% of the aboveground carbon for undisturbed forests at these sites. With RIL harvest management, logged forests had approximately 1.5 times as much total necromass as undisturbed forests. Density and void space estimates for decay classes were similar at the two sites, indicating that these measurements may be

usefully applied for necromass studies conducted in similar forest types in Amazonia. Proportions of standing dead and fallen small, medium, and large CWD size classes were similar across sites within treatments (RIL vs. UF). Decay class proportions were also similar across sites within treatments. RIL treatments showed a proportionate increase in both fallen and standing necromass across sites compared to UF. Small and medium size classes make up about 12-21% percent of total fallen necromass. Standing dead made up 12-17% of the total necromass. Comprehensive studies of necromass in tropical forests need to include both standing dead and smaller size class measurements (< 10 cm diameter) because collectively these contribute a large proportion of the overall necromass pool. A simple compartment model with the assumption of steady state for undisturbed forests indicates that necromass at our two study sites has a residence time of about 7 y in the forests studied. The rapid decay of this necromass suggests that the flux of carbon dioxide from necromass may account for approximately 15% of the gross CO₂ efflux from these undisturbed forests.

CHAPTER IV

NECROMASS PRODUCTION: STUDIES IN UNDISTURBED AND LOGGED AMAZON FORESTS STUDIES³

Introduction

Necromass, including fallen and standing dead wood, is a major component of the carbon cycle in tropical forests. Above-ground coarse necromass (≥ 2 cm diameter) accounts for up to 20% of carbon stored above ground and for 14-19% of the annual above-ground carbon flux in tropical forests (Kira 1976, Clark *et al.* 2002, Grove 2001, Palace *et al.* in press, Chambers *et al.* 2004, Rice *et al.* 2004). The decomposition and production of necromass in tropical forests is important in understanding carbon dynamics, yet it is infrequently studied (Kira 1976, Harmon *et al.* 1995, Keller *et al.* 2004a).

In recent studies in the Brazilian Amazon, necromass decomposition rates have been measured directly and estimated using simple models. Chambers *et al.* (2000 and 2001a) used two different measurement approaches (closed chambers using an infra-red gas analyzer and directly measured density changes to approximate mass loss) and estimated decomposition rates of necromass to be 0.13 and 0.17 y^{-1} in forest sites near Manaus.

Rice *et al.* (2004) combined measured tree mortality rates of 1.7 % per year and an

³ This chapter is based on and contains material from a manuscript that will be submitted for publication in 2006. M. Palace, M. Keller, H. Silva. Necromass Production: Studies in Undisturbed and Logged Amazon Forests. Submitted to *Ecological Applications*.

empirical decomposition model (Chambers *et al.* 2000) to estimate decomposition rates of 0.12 y^{-1} . Palace *et al.* (in press) estimated decomposition of necromass at Tapajos to be 0.14 y^{-1} , using measurements of the biomass and necromass pools and literature estimates of the mortality rate for the Tapajos site.

Few studies have examined necromass production rates in tropical forest. In some recent studies, both direct measurements of fallen debris and mortality data have been used to estimate coarse necromass production. Clark *et al.* (2002) measured production of fallen coarse necromass of $4.8 \text{ Mg ha}^{-1} \text{ yr}^{-1}$ using three repeated surveys in Costa Rica. Eaton and Lawrence (2006), using repeated surveys, found necromass production to be $0.91 \text{ Mg ha}^{-1} \text{ y}^{-1}$ in an undisturbed dry tropical forest in Mexico. Rice *et al.* (2004) estimated a coarse necromass production of 4.8 Mg ha^{-1} using mortality rates from the Tapajos National Forest near Santarem, Brazil. Chambers *et al.* (2000) estimated the production of dead wood in a forest near Manaus to be $4.2 \text{ Mg ha}^{-1} \text{ y}^{-1}$, based on observed mortality rates as well. Using a steady state model, biomass stock measurements, published mortality data, and measurements of necromass stocks, Palace *et al.* (in press) estimated coarse necromass production at the Tapajos National Forest to be $8.5 \text{ Mg ha}^{-1} \text{ y}^{-1}$.

The Amazon region is undergoing drastic changes in land use (Roberts *et al.* 2003, Keller *et al.*, 2004b). Land use change directly alters carbon cycling in terrestrial ecosystems, both in terms of storage and exchange with the atmosphere. One land use practice, selective logging, affects $15,000$ to $20,000 \text{ km}^2 \text{ y}^{-1}$ in the Brazilian Amazon (Asner *et al.* 2005; Asner *et al.* 2006), changing the storage and cycling of carbon in the coarse

necromass pools (Gerwing 2002, Keller *et al.*, 2004a, Feldpausch *et al.* 2005, Palace *et al.* in press). Selective logging actively fells a few trees per hectare, but much of the impact associated with logging results from clearing of roads, log landings, and skid trails (Pereira *et al.* 2002). These activities generate coarse necromass directly, as well as potentially altering tree mortality, and therefore coarse necromass production for at least 2 years after logging (Schulze and Zweede 2006).

Reduced Impact Logging (RIL) is an approach to selective logging that minimizes the damage to the forest as compared to conventional selective logging (CL). Methods employed include tree surveys, vine cutting, road and skid planning, wheeled skidders, and planned directional felling (Pereira *et al.* 2002). Palace *et al.* (in press) found that coarse necromass stocks were 1.5 times greater than in RIL sites one year following logging compared to undisturbed forests in Northwest Mato Grosso, Brazil. Keller *et al.* (2004a) found that CL generated 2.7 times as much fallen coarse necromass compared to RIL sites in Eastern Para, Brazil.

As part of the Large Scale Biosphere-Atmosphere Experiment in Amazonia (LBA; Keller *et al.* 2004b), studies are underway to refine estimates of forest ecosystem carbon storage and fluxes at regional and local scales (Ometto *et al.* 2005; Miller *et al.* 2004, Keller *et al.* 2004b, Rice *et al.* 2004). In LBA plot-based studies of forest stands, as in other forest studies, living biomass is separated from both standing and fallen necromass (e.g. Baker *et al.* 2004). Net carbon flux in forest stands has been expressed as the difference between the carbon increment from the growth of woody biomass minus the carbon lost

through tree mortality. By convention, both of these quantities are most frequently measured for trees greater than 10 cm diameter-at-breast-height (dbh = 1.3 m). It is recognized that carbon fluxes measured this way in stand studies and quantified on an annual basis do not account for the variable production and the relatively slow decomposition of dead wood (Chave *et al.* 2003; Rice *et al.* 2004). Comparisons that have indicated reasonable agreement between plot studies and the net ecosystem exchange measurements made using the eddy covariance technique have accounted for coarse necromass stocks and adjusted fluxes to account for coarse necromass decomposition (e.g. Saleska *et al.* 2003).

Clark *et al.* (2001b) pointed out that forest productivity measurements do not necessarily account for branch fall and other sub-lethal mortality such as crown damage or heart-rot. It is difficult to account for all sub-lethal mortality directly. For example, branches may die and remain attached to trees. Heart rot is concealed within a tree. We note that in a recent study by Nogueira *et al.* (2006), hollows accounted for only 0.6% of stem volume for a forest near Manaus, Brazil.

In the present study, we quantified the production of fallen coarse necromass in a tropical forest over 4.5 y using repeated surveys and attempted to separate the components of this flux owing to branches and stems. We also looked separately at the stocks and loss of standing dead material. We studied the dynamics of coarse necromass in both undisturbed forest (UF) and forests logged using reduced impact logging (RIL) techniques. We compared necromass production estimates calculated from mortality

rates to our field survey data.

Methods

Sites

We examined coarse necromass production and stocks at the Tapajos National Forest, located south of Santarem, Para, Brazil (3.08° S, 54.94° W). The mean annual temperature is about 25° C and the mean annual precipitation is about 2000 mm y⁻¹, with a six month-long dry season (Silver *et al.* 2000). The forest above-ground live biomass is about 282 Mg ha⁻¹ (Keller *et al.* 2001). Our study area included two forest treatment types; one area that was selectively logged using RIL methods and an undisturbed forest (UF). RIL treatments were logged in 2000. Within each forest type, we sampled two approximately 100 ha management blocks. These same areas were examined in Keller *et al.* (2004a) for coarse necromass density and our initial fallen coarse necromass volume and mass measured in 2001. The initial standing dead pool, measured in January 2002, was presented in Palace *et al.* (in press). Comprehensive descriptions of the study sites and the logging techniques are found in Keller *et al.* (2001, 2004a).

Production of Fallen Coarse Necromass

Fallen coarse necromass production in two treatments (RIL and UF) was measured using repeated line intercept transects conducted approximately every six months during 4.5 y from November 2001 through to February 2006. Because of differences among sampling intervals (105 to 257 day), reported values have been adjusted to annual rates. We repeatedly sampled the same line intercept transects (total length 11.1 km) with two blocks per treatment, each containing 3 or 4 transects. The two RIL blocks were sampled

using 2.3 km and 2.8 km of line intercept transects, and the two UF blocks were each sampled using 3 km of line intercept transects. We established the transects six months before our initial measurements conducted in November 2001 by painting and marking all initial necromass crossing the transect lines using the methods described below.

Coarse necromass volume measurements were made using line-intersect transects (Brown 1974, de Vries 1986, Ringvall and Stahl 1999). We separated coarse necromass into three diameter groups, greater than 10 cm diameter (*large*), 5-10 cm (*medium*) and 2-5 cm (*small*). Fallen coarse necromass with a diameter < 2 cm was disregarded, as it is generally included in litter-fall studies (Keller *et al.* 2004a). We recorded diameters for all large necromass pieces intersecting the vertical plane defined by the transect line (Brown 1974). We divided each transect into 50 m segments. Within each 50 m segment of the transect line, we selected at random a 10 m section and counted the number of small and medium necromass pieces intersecting this sub-sample. All large coarse necromass was painted with durable spray enamel during each survey so that the existing necromass could be separated from newly fallen necromass on subsequent surveys; small and medium necromass material was removed from the sample line because painting was impractical. In order to precisely identify the 10 m sub-sampling locations, during every repeat survey, we attached nylon mason line to two large nails pushed into the soil and marked the area with flagging tape. Occasionally between surveys, nylon lines disappeared or were cut by leaf cutter ants, peccaries, or human hunters. If a sub-sample nylon line was cut or if it could not be found, a new sub-sample was randomly selected within the 50 m section and no data on small and medium classes were collected for that

sub-sample for that time interval with an adjustment made to account of the lower number of sub-samples collected.

Each large coarse necromass pieces was classified into one of five decay classes (Harmon *et al.* 1986), ranging from newly fallen necromass with twigs and dead leaves attached (Class 1) to highly decayed material that could be broken apart by hand (Class 5) (Harmon *et al.*, 1995; Keller *et al.*, 2004a). We assigned a mean bulk density value to each class using the same decay class densities measured at Tapajos by Keller *et al.* (2004a) and used in our initial stock estimates. For the two smaller size coarse necromass classes we used a single mean bulk density measurement for each size class determined at Tapajos (Keller *et al.* 2004a). During the final five surveys (January 2003 to November 2004), we classified the sources of each piece of coarse necromass measured as either trunk, branch, or unidentifiable.

Coarse necromass was determined from the product of the volume of material and the respective density of each piece's decay class or size class for small and medium diameter pieces (Harmon *et al.*, 1995; Keller *et al.*, 2004a). When we calculated necromass volume, median diameters for small and medium size classes were used (3.5 and 7.5 cm, respectively) (Keller *et al.* 2004a). We used means weighted by transect length when calculating volume and mass measured from line intercept transects (de Vries 1986).

Coarse Necromass Pool Estimation

In 2004, three years after our initial coarse necromass pool estimates presented in Keller *et al.* (2004a), we conducted a new series of line intersect transects to estimate the fallen coarse necromass pool. These new line intersect transects were randomly selected and parallel to existing lines. We did not resample the same line transects used in the initial coarse necromass pool estimate because foot traffic and removal of coarse necromass from the repeated survey lines would have introduced biases for a resurvey of fallen coarse necromass. For the new fallen coarse necromass pool estimates we sampled a total 12 km of line intercept transects (2 treatments x 2 blocks x 3 one km transects per block). We used the same method to estimate coarse necromass volume and mass as described in our repeated sampling surveys. We classified the source of each piece of necromass in our new line intersect transects as trunk, branch or unidentifiable.

Determination of coarse necromass source was not done in our initial pool measurements (Keller *et al.* 2004a).

We also resurveyed the standing dead (snag) pool in 2004, to compare with initial pool measurements made in 2002 (Palace *et al.* in press). Standing dead volume measurement used strip plots that were 10 m wide along the length of the line intercept transects (~1000 m). The total area resampled for the standing dead necromass pool was 11.1 ha, 5.1 ha were sampled in the RIL treatment (2.3 ha and 2.8 ha in two blocks) and 6 ha were sampled in the undisturbed forest (3 ha each of in two blocks). We used the same five-group decay class classification used in fallen coarse necromass surveys. A laser ranger finder with a built-in clinometer was used to measure snag height (Impulse-200LR, Laser

Technology Inc., Englewood, Colorado). The dbh was recorded for all snags taller than 1.3 m. For snags shorter than 1.3 m, we measured the highest point of the snag and the diameter at the highest point. Volume estimates for snags used the disc method of integration, a taper function (Chambers *et al.* 2000), and height and diameter measurements (Palace *et al.* in press). Mass was calculated by multiplying by the volume of a snag by its respective decay class density (Palace *et al.* in press, Keller *et al.* 2004a).

When we conducted our initial sample of standing dead in 2002, we placed a 20 cm long steel nail attached with numbered flagging tape at the base of each snag. In 2004, we used a metal detector to locate nails and differentiate new snags and from those previously measured. The repeated sampling allowed us to determine changes in the pool of standing necromass and residence time in this pool. In order to avoid double counting, we did not use this data to calculate the decomposition and residence time for the overall fallen necromass pool, because some standing dead falls between survey periods.

Statistical Analysis

We conducted two-way analysis of variance (ANOVA) for treatment (UF and RIL), time, and treatment x time interaction for each of the pool components that we measured (small, medium and large size classes, total fallen coarse necromass, and standing dead). Comparisons were made for treatments for the production of coarse necromass over our 4.5 y study using Tukey-Kramer HSD tests. Statistical significance was considered for results using $\alpha \leq 0.05$. The total coarse necromass (fallen coarse necromass plus standing dead) was not examined with statistical tests because of different sample areas and

methods in data collection between fallen and standing necromass.

We conducted a series of Chi-square tests to examine the proportions of fallen coarse necromass that came from branches, trunks, or undefined sources. We examined production and pool necromass estimates using proportions of total mass for each source to normalize for variable mass (RIL and UF) and different methodology between pool and production measurements. Our analyses examined; (1) proportions between treatments within a source (pool or production), and (2) proportions within treatment and between sources. Results were considered statistically significant for $\alpha \leq 0.05$.

Simple Model to Examine Dynamics

A simple compartmental model of necromass dynamics was developed with three compartments, one for each of the three size classes of fallen necromass. We did not consider transfers among size classes. We also used a single-box model that combined all fallen coarse necromass size classes. The basic model is:

$$dM_i/dt = -k_i M_i + F_i \quad (1)$$

where M_i is the necromass pool (Mg) for a given size class (i) or the aggregate necromass pool, F_i is the rate of necromass production (Mg y^{-1}), and k_i is the decomposition rate (y^{-1}). By definition, at steady state dM/dt is zero, meaning that the amount of necromass produced is the same as the amount that decays. The residence time (τ_i) for necromass is M divided F .

Results

Necromass Production

We measured 668 large, 252 medium and 1168 small pieces of necromass in our repeated line intersect surveys. The mean (std. err.) fallen coarse necromass generated during the study for the RIL treatment was 8.5 (1.3) Mg ha⁻¹ y⁻¹ and was 6.7 (0.8) Mg ha⁻¹ yr⁻¹ for the UF treatment (Table 4.1). The sum of the small and medium size classes made up 30 % of the total fallen coarse necromass produced in UF treatments and 25% in RIL treatments (Table 4.1). We found no significant difference between treatments for the production of fallen coarse necromass.

Table 4.1. Production of necromass over a four and a half year period at Tapajos National Forest, Para, Brazil.

Size Class	RIL			UF		
	Mass (Mg ha ⁻¹ yr ⁻¹)	SE	Percent of Total	Mass (Mg ha ⁻¹ yr ⁻¹)	SE	Percent of Total
Large	6.4	(1.5)	75%	4.7	(0.7)	70%
Small	0.9	(0.0)	10%	0.8	(0.2)	12%
Medium	1.3	(0.3)	15%	1.2	(0.1)	18%
Total Fallen	8.5	(1.3)	100%	6.7	(0.8)	100%

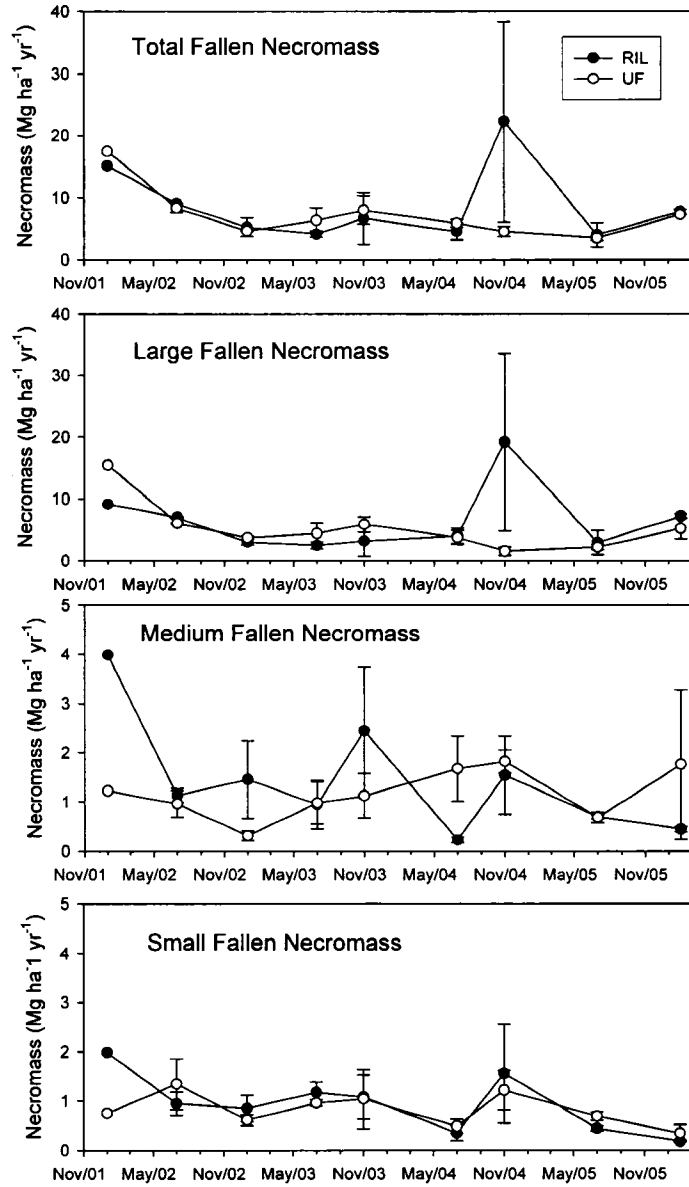


Figure 4.1. Flux of newly fallen coarse necromass shown for RIL (closed circles) and UF (open circles) treatments for nine sampling periods. The fluxes have been annualized for comparison among variable time sampling periods. Error bars are standard errors of the mean. Error bars are not included for the first time period because only one transect was measured in each treatment. Medium and small fallen necromass classes are presented on a different scale compared to large and total fallen coarse necromass.

The time series showed a larger amount of fallen coarse necromass produced at the beginning of the study followed by a nearly constant rate of production in both RIL and UF treatments (Figure 4.1). The initial production estimate only included one transect from RIL and one transect from the UF treatment. Because of this standard error could not be estimated and the mean might be inflated due to under-sampling. The maximum annualized total fallen coarse necromass produced for a single sampling period for the RIL treatment was 22.3 (16.2) Mg ha⁻¹ y⁻¹ and for the UF treatment was 8.4 (0.7) Mg ha⁻¹ y⁻¹. The high value for the RIL forest type in November 2004 sample period was due to one large newly fallen 155 cm diameter tree. Removal of this single extremely large diameter fallen necromass piece changed the RIL necromass production estimate of 22.3 (16.2) to 9.1 (3.0) Mg ha⁻¹ y⁻¹ for that sample period. RIL and UF did not always have correspondingly high and low production measurements. In addition, small and medium necromass production estimates did not follow the same pattern as large necromass production estimates (Figure 4.1). The minimum annualized coarse necromass production was 4.1 (0.5) Mg ha⁻¹ yr⁻¹ and 3.5 (0.4) Mg ha⁻¹ y⁻¹ for RIL and UF respectively.

Necromass Pool Estimates

We measured the volume of 578 snags in November 2004 compared to 640 snags measured in the same 11.1 ha in 2002 (Palace *et al.* in press). Standing dead mass in the RIL treatment was not found to be significantly different between 2002 and 2004 from our initial measurement of 12.9 (4.6) Mg ha⁻¹ and our measurement two years later at the

end of this study at 10.0 (1.9) Mg ha⁻¹ (Table 4.2). The same was true for standing dead measured in undisturbed forest, with 7.7 (2.0) Mg ha⁻¹ 2002 and 8.1 (3.2) Mg ha⁻¹ in 2004 (ANOVA, $p < 0.2918$) (Table 4.2). The logging treatment had no significant effect on the standing dead stocks when compared to the undisturbed forest.

Logging treatment had a significant effect on the mass for all components of fallen coarse necromass when compared to undisturbed forest (Table 4.2). Total fallen coarse necromass was 74.4 (14.2) Mg ha⁻¹ for RIL treatments and 40.8 (4.7) Mg ha⁻¹ for UF treatments in 2004 (Table 4.2). Mass of large fallen coarse necromass and total fallen coarse necromass showed no significant differences for time or time x treatment interaction. Small and medium size classes were found to be significantly different for time, treatment, and time x treatment interaction (ANOVA, $p < 0.001$). In our 2004 resurvey, small and medium size classes for fallen coarse necromass made up 7% of the total fallen coarse necromass in RIL treatments and 11% in UF treatments. RIL treatments had 58% more total coarse necromass (total fallen and standing dead) than UF treatments (Table 4.2). No statistical comparison was conducted on total coarse necromass because of differences in methodology and sampling area between standing dead and fallen coarse necromass pools.

Table 4.2. Coarse necromass pools at Tapajos from two sample periods (2001 and 2004). Standard errors of the mean are in parenthesis. ¹Standing dead was measured in 2002 and 2004. ²Significant differences among sampling period (p), treatment (t) and sampling period x treatment interaction (p*t) in the ANOVA model.

Treatment Measurement	RIL (2001) Mg ha ⁻¹	RIL (2004) Mg ha ⁻¹	UF (2001) Mg ha ⁻¹	UF (2001) Mg ha ⁻¹	Statistics ² (p, t, t*p)
Standing Dead ¹	12.9 (4.6)	10.0 (1.9)	7.7 (2.0)	8.1 (3.2)	
Total Fallen	72.6 (10.4)	74.4 (14.2)	50.7 (1.1)	40.8 (4.7)	t
Fallen Small	5.3 (1.4)	1.2 (0.1)	1.9 (0.4)	1.4 (0.0)	p,t,p*t
Fallen Medium	10.0 (0.1)	3.5 (0.4)	4.0 (1.0)	3.2 (0.3)	p,t,p*t
Fallen Large	57.4 (9.0)	69.7 (14.7)	44.7 (0.4)	36.3 (1.8)	t
Total All Necromass	85.5 (14.9)	84.4 (16.1)	58.4 (3.1)	49.0 (1.1)	NA

Proportion of Necromass Source

Necromass derived from tree trunks dominated the large size class in both necromass production and in pools (Table 4.3). The other size classes were more evenly distributed among sources. We found significant differences between treatments for the proportions of trunk, branch, and unidentified material within both production and pool necromass (X^2 , $p < 0.0001$). Within a treatment proportions between groups (production and pool estimates) were also found to be significantly different (X^2 , $p < 0.0001$).

Table 4.3. Source proportions of fallen coarse necromass from production and pool measurements.

Treatment	Source	Production			Pool		
		Large	Medium	Small	Large	Medium	Small
RIL	Branch	0.16	0.46	0.38	0.32	0.47	0.66
	Unidentified	0.05	0.32	0.41	0.05	0.22	0.25
	Trunk	0.79	0.22	0.20	0.63	0.31	0.09
UF	Branch	0.35	0.57	0.53	0.23	0.49	0.71
	Unidentified	0.08	0.22	0.39	0.03	0.29	0.25
	Trunk	0.57	0.21	0.08	0.74	0.22	0.04

Simple Model Outputs

We used measured necromass production (Table 4.1) together with the mean of stock estimates from 2001 and 2004 (Table 4.2) and the assumption of steady state to calculate decomposition rates for necromass using our simple compartment model (Equation 1; Table 4.4). We calculated CWD decomposition rates (k) to be 0.12 y^{-1} for the large size class, 0.33 y^{-1} for the medium size class, and 0.47 y^{-1} for the small size class; the overall decomposition rate for all fallen coarse necromass was 0.15 y^{-1} . Calculated residence times ($\tau = 1/k$) are 8.6 y, 3.0 y, and 2.1 y for the large, medium, and small size classes, respectively (Table 4.4, 4.5).

Table 4.4. Results from a simple model to estimate pools and fluxes of coarse fallen necromass in an undisturbed forest assuming steady state. Measured values are show in **bold face type**.

Site	Large	Medium	Small	Total
Production of Fallen Coarse Necromass ($\text{Mg ha}^{-1} \text{ y}^{-1}$)	4.7	1.2	0.8	6.7
Fallen Coarse Necromass Pool ($\text{Mg ha}^{-1} \text{ y}^{-1}$)	40.5	3.6	1.7	45.8
Estimated Decay Rate if at Steady State (y^{-1})	0.12	0.33	0.47	0.15
Residence Time (y)	8.6	3.0	2.1	6.8

Table 4.5. Production and mortality calculations are based on above-ground biomass of 282 Mg ha^{-1} (Keller *et al.* 2001). Measured values are show in **bold face type**.
^aSchulze and Zweede (2006), ^bSilva *et al.* (1995).

Mortality (y^{-1})	Necromass Production (Mg y^{-1})	Decomposition Rate (y^{-1})
0.015^a	4.2	0.08
0.024	6.7	0.15
0.030^b	8.5	0.16

For standing dead, in undisturbed forests, we based our model on the pool values and the measurement of new standing dead during two years of study (Table 4.6). We found that 1.9 Mg ha^{-1} of standing dead was produced each year. Considering this value, we calculated the rate of movement through the pool to be 0.24 y^{-1} with a corresponding

residence time of 4.2 y. Using the decomposition rate estimated for large fallen necromass we estimate respiration while in the standing dead pool to be $0.9 \text{ Mg ha}^{-1} \text{ y}^{-1}$. Standing dead necromass dynamics in a RIL treatment was similar to undisturbed forest standing dead (Table 4.6).

Table 4.6. Examination of standing dead and estimation of time in pool and respiration from the pool. Only one RIL treatment was used in this analysis due to missing data.

Necromass Component	UF
Standing Dead Pool (Mg ha^{-1})	7.9
Standing Dead Production ($\text{Mg ha}^{-1} \text{ y}^{-1}$)	1.9
Rate of movement through pool (y^{-1})	0.24
Time in Pool (y)	4.2
<u>Estimated Decomposition while in pool ($\text{Mg ha}^{-1} \text{ y}^{-1}$)*</u>	<u>0.9</u>

* using decay rate from large fallen coarse necromass

Discussion

Production and Decomposition of Necromass

Measurements of total fallen necromass stocks and large fallen necromass in 2001 and 2004 showed no significant difference between the two sample periods for each treatment type (Table 4.2). In contrast, there were significant differences for the small and medium categories. The RIL treatments were first examined approximately one year after logging therefore the difference in pool size between the treatments may be attributed to the effects of logging. Large fallen necromass stocks were always greater at the RIL treatment compared to the UF treatment. After the initial impact of logging, it appears that the forests functioned similarly with respect to the production and decomposition of large necromass. However, small and medium sized fallen necromass stocks decreased notably in the RIL treatments between 2001 and 2004, leading to a treatment effect and a period by treatment interaction in the ANOVA model. The rapid decomposition of small

and medium sized necromass is consistent with our residence time estimates for necromass size classes derived from our simple model (Table 4.5).

Fallen CWD production measured over a 4.5 year period indicated no significant difference between RIL logged ($8.5 (1.3) \text{ Mg ha}^{-1} \text{ y}^{-1}$) and undisturbed treatments ($6.7 (0.8) \text{ Mg ha}^{-1} \text{ y}^{-1}$). There was tendency for greater amount of necromass created at the initial stages of our study for both RIL and UF treatments. Possibly a disturbance, not specific to the logged site, may have occurred on a landscape level. It has been suggested that large-scale mortality occurred at Tapajos in the late 1990's resulting from drought during the 1997-1998 El Niño (Saleska *et al.* 2003; Rice *et al.* 2004). The elevated production of fallen coarse necromass early in our study may represent a delayed response to a landscape level disturbance. This long delay is plausible in light of the approximately 4 year residence time of standing dead. Alternatively, it is possible that the initial estimate of necromass production may be elevated simply because of under-sampling.

Other direct measurements of coarse necromass production include $0.91 \text{ Mg ha}^{-1} \text{ y}^{-1}$ in a dry tropical forest in Mexico (Eaton and Lawrence 2006), $2 \text{ Mg ha}^{-1} \text{ yr}^{-1}$ in Jamaica (Tanner 1980), $14.4 \text{ Mg ha}^{-1} \text{ yr}^{-1}$ in Pasoh Forest in Western Malaysia (Kira 1976) and 4.9 Mg ha^{-1} in Costa Rica (Clark *et al.* 2002). Eaton and Lawrence (2006) examined coarse necromass production in a dry tropical forest and found a higher amount of input during the dry season using four repeated measurements at 6 month intervals. In our 4.5 year study, with 9 repeated measurements conducted in a moist tropical forest at Tapajos,

no seasonality was found in the production of fallen coarse necromass for both RIL and undisturbed treatments for any of the size classes.

In the Tapajos forest, Rice *et al.* (2004) calculated a coarse necromass production value of $4.8 \text{ Mg ha}^{-1} \text{ y}^{-1}$ using a mortality rate of $1.7\% \text{ y}^{-1}$ for trees greater than 10 cm DBH. Vieira *et al.* (2004) estimated a steady state live wood production in the Tapajos National forest of $3.0 \text{ Mg ha}^{-1} \text{ y}^{-1}$ based on diameter increments implying that coarse necromass was also $3.0 \text{ Mg ha}^{-1} \text{ y}^{-1}$. These two estimates are 2 to $4 \text{ Mg ha}^{-1} \text{ yr}^{-1}$ lower than our measurement of coarse necromass production for undisturbed forest at Tapajos. The difference between mortality based estimates of wood or coarse necromass creation and our measurements may reflect two problems with using mortality rates to estimate necromass production. First, mortality-based estimates of necromass creation are most frequently applied to biomass of trees only above 10 cm, ignoring smaller trees, shrubs, and vines. These biomass components may be important components of overall forest productivity (Chave *et al.* 2003). Second, mortality based estimates do not include non-lethal mortality wherein only a portion of a tree dies. Clark *et al.* (2001ab) noted the potential importance of branch-fall to estimation of net primary productivity. Chave *et al.* (2003) found that branch falls and crown damage contributed about $0.5 \text{ Mg ha}^{-1} \text{ y}^{-1}$ to above ground biomass loss in a 50 ha forest plot at Barro Colorado, Panama. Chambers *et al.* (2001b) estimated that branchfall at an old-growth forest site near Manaus, Brazil was $0.9 \text{ Mg ha}^{-1} \text{ y}^{-1}$ based upon allometric arguments.

Palace *et al.* (in press) estimated necromass production to be $8.5 \text{ Mg ha}^{-1} \text{ y}^{-1}$ using a

mortality rate of 0.03 y^{-1} and measured biomass from Keller *et al.* (2001) (Table 4.5). The mortality rate used in that work was selected from the high end of available mortality measurements for tropical moist forests in order to generate agreement with published estimates of coarse necromass decomposition (Silva *et al.* 1995).

We calculated production of $4.2 \text{ Mg ha}^{-1} \text{ y}^{-1}$ for coarse necromass using a using mortality rate of $1.5\% \text{ y}^{-1}$ from Schulze and Zweede (2006) and an above-ground biomass of 282 Mg ha^{-1} from Keller *et al.* (2001) that includes non-tree components. This approach underestimates coarse necromass production by $2.5 \text{ Mg ha}^{-1} \text{ y}^{-1}$ (Table 4.5). Using this production amount and assuming steady state, the decomposition rates would be 0.08 y^{-1} , only about half the decomposition rate we found using our production and stock measurements.

If we take measurements of coarse necromass production divided by an above-ground biomass of 282 Mg ha^{-1} from Keller *et al.* (2001) (Table 4.5) then we calculate a mortality rate of $2.4\% \text{ y}^{-1}$, 0.9% higher than the mortality rate of $1.5\% \text{ y}^{-1}$ observed by Schulze and Zweede (2006) (Table 4.5). We stress that using a mortality rate to estimate necromass production may lead to a substantial underestimation. This 0.9% of unaccounted for mortality based on our measurements of coarse necromass production may result from branchfall and other non-lethal disturbances.

Although our study was more extensive spatially and temporally than any other study discussed here, the effect of a single large tree fall ($>150 \text{ cm}$ diameter) nonetheless had a

substantial effect on the necromass production measurement for the RIL treatment in November 2004. Trees of this size or greater occur with a frequency of only about 0.079 ha⁻¹ at Tapajos based on a 400 ha survey (Keller *et al.* 2001). Assuming that we adequately sampled our 100 ha blocks, we would have only 7.9 trees of this size class per 100 ha block. If these trees have a 1.7 % annual mortality rate (Rice *et al.* 2004) then our chance of seeing a fall of this size is $(1-0.983^{7.9})$ or 12.7% per year per 100 ha block. Considering that our study was conducted over a 4.5 year period, our estimate of the probability of encountering a treefall over 150 cm DBH is $(1 - 0.873^{4.5})$ or 45.7% per block. In order to have a 95% chance of measuring the death of a 150 cm diameter tree in a single year, we would need to sample an area that contained about 175 trees of this size equivalent to about 2215 ha. Our coarse necromass production estimate may represent a slight underestimate. About 0.8% of the biomass at Tapajos is found in trees > 150 cm DBH. If trees in this size class die on average with the same frequency of other trees, then their contribution (by complete mortality) to coarse necromass production would be about 2.4 Mg ha⁻¹ x 0.017 y⁻¹ equal to about 0.5% of the annual coarse necromass production that we measured.

Necromass Pools

Our two pool measurements of necromass (Table 4.2) are consistent with literature values for tropical forests. Edwards and Grubb (1977) found fallen dead wood mass of 10.9 Mg ha⁻¹ in a rainforest in New Guinea. In a tropical forest in Australia, dead wood mass was 12 Mg ha⁻¹ (Grove 2001). In the Brazilian Amazon, measurements of fallen coarse necromass in undisturbed forests in *terra firma* include 48.0 Mg C ha⁻¹ (Rice *et al.* 2004)

and 42.8 Mg C ha⁻¹ (Summers 1998) on the higher end, 27.6 Mg C ha⁻¹ (Keller *et al.* 2004a), 15 Mg C ha⁻¹ (Brown *et al.* 1995), and 16.5 Mg C ha⁻¹ (Gerwing 2002) for more central values, and 9.5 Mg ha⁻¹ (Martius and Bandeira 1998) and 5.8 Mg ha⁻¹ Scott *et al.* (1992) on the lower end. In the floodplains of the Amazon, necromass was 1.8 to 5.7 Mg C ha⁻¹ (Martius 1997). Other studies have examined coarse necromass in secondary forests and logged forests (Gerwing 2002, Uhl *et al.* 1988, Keller *et al.* 2004a, Palace *et al.* in press).

The proportion of carbon in coarse necromass to total carbon in tropical forests has a wide range, 2% to 40%, with much variability (Edwards and Grubb 1977, Brown 1997). The proportion of above ground coarse necromass to above ground biomass in tropical forests was measured recently at a range of tropical forest sites including 18% (Keller *et al.* 2004a) to 33% Rice *et al.* 2004) at the Tapajos National Forest, 33% at the wet forest at La Selva in Costa Rica (Clark *et al.* 2002), and 2-18% for an altitudinal transect in Venezuela (Delaney *et al.* 1998).

Standing dead stock was found to add an additional 11 to 30% to the total above ground coarse necromass stock in central Amazonia (Klinge *et al.* 1975, Higuchi and Biot 1995). Gerwing (2002) found standing dead to be 40% of the total coarse wood necromass stock in a disturbed forest that had been lightly logged and burned.

Measurements of standing dead stock often do not include stumps. We found that standing dead less than 1.3 m in height accounted for 1.7 to 27.2% of the standing dead

stock for our survey plots with an average of 4.9%. This high proportion for both standing dead and stumps to necromass suggests that necromass measurements in moist tropical forests should always include standing dead and preferably should also include stumps.

Necromass Sources

Our examination of the proportions of fallen necromass source (trunk, branch, and unidentified) indicated that there is a significant difference between treatments within a production estimate or a pool estimate. We also found that the source proportions of fallen necromass were significantly different between production and pool estimates within treatments. RIL may have more material created from trunks than UF because the RIL logging process includes vine cutting which may strip out senescent branches. Also, logging damages trees, which leads to subsequent mortality and greater whole tree death (Verissimo *et al.* 1992). Small and medium size class production proportionally had more branches in UF than RIL treatments. The small size class production source was made up of more trunks in RIL than UF. When we compare source proportions for production compared to pools, we do not find consistent proportions. UF treatments had more branch produced than in the pool, and RIL treatments had more trunks produced than in the pool. This could both show the influence of branchfall in an undisturbed forest and the influence of RIL methods of vine cutting and tree canopy loss due to tree felling.

We believe that branchfall from both live and standing dead trees is an important source

of necromass production. Our field observations of standing dead necromass indicated that many trunks remain upright after limbs fall to the ground. Branches also fall from live trees. While we separated branches from trunks in our study, we did not directly measure branchfall because in the field it was frequently difficult to identify whether a branch had broken off from a tree before or after a whole tree fell. Ideally, measurements of coarse necromass source and pool would determine not just the source (trunk, unidentified, and branch), but also the mechanism that produced the coarse necromass (sub-lethal disturbance or whole tree death).

Simple Model of Production and Decomposition

The stock of necromass in a forest depends upon both the production and the decomposition of dead wood. The production of coarse necromass is an episodic event and decomposition of wood is a gradual process. We found it was easier to measure necromass production compared to decomposition so we modeled necromass with a simple first-order differential equation (Equation 1) in order to estimate size-specific rates of decomposition. Stock estimates for necromass at the beginning and end of our study indicate only a small and statistically insignificant change in total necromass, therefore we believe that our steady-state assumption provides reasonable estimates, though the production data show some notable fluctuations, especially in 2004, as discussed above.

For comparison with studies at other tropical forest sites, we focus on the necromass dynamics of undisturbed old-growth forests (UF). Our finding for the overall necromass

pool decomposition rate (0.15 y^{-1}), based on the steady state assumption, are similar to those found in Chambers *et al.* (2000, 2001a) and Rice *et al.* (2004), 0.13 y^{-1} and 0.12 y^{-1} respectively. Chambers *et al.* (2000, 2001a) estimated decomposition rates for material greater than 10 cm diameter, and Rice *et al.* (2004) based their estimates on work by Chambers *et al.* (2001a). Given the much more rapid decomposition of necromass less than 10 cm diameter, the apparent agreement between our study and these others is fortuitous. A comparison of our results and those of Chambers *et al.* (2001a) suggests that coarse necromass greater than 10 cm diameter decomposes more rapidly in the forest studied at Manaus than at the Tapajos National Forest. This may be a result of the moister environment near Manaus or it could also be related to wood properties such as density.

Decomposition rates varied from 0.03 to 0.52 y^{-1} across six life zones in tropical forests in Venezuela (Delaney *et al.* 1998). In a dry tropical forest in Mexico, decomposition rates for coarse necromass varied from 0.008 to 0.615 y^{-1} (Harmon *et al.* 1995). Wilcke *et al.* (2005) estimated a decomposition rate of 0.09 y^{-1} in a montane forest in Ecuador. A dry tropical forest study by Eaton and Lawrence (2006) yielded decomposition rates for large coarse necromass ranging from 0.134 to 0.643 y^{-1} and decomposition rates from 0.368 to 0.857 y^{-1} for small and medium necromass (with a minimum diameter of 1.8 cm).

We summarize fluxes of coarse necromass in undisturbed forest in Figure 4.2. There is a fundamental difference between our measured necromass production ($a + b + c' = 6.7 \text{ Mg}$

$\text{ha}^{-1} \text{y}^{-1}$) and the estimation of necromass production based on mortality rates ($b + c$). Necromass production from sub-lethal mortality (a) was found to be $3.4 \text{ Mg ha}^{-1} \text{y}^{-1}$ using a combination of our measured production of standing dead (c) and coarse necromass production from mortality rates ($b + c$). When we compare the estimate of necromass production by a mortality estimate (0.015 y^{-1}) multiplied by the above-ground biomass (282 Mg ha^{-1}), we find the resulting value ($4.2 \text{ Mg ha}^{-1} \text{y}^{-1}$) is only 55% of the sum of our measured annual fallen necromass production ($6.7 \text{ Mg ha}^{-1} \text{y}^{-1}$) plus the decomposition of standing necromass ($0.9 \text{ Mg ha}^{-1} \text{y}^{-1}$).

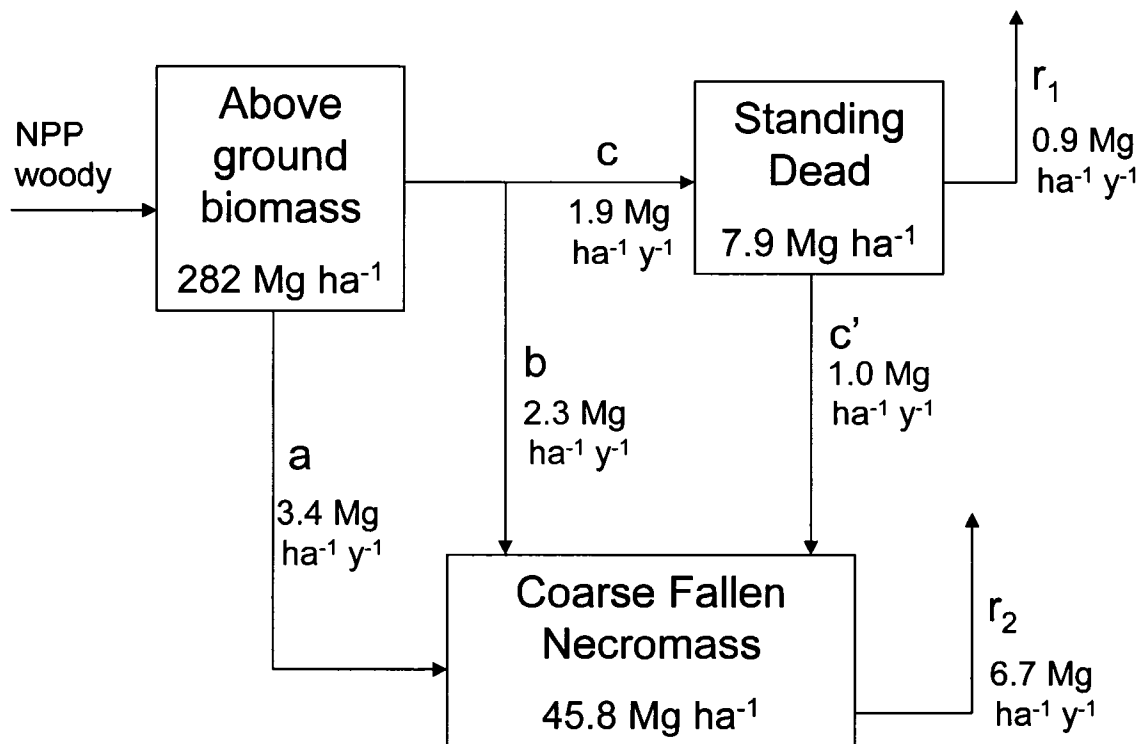


Figure 4.2. A compartmental model of measured and estimated coarse necromass components where:

- a = sub-lethal mortality;
- b = fallen mortality that is not a and c ;
- c = mortality that goes into the standing dead pool;
- c' = standing dead that falls to forest floor (assumed steady state);
- r_1 = decomposition from standing dead;
- r_2 = decomposition from fallen coarse necromass (assumed steady state);

Our measurement of coarse necromass production is close to the measurement of woody increment in living trees at Tapajos ($6.4 \text{ Mg ha}^{-1} \text{ y}^{-1}$) found by Rice *et al.* (2004). The woody increment includes growth of branches and trunks based on allometric equations. Based on carbon balance from studies near Manaus, Brazil, Malhi *et al.* (2004) estimated that above ground coarse wood production is $6.2 \text{ Mg ha}^{-1} \text{ y}^{-1}$.

Based on field measurements, the annual production of necromass pool was $8.5 (1.3) \text{ Mg ha}^{-1} \text{ y}^{-1}$ in the RIL treatment and $6.7 (0.8) \text{ Mg ha}^{-1} \text{ y}^{-1}$ in the undisturbed forest. Using the estimate from Chambers *et al.* (2001a) that approximately 80% of necromass decomposition is lost to the atmosphere, we estimate carbon dioxide flux from fallen coarse necromass to be $3.4 \text{ Mg-C ha}^{-1} \text{ y}^{-1}$ for RIL sites and $2.7 \text{ Mg-C ha}^{-1} \text{ y}^{-1}$ for UF sites. Also we get an estimate of 20% or 1.7 for RIL sites and 1.3 for UF sites leached out of necromass or contributing to soil organic matter. When we add $0.3 \text{ Mg-C ha}^{-1} \text{ y}^{-1}$ for standing dead decomposition, total necromass carbon dioxide flux to the atmosphere is equivalent to about 11 to 13% of the gross primary productivity based on a measurement of $30 \text{ Mg-C ha}^{-1} \text{ y}^{-1}$ by Miller *et al.* (2004) from the Tapajos National Forest. Coarse necromass production is 63% as large as the far more frequently measured fine litter production ($6.0 \text{ Mg-C ha}^{-1} \text{ y}^{-1}$ at Tapajos; Rice *et al.* (2004)).

Conclusions

RIL selective logging altered the stock of fallen necromass, but not the standing dead stock. Compared to the undisturbed forest, we found that RIL also had no significant influence on coarse necromass production from the time we started measurement about

one year following logging. In the undisturbed forest, necromass was equal to 14% of the total above ground biomass and accounted for about 13% of the total ecosystem respiration. Small diameter necromass (2 to 5 cm) and medium diameter (5 to 10 cm) necromass respectively decomposed 4.2 and 3.0 times more rapidly than large (> 10 cm diameter) fallen necromass. The small and medium size classes accounted for 30% of the fallen necromass created, but only 14% of the total fallen coarse woody debris pools. Standing dead necromass accounts for up to 15% of the total necromass. Based on these findings, we encourage the inclusion of standing dead and fallen necromass less than 10 cm diameter in future studies of coarse necromass in tropical forests.

We measured coarse necromass production to be 1.8 times greater than an estimate based on measured mortality rate and biomass stocks. Use of tree mortality alone to estimate coarse necromass production ignores branchfall, crown damage, and other sub-lethal processes and leads to a substantial (45% in our case) underestimate of coarse necromass production. . For carbon cycling studies, direct measurement of the production of coarse necromass is more comprehensive than the estimation of necromass production from mortality statistics.

CHAPTER V

REVIEW OF COARSE NECROMASS IN TROPICAL FORESTS

Introduction

Necromass, dead organic material, is an important component in the carbon cycle of forests accounting for 20-40% of carbon stocks and 12% of the total above ground respiration (Harmon and Sexton 1996, Brown 1997, Palace *et al.* in press). Coarse necromass or coarse woody debris (CWD) is defined as large pieces of necromass, greater than 2 cm DBH, from tree trunks, vines, and branches (Maser *et al.* 1979).

Coarse necromass is also important in nutrient cycling and provides habitat for many organisms (MacNally *et al.* 2001; Norden and Paltto 2001). With deforestation and land-use change occurring throughout the tropics, improved understanding of these dynamic and complex forests and their carbon cycles are vital for the development of regional carbon budgets (Nobre *et al.* 1991, Werth and Avissar 2002, Houghton *et al.* 2001, Davidson and Artaxo 2004). Knowledge of coarse necromass production, decay, and stocks prove useful in quantifying carbon dynamics in tropical forests.

The dynamics of necromass production and loss, through disturbance and decay, are poorly understood and quantified in tropical forests in regard to biomass estimates and leaf litter studies (Martius and Banderia 1998, Eaton and Lawrence 2006). The slow

process of decomposition is dependent upon the chemical and structural complexity of wood as well as the influence of a multitude of organisms involved with decomposition.

Decomposition rates depend upon physical climate properties that vary over time (Harmon *et al.* 1995, Chambers *et al.* 2000). The production of necromass through the death of whole trees or portions of trees is episodic, ranging greatly over temporal and spatial scales (Wessman 1992). The ranges in scale makes necromass measurement difficult, requiring large plots or long transects to catch rare large tree falls, and long periods of study to estimate both necromass production and decomposition (Harmon *et al.* 1986).

In this chapter, we review coarse necromass studies conducted in tropical forested ecosystems. We define and describe important terms and components in necromass research. In conjunction with this discussion, we examined various methodologies designed to measure these components and current literature involved with field based estimates of necromass. A simple model was developed to examine pool and decay estimates throughout these forested regions where literature estimates were unavailable. General relationships between coarse necromass components were explored such as proportion of coarse necromass to biomass and fallen to standing dead necromass.

Methods

We reviewed peer-reviewed literature that dealt with field measurements of above ground coarse necromass stocks, production of dead wood, and decomposition of coarse

necromass. We gathered sources on necromass, with a focus on tropical forests, through library searches, references cited in seminal ecological articles, peer suggestion, Web of Science©, a necromass database (compiled by Mark Harmon, OSU, personal communication), and an Yahoo© newsgroup focusing on dead wood. We excluded the abundant studies focused on fine litter dynamics or soil respiration, although these aspects of carbon cycling would be important for comprehensive review and site comparison of carbon budgets. This study did not examine remote sensing or modeling literature with regard to coarse necromass, although these two approaches may provide fruitful means for estimation and understanding of necromass production and cycling.

More than 100 papers were examined for coarse necromass stock, production and decay information and field estimated values. Data relevant to tropical forests is presented in Table 5.1 and 5.2. Data in Table 5.1 presents measured coarse necromass components and information about the site location. Table 5.2 includes site information along with measured and estimated values of production and decomposition rates. Methodology was included in our database and is presented in Table 5.3. We recorded stocks of necromass, production of dead wood, and decomposition rates when available. A few papers did not include biomass estimates so we attempted to gather biomass estimates from other papers and in some cases we were able to contact authors directly for biomass information (personal communications, Simon Grove and Michael Liddell). In each of the following three sections, coarse necromass stocks, production of coarse necromass, and decomposition of coarse necromass, we review the component, present methodologies, and review the literature pertaining to the tropical forests.

Table 5.1. Reviewed literature for tropical coarse necromass, field measurements of coarse necromass, biomass, fallen and standing pools, and production and decomposition rates.

Reference	Location	type of site	UF or DF	Forest Type	CWD (Mg ha ⁻¹)	Biomass (Mg ha ⁻¹)
Bernhard-Reversal et al., 1978	Banco, Ivory Coast	UF	UF	TRF	3.8	538.3
Bernhard-Reversal et al., 1978	Yapo, Ivory Coast	light disturbance	DF	TRF	3.6	429.4
Brown et al., 1992	Acre, Brazil	UF	UF	TMF	43.0	320.0
Brown et al., 1992	Acre, Brazil	regrowth forest	DF	TMF	13.0	95.0
Brown et al., 1995	Rondonia, Brazil	UF	UF	TMF	40.0	285.0
Buxton 1981	Tsavo National Park, Kenya	2nd-growth (fire and elephants)	DF	DTF	3.2	
Carey et al. 1994	Venezuela	UF	UF	TMF		326.0
Carey et al. 1994	Venezuela	UF	UF	LMMF		397.0
Chambers et al., 2000	Manaus, Brazil	UF	UF	LEF	21.0	
Clark et al., 2002	La Selva, Costa Rica	UF	UF	TRF	52.8	155.8
Cochrane et al. 1999	Tailandia, Para, Brazil	UF	UF	TMF	53.0	242.0
Cochrane et al. 1999	Tailandia, Para, Brazil	first burn	DF	TMF	50.0	220.0
Cochrane et al. 1999	Tailandia, Para, Brazil	second burn	DF	TMF	71.0	129.0
Cochrane et al. 1999	Tailandia, Para, Brazil	third burn	DF	TMF	116.0	47.0
Collins 1981	Southern Guinea Savanna, Nigeria	UF (savanna fires)	DF	Savanna	2.5	
Delaney et al., 1998	Venezuela	UF	UF	TTW	2.4	13.1
Delaney et al., 1998	Venezuela	UF	UF	TDF	4.8	141.2
Delaney et al., 1998	Venezuela	UF	UF	T MDF	6.6	330.0
Delaney et al., 1998	Venezuela	UF	UF	TMF	33.3	346.9
Delaney et al., 1998	Venezuela	UF	UF	TLMF	42.3	341.1
Delaney et al., 1998	Venezuela	UF	UF	TMF	34.5	325.5
Eaton and Lawrence 2006	Southern Mexico	Milpa cleared for Montana	DF	DTF	51.6	
Eaton and Lawrence 2006	Southern Mexico	2nd-growth 1-5	DF	DTF	19.9	
Eaton and Lawrence 2006	Southern Mexico	2nd-growth 6-12	DF	DTF	11.4	
Eaton and Lawrence 2006	Southern Mexico	2nd-growth 12-16	DF	DTF	15.0	
Eaton and Lawrence 2006	Southern Mexico	Montana	DF	DTF	37.5	147.0
Edwards and Grubb 1977	New Guinea	UF	UF	TMonF	10.9	490.0
Gerwing, 2002	Paragominas, Brazil	UF	UF	TMF	55.0	309.0
Gerwing, 2002	Paragominas, Brazil	moderate int. log.	DF	TMF	76.0	245.0
Gerwing, 2002	Paragominas, Brazil	high intensity log.	DF	TMF	149.0	168.0
Gerwing, 2002	Paragominas, Brazil	logged lightly burned	DF	TMF	101.0	177.0
Gerwing, 2002	Paragominas, Brazil	logged and heavily burned	DF	TMF	152.0	50.0
Golley et al. 1973, 1969	Darien, Panama	UF	UF	TMF	17.6	370.5
Golley et al. 1973, 1969	Darien, Panama	UF	UF	TMF	6.2	263.5
Golley et al. 1973, 1969	Darien, Panama	UF	UF	TMF	4.8	271.4
Golley et al. 1973, 1969	Darien, Panama	UF	UF	TMF	19.1	176.6
Golley et al. 1973, 1969	Darien, Panama	UF	UF	TMF	102.1	279.2
Golley et al. 1975	Darien, Panama	UF	UF	TMF	14.6	377.8
Golley et al. 1975	Darien, Panama	UF	UF	Riverine Forest	4.9	284.1
Greenland and Kowal 1960	Kade, Ghana	2nd-growth 50 y	DF	MTF	71.8	213.7
Greenland and Kowal 1960	Yangambi, Belgian Congo	2nd-growth 18 y	DF	MTF	17.4	128.7
Grove 2001, biomass Liddell personal	Australia	UF	UF	TRF	9.3	270.0
Grove 2001, biomass Liddell personal	Australia	Logged	DF	TRF	7.3	
Grove 2001, biomass Liddell personal	Australia	regrowth forest	DF	TRF	5.1	
Harmon et al., 1995	Quintana Roo, Mexico	moderate distur (hurricane)	DF	TDF	48.5	112.0
Harmon et al., 1995	Quintana Roo, Mexico	moderate distur (fire)	DF	TDF	128.2	112.0
Harmon et al., 1995	Quintana Roo, Mexico	UF	UF	TDF	38.0	209.0
Harmon et al., 1995	Quintana Roo, Mexico	moderate distur (hurricane)	DF	TDF	60.8	133.0
Harmon et al., 1995	Quintana Roo, Mexico	moderate distur (fire)	DF	TDF	122.5	133.0
Harmon et al., 1995	Quintana Roo, Mexico	heavy distur (hurricane)	DF	TDF	28.0	94.0
Harmon et al., 1995	Quintana Roo, Mexico	heavy distur (fire)	DF	TDF	118.6	94.0
Hughes et al. 2000	Tuxtias, Mexico	UF	UF	TEF	14.0	382.5
Kauffman et al., 1988	Rio Negro, Venezuela	UF	UF	TRF	1.6	11.4
Kauffman et al., 1988	Rio Negro, Venezuela	UF	UF	TRF	5.3	38.7
Kauffman et al., 1988	Rio Negro, Venezuela	UF	UF	TRF	42.4	20.6
Kauffman et al., 1988	Rio Negro, Venezuela	UF	UF	TRF	12.9	51.1
Kauffman et al., 1988	Rio Negro, Venezuela	disturbed	DF	TRF	48.5	47.5
Kauffman et al., 1988	Rio Negro, Venezuela	disturbed	DF	TRF	26.9	80.1
Kauffman et al., 1988	Rio Negro, Venezuela	UF	UF	TRF	14.4	238.6
Kauffman et al., 1993	Serra Talhada, Pernambuco, Brazil	2nd-growth pre-fire	DF	TDF		72.0
Kauffman et al., 1993	Serra Talhada, Pernambuco, Brazil	2nd-growth pre-post	DF	TDF		72.0
Keller et al., 2004, Asner et al. 2002	Cauaxi, Brazil	UF	UF	TMF	66.2	203.0
Keller et al., 2004, Asner et al. 2002	Cauaxi, Brazil	RIL	DF	TMF	89.6	203.0
Keller et al., 2004, Asner et al. 2002	Cauaxi, Brazil	CL	DF	TMF	129.4	203.0
Keller et al., 2004, Keller et al. 2001	Tapajos, Brazil	UF	UF	TMF	60.8	282.0
Keller et al., 2004, Keller et al. 2001	Tapajos, Brazil	RIL	DF	TMF	91.4	282.0

Table 5.1 (continued).

Reference	Fallen CWD (Mg ha-1)	Standing Dead (Mg ha-1)	Creation Amount (Mg ha-1 y-1)	k (y-1)
Bernhard-Reversat et al., 1978				
Bernhard-Reversat et al., 1978				
Brown et al., 1992				
Brown et al., 1992				
Brown et al., 1995				
Buxton 1981			0.31	0.07
Carey et al. 1994			8.80	
Carey et al. 1994			9.53	
Chambers et al., 2000			4.20	0.17
Clark et al., 2002	46.3	6.5	4.90	0.09
Cochrane et al. 1999				
Cochrane et al. 1999				
Cochrane et al. 1999				
Cochrane et al. 1999				
Collins 1981	1.4	1.1	1.27	0.51
Delaney et al., 1998	1.0	1.4		0.06
Delaney et al., 1998	1.9	2.9		0.20
Delaney et al., 1998	3.8	2.8		0.52
Delaney et al., 1998	18.5	14.8		0.03
Delaney et al., 1998	21.0	21.3		0.13
Delaney et al., 1998	8.2	26.3		0.11
Eaton and Lawrence 2006	51.6			0.38
Eaton and Lawrence 2006	19.9		0.11	0.38
Eaton and Lawrence 2006	11.4		0.11	0.38
Eaton and Lawrence 2006	15.0		0.11	0.38
Eaton and Lawrence 2006	37.5		0.91	0.38
Edwards and Grubb 1977				
Gerwing, 2002	33.0	22.0		
Gerwing, 2002	68.0	8.0		
Gerwing, 2002	140.0	9.0		
Gerwing, 2002	70.0	31.0		
Gerwing, 2002	128.0	24.0		
Golley et al. 1973, 1969				
Golley et al. 1973, 1969				
Golley et al. 1973, 1969				
Golley et al. 1973, 1969				
Golley et al. 1973, 1969				
Golley et al. 1975				
Golley et al. 1975				
Greenland and Kowal 1960				
Greenland and Kowal 1960				
Grove 2001, biomass Liddell personal				
Grove 2001, biomass Liddell personal				
Grove 2001, biomass Liddell personal				
Harmon et al., 1995	45.7	2.8		
Harmon et al., 1995	72.4	55.8		
Harmon et al., 1995	24.8	13.2		
Harmon et al., 1995	47.3	13.5		
Harmon et al., 1995	1.6	120.9		
Harmon et al., 1995	21.2	6.8		
Harmon et al., 1995	25.8	92.8		
Hughes et al. 2000	14.0			
Kauffman et al., 1988				
Kauffman et al., 1988				
Kauffman et al., 1988				
Kauffman et al., 1988				
Kauffman et al., 1988				
Kauffman et al., 1988				
Kauffman et al., 1988				
Kauffman et al., 1993	63.1			
Kauffman et al., 1993	11.9			
Keller et al., 2004, Asner et al. 2002	55.2			
Keller et al., 2004, Asner et al. 2002	74.7			
Keller et al., 2004, Asner et al. 2002	107.8			
Keller et al., 2004, Keller et al. 2001	50.7			
Keller et al., 2004, Keller et al. 2001	76.2			

Table 5.1 (continued).

Reference	Location	type of site	UF or DF	Forest Type	CWD (Mg ha ⁻¹)	Biomass (Mg ha ⁻¹)
Kira, 1978	Pasoh Forest, West Malaysia	UF	UF	TRF	50.9	421.3
Kira, 1978	Pasoh Forest, West Malaysia	UF	UF	TRF		374.2
Kira, 1978	Pasoh Forest, West Malaysia	UF	UF	TRF		379.8
Klinge 1973	Central Amazon, Brazil	UF	UF	TRF	18.0	731.7
Lang and Knight 1979	Barro Colorado, Panama	UF	UF	TRF		
Lang and Knight 1983	Panama	2nd-growth 60 y	DF	TMF		
Martius 1997	Central Amazon, Brazil	UF	UF	Varzea Forest	11.4	
Martius and Bandeira 1998	Reserva Ducke, Manaus, Brazil	UF	UF	TMF	9.5	
Nascimento and Laurence 2002	Mauaus, Brazil	UF	UF	TMF	30.95	356.2
Palace et al. in press	Juruena, Mato Grosso, Brazil	RIL	DF	TMF	67.0	263.0
Palace et al. in press	Juruena, Mato Grosso, Brazil	UF	UF	TMF	44.9	281.0
Palace et al. in press, Keller et al. 2001, 2004	Tapajos, Brazil	RIL	DF	TMF	72.6	282.0
Palace et al. in press, Keller et al. 2001, 2004	Tapajos, Brazil	UF	UF	TMF	50.7	282.0
Rice et al., 2003	Tapajos, Brazil	UF	UF	TMF	70.0	298.1
Rice et al., 2003	Tapajos, Brazil	UF	UF	TRF	99.6	298.1
Roberston and Daniel 1989	Australia	UF	UF	Young Mangrove	1.8	387.0
Roberston and Daniel 1989	Australia	UF	UF	Old Mangrove	14.3	465.0
Scott et al. 1992	Roraima, Brazil	UF	UF	LEF	5.1	
Summers, 1998	Central Amazon, Brazil		DF	TMF	88.8	
Tanner, 1980	Jamaica (a)	UF	UF	DTF	7.6	231.0
Tanner, 1980	Jamaica (b)	UF	UF	DTF	12.0	338.0
Uhl & Kauffman, 1990, Kauffman and Uhl 1990	Vitoria Ranch,Paragominas,Brazil	pasture	DF	TMF	40.0	
Uhl & Kauffman, 1990, Kauffman and Uhl 1990	Vitoria Ranch,Paragominas,Brazil	UF	UF	TMF	51.0	250.0
Uhl & Kauffman, 1990, Kauffman and Uhl 1990	Vitoria Ranch,Paragominas,Brazil	logged forest	DF	TMF	173.0	
Uhl & Kauffman, 1990, Kauffman and Uhl 1990	Vitoria Ranch,Paragominas,Brazil	2nd-growth for	DF	TMF	23.0	28.0
Uhl et al., 1988	Paragominas, Brazil	UF	UF	TMF	41.9	300.0
Uhl et al., 1988	Paragominas, Brazil	light/young	DF	TMF	78.3	29.4
Uhl et al., 1988	Paragominas, Brazil	light/old	DF	TMF	87.8	86.1
Uhl et al., 1988	Paragominas, Brazil	light/old	DF	TMF	49.9	88.9
Uhl et al., 1988	Paragominas, Brazil	moderate/young	DF	TMF	16.3	5.8
Uhl et al., 1988	Paragominas, Brazil	moderate/young	DF	TMF	21.6	8.3
Uhl et al., 1988	Paragominas, Brazil	moderate/young	DF	TMF	47.4	16.8
Uhl et al., 1988	Paragominas, Brazil	moderate/young	DF	TMF	11.2	17.0
Uhl et al., 1988	Paragominas, Brazil	moderate/old	DF	TMF	20.3	37.0
Uhl et al., 1988	Paragominas, Brazil	moderate/old	DF	TMF	20.4	32.8
Uhl et al., 1988	Paragominas, Brazil	heavy/young	DF	TMF	10.4	7.6
Uhl et al., 1988	Paragominas, Brazil	heavy/young	DF	TMF	8.6	15.5
Uhl et al., 1988	Paragominas, Brazil	heavy/old	DF	TMF	5.7	4.7
Uhl et al., 1988	Paragominas, Brazil	UF	UF	TMF	35.6	327.6
Uhl et al., 1988	Paragominas, Brazil	UF	UF	TMF	48.1	284.7
Wilcke et al. 2005	Ecuadorian Andes, Ecuador	UF	UF	TMonF	9.1	
Yoda & Kira, 1982	Malaysia		DF	TRF	46.7	

Table 5.2. Reviewed literature for tropical coarse necromass, coarse necromass to biomass ratio, field measurements of production and decomposition rates compared with estimate production and decomposition rates.

Reference	Location	type of site	UF or DF	Forest Type	Necro/Bio	Creation Measured (Mg ha ⁻¹ y ⁻¹)	k Measured (y ⁻¹)
Bernhard-Reversat et al., 1978	Banco, Ivory Coast	UF	UF	TRF	0.01		
Bernhard-Reversat et al., 1978	Yapo, Ivory Coast	light disturbance	DF	TRF	0.01		
Brown et al., 1992	Acre, Brazil	UF	UF	TMF	0.13		
Brown et al., 1992	Acre, Brazil	regrowth forest	DF	TMF	0.14		
Brown et al., 1995	Rondonia, Brazil	UF	UF	TMF	0.14		
Buxton 1981	Tsavo National Park, Kenya	2nd-growth (fire and elephants)	DF	DTF		0.31	0.07
Carey et al., 1994	Venezuela	UF	UF	TMF	0.00	8.80	
Carey et al., 1994	Venezuela	UF	UF	LMMF	0.00	9.53	
Chambers et al., 2000	Manaus, Brazil	UF	UF	LEF		4.20	0.17
Clark et al., 2002	La Selva, Costa Rica	UF	UF	TRF	0.34	4.90	0.09
Cochrane et al., 1999	Tailandia, Para, Brazil	UF	UF	TMF	0.22		
Cochrane et al., 1999	Tailandia, Para, Brazil	first burn	DF	TMF	0.23		
Cochrane et al., 1999	Tailandia, Para, Brazil	second burn	DF	TMF	0.55		
Cochrane et al., 1999	Tailandia, Para, Brazil	third burn	DF	TMF	2.47		
Collins 1981	Southern Guinea Savanna, Nigeria	UF (savanna fires)	DF	Savanna		1.27	0.51
Delaney et al., 1998	Venezuela	UF	UF	TTW	0.18		0.06
Delaney et al., 1998	Venezuela	UF	UF	TDF	0.03		0.20
Delaney et al., 1998	Venezuela	UF	UF	TMDF	0.02		0.52
Delaney et al., 1998	Venezuela	UF	UF	TMF	0.10		0.03
Delaney et al., 1998	Venezuela	UF	UF	TLMF	0.12		0.13
Delaney et al., 1998	Venezuela	UF	UF	TMF	0.11		0.11
Eaton and Laurence 2006	Southern Mexico	Milpa cleared for Montana	DF	DTF		0.11	0.38
Eaton and Laurence 2006	Southern Mexico	2nd-growth 1-5	DF	DTF		0.11	0.38
Eaton and Laurence 2006	Southern Mexico	2nd-growth 6-12	DF	DTF		0.11	0.38
Eaton and Laurence 2006	Southern Mexico	2nd-growth 12-16	DF	DTF	0.25	0.91	0.38
Laurence 2006, biomass from Read and Lawr	Southern Mexico	Montana	DF	DTF			0.38
Edwards and Grubb 1977	New Guinea	UF	UF	TMonF	0.02		
Gerwing, 2002	Paragominas, Brazil	UF	UF	TMF	0.18		
Gerwing, 2002	Paragominas, Brazil	moderate int. log.	DF	TMF	0.31		
Gerwing, 2002	Paragominas, Brazil	high intensity log.	DF	TMF	0.89		
Gerwing, 2002	Paragominas, Brazil	logged lightly burned	DF	TMF	0.57		
Gerwing, 2002	Paragominas, Brazil	logged and heavily burned	DF	TMF	3.04		
Golley et al., 1973, 1969	Darien, Panama	UF	UF	TMF	0.05		
Golley et al., 1973, 1969	Darien, Panama	UF	UF	TMF	0.02		
Golley et al., 1973, 1969	Darien, Panama	UF	UF	TMF	0.02		
Golley et al., 1973, 1969	Darien, Panama	UF	UF	TMF	0.11		
Golley et al., 1973, 1969	Darien, Panama	UF	UF	TMF	0.37		
Golley et al., 1975	Darien, Panama	UF	UF	TMF	0.04		
Golley et al., 1975	Darien, Panama	UF	UF	Riverine Forest	0.02		
Greenland and Kowal 1960	Kade, Ghana	2nd-growth 50 y	DF	MTF	0.34		
Greenland and Kowal 1960	Yangambi, Belgian Congo	2nd-growth 18 y	DF	MTF	0.14		
Grove 2001, biomass Liddell personal	Australia	UF	UF	TRF	0.03		
Grove 2001, biomass Liddell personal	Australia	Logged	DF	TRF			
Grove 2001, biomass Liddell personal	Australia	regrowth forest	DF	TRF			
Harmon et al., 1995	Quintana Roo, Mexico	moderate disturb (hurricane)	DF	TDF	0.43		
Harmon et al., 1995	Quintana Roo, Mexico	moderate disturb (fire)	DF	TDF	1.14		
Harmon et al., 1995	Quintana Roo, Mexico	UF	UF	TDF	0.18		
Harmon et al., 1995	Quintana Roo, Mexico	moderate disturb (hurricane)	DF	TDF	0.46		
Harmon et al., 1995	Quintana Roo, Mexico	moderate disturb (fire)	DF	TDF	0.92		
Harmon et al., 1995	Quintana Roo, Mexico	heavy disturb (hurricane)	DF	TDF	0.30		
Harmon et al., 1995	Quintana Roo, Mexico	heavy disturb (fire)	DF	TDF	1.26		
Hughes et al., 2000	Tuxtias, Mexico	UF	UF	TEF	0.04		
Kauffman et al., 1988	Rio Negro, Venezuela	UF	UF	TRF	0.14		
Kauffman et al., 1988	Rio Negro, Venezuela	UF	UF	TRF	0.14		
Kauffman et al., 1988	Rio Negro, Venezuela	UF	UF	TRF	2.06		
Kauffman et al., 1988	Rio Negro, Venezuela	UF	UF	TRF	0.25		
Kauffman et al., 1988	Rio Negro, Venezuela	disturbed	DF	TRF	1.02		
Kauffman et al., 1988	Rio Negro, Venezuela	disturbed	DF	TRF	0.34		
Kauffman et al., 1988	Rio Negro, Venezuela	UF	UF	TRF	0.06		
Kauffman et al., 1993	Serra Talhada, Pernambuco, Brazil	2nd-growth pre-fire	DF	TDF	0.00		
Kauffman et al., 1993	Serra Talhada, Pernambuco, Brazil	2nd-growth pre-post	DF	TDF	0.00		
Keller et al., 2004, Asner et al. 2002	Cauaxi, Brazil	UF	UF	TMF	0.33		
Keller et al., 2004, Asner et al. 2002	Cauaxi, Brazil	RIL	DF	TMF	0.44		
Keller et al., 2004, Asner et al. 2002	Cauaxi, Brazil	CL	DF	TMF	0.64		
Keller et al., 2004, Keller et al. 2001	Tapajos, Brazil	UF	UF	TMF	0.22		
Keller et al., 2004, Keller et al. 2001	Tapajos, Brazil	RIL	DF	TMF	0.32		

Table 5.2 (continued).

Reference	Creation Estimated (biomass * 0.02) (Mg ha ⁻¹ y ⁻¹)	k Estimated (biomass) (y ⁻¹)	Creation Estimated (necromass * 0.15) (Mg ha ⁻¹ y ⁻¹)
Bernhard-Reversat et al., 1978	10.77	2.83	0.57
Bernhard-Reversat et al., 1978	8.59	2.39	0.54
Brown et al., 1992	6.40	0.15	6.45
Brown et al., 1992	1.90	0.15	1.95
Brown et al., 1995	5.70	0.14	6.00
Buxton 1981			0.48
Carey et al. 1994	6.52		
Carey et al. 1994	7.94		
Chambers et al., 2000			3.15
Clark et al., 2002	3.12	0.06	7.92
Cochrane et al. 1999	4.84	0.09	7.95
Cochrane et al. 1999	4.40	0.09	7.50
Cochrane et al. 1999	2.58	0.04	10.65
Cochrane et al. 1999	0.94	0.01	17.40
Collins 1981			0.37
Delaney et al., 1998	0.26	0.11	0.36
Delaney et al., 1998	2.82	0.59	0.72
Delaney et al., 1998	6.60	1.00	0.99
Delaney et al., 1998	6.94	0.21	5.00
Delaney et al., 1998	6.82	0.16	6.35
Delaney et al., 1998	6.51	0.19	5.18
Eaton and Laurence 2006			7.74
Eaton and Laurence 2006			2.98
Eaton and Laurence 2006			1.71
Eaton and Laurence 2006	2.94	0.08	2.25
Laurence 2006, biomass from Read and Lawr			5.62
Edwards and Grubb 1977	9.80	0.90	1.64
Gerwing, 2002	6.18	0.11	8.25
Gerwing, 2002	4.90	0.06	11.40
Gerwing, 2002	3.36	0.02	22.35
Gerwing, 2002	3.54	0.04	15.15
Gerwing, 2002	1.00	0.01	22.80
Golley et al. 1973, 1969	7.41	0.42	2.64
Golley et al. 1973, 1969	5.27	0.85	0.93
Golley et al. 1973, 1969	5.43	1.13	0.72
Golley et al. 1973, 1969	3.53	0.18	2.87
Golley et al. 1973, 1969	5.58	0.05	15.32
Golley et al. 1975	7.56	0.52	2.19
Golley et al. 1975	5.68	1.16	0.74
Greenland and Kowal 1960	4.27	0.06	10.77
Greenland and Kowal 1960	2.57	0.15	2.61
Grove 2001, biomass Liddell personal	5.40	0.58	1.40
Grove 2001, biomass Liddell personal			1.09
Grove 2001, biomass Liddell personal			0.76
Harmon et al., 1995	2.24	0.05	7.28
Harmon et al., 1995	2.24	0.02	19.23
Harmon et al., 1995	4.18	0.11	5.70
Harmon et al., 1995	2.66	0.04	9.12
Harmon et al., 1995	2.66	0.02	18.38
Harmon et al., 1995	1.88	0.07	4.20
Harmon et al., 1995	1.88	0.02	17.79
Hughes et al. 2000	7.65	0.55	2.10
Kauffman et al., 1988	0.23	0.14	0.24
Kauffman et al., 1988	0.77	0.15	0.80
Kauffman et al., 1988	0.41	0.01	6.36
Kauffman et al., 1988	1.02	0.08	1.94
Kauffman et al., 1988	0.95	0.02	7.28
Kauffman et al., 1988	1.60	0.06	4.04
Kauffman et al., 1988	4.77	0.33	2.16
Kauffman et al., 1993	1.44		
Kauffman et al., 1993	1.44		
Keller et al., 2004, Asner et al. 2002	4.06	0.06	9.94
Keller et al., 2004, Asner et al. 2002	4.06	0.05	13.45
Keller et al., 2004, Asner et al. 2002	4.06	0.03	19.40
Keller et al., 2004, Keller et al. 2001	5.64	0.09	9.13
Keller et al., 2004, Keller et al. 2001	5.64	0.06	13.72

Table 5.2 (continued).

Reference	Location	type of site	UF or DF	Forest Type	Necro/Bio	reaction Measure (Mg ha ⁻¹ y ⁻¹)	Measured (y ⁻¹)
Kira, 1978	Pasoh Forest, West Malaysia	UF	UF	TRF	0.12	3.30	0.30
Kira, 1978	Pasoh Forest, West Malaysia	UF	UF	TRF	0.00		
Kira, 1978	Pasoh Forest, West Malaysia	UF	UF	TRF	0.00		
Klinge 1973	Central Amazon, Brazil	UF	UF	TRF	0.02		
Lang and Knight 1979	Barro Colorado, Panama	UF	UF	TRF			0.46
Lang and Knight 1983	Panama	2nd-growth 60 y	DF	TMF			
Martius 1997	Central Amazon, Brazil	UF	UF	Varzea Forest		6.00	0.33
Martius and Bandeira 1998	Reserva Ducke, Manaus, Brazil	UF	UF	TMF			
Nascimento and Laurence 2002	Mauaus, Brazil	UF	UF	TMF	0.09		
Palace et al. in review	Juruena, Mato Grosso, Brazil	RIL	DF	TMF	0.29		
Palace et al. in review	Juruena, Mato Grosso, Brazil	UF	UF	TMF	0.18		
Palace et al. in review, Keller et al. 2001, 2004	Tapajos, Brazil	RIL	DF	TMF	0.30		
Palace et al. in review, Keller et al. 2001, 2004	Tapajos, Brazil	UF	UF	TMF	0.21		
Rice et al., 2004	Tapajos, Brazil	UF	UF	TMF	0.23	5.00	0.17
Rice et al., 2004	Tapajos, Brazil	UF	UF	TRF	0.33	5.00	0.12
Roberston and Daniel 1989	Australia	UF	UF	Young Mangrove	0.00	0.10	0.06
Roberston and Daniel 1989	Australia	UF	UF	Old Mangrove	0.03	0.97	2.00
Scott et al. 1992	Roraima, Brazil	UF	UF	LEF			
Summers, 1998	Central Amazon, Brazil		DF	TMF			
Tanner, 1980	Jamaica (a)	UF	UF	DTF	0.03	2.00	0.26
Tanner, 1980	Jamaica (b)	UF	UF	DTF	0.04	2.00	0.17
Uhl & Kauffman, 1990, Kauffman and Uhl 1990	Vitoria Ranch,Paragominas,Brazil	pasture	DF	TMF			
Uhl & Kauffman, 1990, Kauffman and Uhl 1990	Vitoria Ranch,Paragominas,Brazil	UF	UF	TMF	0.20		
Uhl & Kauffman, 1990, Kauffman and Uhl 1990	Vitoria Ranch,Paragominas,Brazil	logged forest	DF	TMF			
Uhl & Kauffman, 1990, Kauffman and Uhl 1990	Vitoria Ranch,Paragominas,Brazil	2nd-growth for	DF	TMF	0.82		
Uhl et al., 1988	Paragominas, Brazil	UF	UF	TMF	0.14		
Uhl et al., 1988	Paragominas, Brazil	light/young	DF	TMF	2.66		
Uhl et al., 1988	Paragominas, Brazil	light/old	DF	TMF	1.02		
Uhl et al., 1988	Paragominas, Brazil	light/old	DF	TMF	0.56		
Uhl et al., 1988	Paragominas, Brazil	moderate/young	DF	TMF	2.81		
Uhl et al., 1988	Paragominas, Brazil	moderate/young	DF	TMF	2.60		
Uhl et al., 1988	Paragominas, Brazil	moderate/young	DF	TMF	2.82		
Uhl et al., 1988	Paragominas, Brazil	moderate/young	DF	TMF	0.66		
Uhl et al., 1988	Paragominas, Brazil	moderate/old	DF	TMF	0.55		
Uhl et al., 1988	Paragominas, Brazil	moderate/old	DF	TMF	0.62		
Uhl et al., 1988	Paragominas, Brazil	heavy/young	DF	TMF	1.37		
Uhl et al., 1988	Paragominas, Brazil	heavy/young	DF	TMF	0.55		
Uhl et al., 1988	Paragominas, Brazil	heavy/old	DF	TMF	1.21		
Uhl et al., 1988	Paragominas, Brazil	UF	UF	TMF	0.11		
Uhl et al., 1988	Paragominas, Brazil	UF	UF	TMF	0.17		
Wilcke et al. 2005	Ecuadorian Andes, Ecuador	UF	UF	TMonF		0.82	0.09
Yoda & Kira, 1982	Malaysia		DF	TRF			

Table 5.2 (continued).

Reference	(biomass * 0.02) (Mg ha ⁻¹ y ⁻¹)	Estimated (biomass) (y ⁻¹)	(necromass * 0.15) (Mg ha ⁻¹ y ⁻¹)
Kira, 1978	8.43	0.17	7.64
Kira, 1978	7.48		
Kira, 1978	7.60		
Klinge 1973	14.63	0.81	2.70
Lang and Knight 1979			
Lang and Knight 1983			
Martius 1997			1.71
Martius and Bandeira 1998			1.43
Nascimento and Laurence 2002	7.124	0.230177706	4.64
Palace et al. in review	5.26	0.07	10.05
Palace et al. in review	5.62	0.11	6.74
Palace et al. in review, Keller et al. 2001, 2004	5.64	0.07	10.89
Palace et al. in review, Keller et al. 2001, 2004	5.64	0.10	7.61
Rice et al., 2004	5.96	0.09	10.50
Rice et al., 2004	5.96	0.06	14.94
Roberston and Daniel 1989	7.74	4.27	0.27
Roberston and Daniel 1989	9.30	0.65	2.14
Scott et al. 1992			0.76
Summers, 1998			13.32
Tanner, 1980	4.62	0.61	1.14
Tanner, 1980	6.76	0.56	1.80
Uhl & Kauffman, 1990, Kauffman and Uhl 1990			6.00
Uhl & Kauffman, 1990, Kauffman and Uhl 1990	5.00	0.10	7.65
Uhl & Kauffman, 1990, Kauffman and Uhl 1990			25.95
Uhl & Kauffman, 1990, Kauffman and Uhl 1990	0.56	0.02	3.45
Uhl et al., 1988	6.00	0.14	6.28
Uhl et al., 1988	0.59	0.01	11.75
Uhl et al., 1988	1.72	0.02	13.17
Uhl et al., 1988	1.78	0.04	7.49
Uhl et al., 1988	0.12	0.01	2.45
Uhl et al., 1988	0.17	0.01	3.24
Uhl et al., 1988	0.34	0.01	7.11
Uhl et al., 1988	0.34	0.03	1.68
Uhl et al., 1988	0.74	0.04	3.05
Uhl et al., 1988	0.66	0.03	3.06
Uhl et al., 1988	0.15	0.01	1.56
Uhl et al., 1988	0.31	0.04	1.29
Uhl et al., 1988	0.09	0.02	0.86
Uhl et al., 1988	6.55	0.18	5.34
Uhl et al., 1988	5.69	0.12	7.22
Wilcke et al. 2005			1.37
Yoda & Kira, 1982			7.01

Table 5.3. Literature reviewed with methods presented.

Reference	Method	Coarse Woody Debris Size Classes	Standing Dead Size Cutoff	Density or decay class density
Brown et al. 1995	LIS	≥ 10 cm	≥ 10 cm	Yes
Buxton 1981	Plot	measured all		Weighed Dead Wood
Chambers et al. 2000	Plot	10-20 cm, 20 - 50 cm, > 50 cm		Yes
Clark et al., 2002	Plot	≥10 cm	≥ 10 cm	Yes
Collins 1981	Plot	≤ 2 cm, ≥ 2 cm	≥ 5 cm	Weighed Dead Wood
Delaney et al. 1998	LIS	2.5 - 4.99 cm, 5 - 9.99 cm, 10 - 29.9 cm, 30 - 49.9 cm, ≥ 50 cm	≥ 10 cm	Yes
Eaton and Lawrence 2006	Plot	1.8 - 10 cm, ≥ 10 cm		Yes
Edwards and Grubb 1977	Plot	measured all	measured all	Weighed Dead Wood
Gerwing 2002	LIS	≥ 10 cm		Yes
Golley et al. 1975	Plot	measured all		Weighed Dead Wood
Greenland and Kowal 1960	Plot	measured all	measured all	Weighed Dead Wood
Grove 2001	Plot LIS	≥ 7.5	≥ 7.5	Yes
Harmon et al. 1995	Plot	≤ 10cm, ≥ 10cm		Yes
Hughes et al. 2000	LIS	2.45 - 7.6 cm, ≥ 7.6 cm	≥ 10 cm	Yes
Kauffman et al. 1993	LIS	0.6-2.5 cm, 2.5-7.6 cm, ≥ 7.6 cm		No
Keller et al. 2004	LIS	2 - 4.99 cm, 5 - 9.99 cm, ≥ 10 cm		Yes
Kira 1978	Plot	≥10 cm		Yes
Martius 1997, Martius 1980	Plot	≥10 cm		No
Martius and Bandeira 1998	Plot	1 -3 cm, ≥ 3 cm		Yes
Nascimento and Laurence 2002	Plot LIS	2.5-9.9, gt 10		Yes
Palace et al. in press	Plot LIS	2 - 4.99 cm, 5 - 9.99 cm, ≥ 10 cm	≥ 10 cm	Yes
Rice et al. 2004	Plot LIS	2 - 10 cm, 10 - 30 cm, ≥ 30 cm	≥ 10 cm	Yes
Roberston and Daniel 1989	Plot	measured all	measured all	Yes
Scott et al. 1992	Plot	2 - 4.99 cm, 5 - 9.99 cm, ≥ 10 cm, palm fragments	≥ 5 cm	Yes
Uhl & Kauffman, 1990, Kauffman and Uhl 1990	LIS	≤ 0.64 cm, 0.65 - 2.54 cm, 2.55 - 7.6 cm, ≥ 7.6cm		
Uhl et al. 1988	Plot	≥10 cm		
Wilcke et al. 2005	Plot	≥10 cm, length limits		Yes

Coarse Necromass Stocks

Necromass stocks aboveground include fine litter and coarse necromass where coarse necromass has generally been defined as necromass with a diameter greater than 2 cm (Harmon *et al.* 1986). Coarse necromass is often divided into two categories: (1) fallen or downed necromass and (2) standing dead wood (snags) (Harmon *et al.*, 1986). Similar stocks for coarse and fine material are found below ground. Below ground necromass is not treated in this review. The diameter of coarse necromass and the degree of decomposition (decay class) have been used to further refine coarse necromass categories (Harmon *et al.* 1986).

Measurement of fallen coarse necromass is done primarily by one of two methods, line intercept or plot sampling (Harmon *et al.* 1986). Another method, relascope sampling (Gove *et al.* 2002) has not been used in tropical field studies and is not discussed here. Line intercept sampling (also termed planar intercept sampling) uses a straight line where all pieces of coarse necromass that intersect a two dimensional plane defined by the line and perpendicular to the earth's gravity. Volume (V) (m³ ha⁻¹) of CWD for an individual transect is calculated using the following equation:

$$V = \frac{\pi^2 \sum (d_n)^2}{(8 * L)}$$

where d_n is the diameter of a piece of necromass at the line intercept and L is the length of the transect used in sampling (De Vries, 1986).

In plot based sampling a fixed area is identified and all pieces of CWD are measured in that area. Plot measurements of coarse necromass often require more work, but retain spatial information that can be compared with other biometric or other environmental variables. Plot estimates of fallen and standing dead coarse necromass use a variety of methods to estimate volume. These include the assumption that a piece of necromass is a cylinder or frustum, or using multiple measurements along the length of the log to calculate volume. Taper functions have also been used to calculate the volume of fallen and standing dead (Rice *et al.* 2004; Palace *et al.* in press).

Some studies divide fallen coarse necromass has been divided into diameter size classes. Depending on the sampling methodology, diameter can have different meanings. In line intercept sampling, the fallen necromass diameter is only measured at the point in which the two-dimensional plane is intersected by the piece of necromass (Brown 1974). If the necromass curves back across the plan it is measured again (De Vries 1986). For plot level sampling, diameter often refers to the average diameter of the entire log, along which multiple diameters have been measured (Harmon *et al.* 1986). In order to save time and effort, small diameter fallen coarse necromass is often grouped into a range of diameters, tallied, and a median diameter is used in calculations (Brown 1974, Keller *et al.* 2004a). Many studies have used a diameter of 2 cm as a low-end cutoff for sampling, although there are a few exceptions (Table 5.4).

Plot and line intercept sampling provide measurements of volume, except when all pieces

of necromass are weighed in a plot. Five studies in our review, all published prior to 1980, weighed all pieces of necromass (Table 5.1). In order to quantify coarse necromass from volume estimates, measurements of the densities of necromass pieces are required. More highly decayed logs theoretically should have less mass (Harmon *et al.* 1995). A common approach to quantification of coarse necromass is the stratification of necromass into decay classes and the application of decay-class-wide densities to the volume quantified by decay class. Other approaches to the estimation of necromass density include application of average density of live trees (Gerwig 2002, Nascimento and Laurence 2002), application of guesses (Gerwing 2002), and use of values from other sites (Rice *et al.* 2004). One study did not mention how mass was derived from volume estimates (Uhl and Kauffman 1990). Another used measured values for classes of coarse necromass, such as trunks, prop roots, branches, and twigs (Roberston and Daniel 1989)

Decay classes are easily determined by the data collector and allow for a stratification of coarse necromass sampling. Densities are measured for a sample of all coarse necromass by decay class. Measurement approaches for density include weighing entire pieces of coarse necromass, disks cut out of a log, and smaller plugs or samples across a cut disk (Harmon *et al.* 1986, Chambers *et al.* 2001, Keller *et al.* 2004a). In all cases, samples must be dried to a constant weight for disk and plug sampling. Large void spaces, created by organisms like termites or beetles, are often not considered in necromass density estimates. Larger samples used in density estimate include these void spaces, but smaller samples need to account for this. Keller *et al.* (2004a) used digitized images of disks cut through large pieces of fallen coarse necromass in order to measure void spaces

and adjust density estimates accordingly.

Decay classes usually consist of two or more categories (Harmon *et al.* 1986, Chambers *et al.* 2000), ranging from newly fallen coarse necromass to highly decayed material that can be broken apart by hand (Harmon *et al.*, 1995; Keller *et al.*, 2004a). A description of each of five decay classes is found in Table 5.4.

Table 5.4. Description of five decay classes used in numerous coarse necromass studies.

Decay Class	Description
1	newly fallen solid wood with leaves and/or fine twigs still attached
2	solid and has intact bark but no fine twigs or leaves
3	necromass resembles class 2 except the bark is rotten or sloughing
4	material is rotten and can be broken when kicked
5	highly friable and rotten and it can be broken apart with bare hands

Decay class estimates of density were used in 20 studies, 5 studies weighed all material, and 10 did not use decay class density estimates, but density site averages or were unclear as to their methodology. We compiled eleven studies and reported their decay class density estimates in detail (Table 5.5). Decay classes and density measurements for such decay classes were similar across many studies (Table 5.5). Harmon *et al.* (1995), Eaton and Lawrence (2006), Keller *et al.* (2004a), and Palace *et al.* (in press), all used five decay classes in their studies. Although Palace *et al.* (in press) and Keller *et al.* (2004a) conducted field work in the same biome, moist tropical forest, Eaton and Lawrence (2006) worked in a dry tropical forest. These studies had consistent decay class density estimates between biomes suggesting that the apparently arbitrary classification is robust. Clearly, site specific density measurements will be the most accurate approach, however, we have suggested based on studies at two sites in the Amazon, that coarse necromass

density measurements may be applied across broad areas provided that the decay classes are defined uniformly across sites (Palace *et al.* in press). This remains to be tested.

Standing dead trees or snags include whole dead trees and portions of dead trees that remain upright (Harmon *et al.* 1986). In tropical forests, standing dead was measured 47% less frequently than fallen coarse necromass. Many studies use a percentage of total fallen coarse necromass to estimate standing dead necromass (Keller *et al.* 2004a). The size of standing dead included in tallies differs between studies. Palace *et al.* (in press) and others have used a cutoff of 10 cm dbh, while others have measured standing dead down to 2 cm dbh (Edwards and Grubb 1997).

The methodology of height measurement also varies among studies. Visual estimates or average heights (Rice *et al.* 2004) are used when standing dead heights are not measured. For more precise studies, measuring tapes and clinometers or laser range finders have been used (Palace *et al.* in press). Only Palace *et al.* (in press) included in their methodology specific mention of stumps or standing dead less than 1.3 m in height in estimates of standing dead.

Table 5.5. Comparison of coarse necromass density based on decay groups or classes for different studies in tropical forests

Location and Reference	Forest Type	Group	Decay Groups or Classes						
			Heavy Wood	Light Wood					
Manaus, Brazil			0.85	0.45					
Chambers et al., 2000	LEF		0.85	0.45					
La Selva, Costa Rica			Sound	Partial Decomp.	Full Decomp				
Clark et al., 2002	TRF		0.45	0.35	0.25				
Venezuela			Sound	Intermed.	Rotten	small 2.5-4.99	med 5-9.99		
Delaney et al., 1998	TTW		NW	0.69	NW	0.29	NW		
Delaney et al., 1998	TDF		NW	0.59	0.40	0.29	0.70		
Delaney et al., 1998	T MDF		0.42	0.37	0.25	0.24	0.22		
Delaney et al., 1998	TMF		0.58	0.59	0.50	0.29	0.29		
Delaney et al., 1998	TLMF		0.52	0.39	0.31	0.20	0.12		
Delaney et al., 1998	TMF		NW	0.48	0.32	0.19	0.13		
Southern Mexico			DC1	DC2	DC3	DC4	DC5		
Eaton and Laurence 2006	DTF		None	0.74	0.78	0.62	0.36		
Australia			DC1	DC2	DC3	DC4	None		
Grove 2001	TRF	Yellow fibrous	0.29	0.23	0.18	0.11	None		
Grove 2001	TRF	Hard	0.35	0.36	0.38	0.35	None		
Grove 2001	TRF	Brown crumbly	0.29	0.23	0.20	0.16	None		
Grove 2001	TRF	Brown fibrous	0.29	0.23	0.20	0.23	None		
Grove 2001	TRF	Red Block	None	0.23	0.19	0.17	None		
Quintana Roo, Mexico			By Species	DC2	DC3	DC4	DC5		
Hammon et al., 1995	TDF	Used Range	0.25 - 0.81	0.19 - 0.84	0.06 - 0.81	0.49 - 0.64	0.22		
Australia			Mod. Decayed	Very Decayed	Extremely Decayed				
Roberston and Daniel 1989	Mangrove	Trunk	0.34	0.34	0.23				
Roberston and Daniel 1989		Prop Roots	0.51	0.28	0.39				
Roberston and Daniel 1989		Branches	0.60	0.43	0.28				
Roberston and Daniel 1989		Twigs	0.63	0.41	0.35				
Reserva Ducke, Manaus, Brazil			Fine Wood	Coarse Wood					
Martius and Bandeira 1998	TMF	Fresh to Dry Mass	0.55	0.46					
Ecuadorian Andes, Ecuador			Intact	Rotten	Full Decomp.	Bark			
Wilcke et al. 2005	T MonF		0.38	0.22	0.25	0.37			
Tapajos, Brazil			DC1	DC2	DC3	DC4	DC5	Small 2-5 cm	Med. 5-10
Keller et al., 2004	TMF	Plug Density	0.61	0.71	0.63	0.58	0.46	0.36	0.45
Keller et al., 2004	TMF	Void Density	0.02	0.02	0.08	0.21	0.26	NA	NA
Keller et al., 2004	TMF	Density Adjusted for Void	0.60	0.70	0.58	0.45	0.34	0.36	0.45
Juruaena, Brazil			DC1	DC2	DC3	DC4	DC5	Small 2-5 cm	Med. 5-10
Palace et al. in press	TMF	Plug Density	0.72	0.70	0.66	0.67	0.44	0.52	0.50
Palace et al. in press	TMF	Void Density	0.01	0.02	0.08	0.12	0.20	NA	NA
Palace et al. in press	TMF	Density Adjusted for Void	0.71	0.69	0.60	0.59	0.33	0.52	0.50

Out of a total of 39 papers that examined coarse necromass in tropical forests, 35 reported stock measurements. All but five of the 35 papers used a volume sampling method, either plots (19 studies) or line intercepts (7 studies) or both methods (4 studies). Fallen coarse necromass was measured using line intercept sampling and standing dead was measured using plots in a few studies (Nascimento and Laurence 2002, Palace *et al.* 2004). One study used plots except for one area in which dense understory prohibited movement and line intercept sampling was used (Grove 2001). Reported values of coarse necromass stock were evenly distributed between disturbed and undisturbed sites. Standing dead and fallen coarse necromass were both measured at 29 sites in only 10 articles, with the ratio of standing dead to total coarse necromass ranging from 6% in a disturbed forest and 98% at a heavily disturbed site (Gerwing 2002, Harmon *et al.*, 1995). In undisturbed forests, standing dead to total coarse necromass stock measurements ranged from 11% to 76% (Palace *et al.* in press, Delaney *et al.*, 1998). We do not present averages of coarse necromass stock or other components because this would be misleading; the literature examined do not represent a valid statistical sample of the necromass or forest types found in the tropics.

Size class criteria differed slightly among studies (Table 5.3). Of the 39 studies that reported stock estimates, only 28 explained their size class methodology. A cutoff of less than 2 cm was used in 5 of 28 studies that reported size class methodology. Five studies used a cutoff of 2.5 cm. Many (18 %) used a cutoff greater than 10 cm. Five studies used a 10 cm cutoff to define the difference between small and large diameter coarse necromass. Half of all studies used a cutoff of 10 cm for standing dead measurement.

We suggest standardization, with the use of three size classes, small diameter (2-5 cm), medium diameter (5-10 cm), and large diameter (greater than 10 cm) for fallen coarse necromass. For standing dead measurements, we suggest the use of a standardized cutoff of greater than 10 cm at diameter at breast height.

The stock of coarse necromass makes up a large percentage of the carbon pool in a forest, including tropical forests. Coarse necromass was found to range from 1.6 to 173 Mg ha⁻¹ (Table 5.1). In dry tropical forests, coarse necromass amounts tended to be lower than moist tropical forests, with dry forests ranging from 2.5 (Collins 1981) to 118.6 Mg ha⁻¹ (Harmon *et al.*, 1995) in a heavy logged area. In moist tropical forests coarse necromass ranged from 2.4 (Delaney *et al.*, 1998) to 213.7 Mg ha⁻¹ (Greenland and Kowal 1960) (Table 5.2). In tropical forest areas outside of the Brazilian Amazon researchers found coarse necromass ranging from 3.8 to 6.0 Mg C ha⁻¹ in montane forest in Jamaica (Tanner 1980), 22.4 Mg C ha⁻¹ in wet forest in Costa Rica (Clark et al 2002) and 22.5 Mg C ha⁻¹ in dipterocarp forests in Malaysia (Yoda and Kira 1982). In the Brazilian Amazon, where much recent work on coarse necromass is concentrated, estimates of fallen coarse necromass in undisturbed moist forests in terra firma included 42.8 Mg C ha⁻¹ (Summers 1998) and 48.0 Mg C ha⁻¹ (Rice et al in press) on the high end and 27.6 Mg C ha⁻¹ (Keller *et al.* 2004a), 15 Mg C ha⁻¹ (Brown et al 1995), and 16.5 Mg C ha⁻¹ (Gerwing 2002) on the low end. Other studies examined coarse necromass in secondary forests and the effects of logging on coarse necromass (Gerwing 2002, Uhl et al 1988, Keller *et al.* 2004a). The proportion of coarse necromass to total above ground biomass can be surprisingly high, 18 to 25% (Keller *et al.* 2004a; Rice *et al.* (2004) even in

unmanaged forests. These values are for the Tapajos National Forest near Santarem, Brazil where Saleska *et al.* (2003) hypothesized that the 1997-1998 El Niño drought led to substantial mortality prior to the coarse necromass measurements cited above.

Production of Necromass

Death of whole trees or portions of trees creates necromass and the mechanisms that lead to tree death are termed disturbances. The processes and influences of these disturbances function on different temporal and spatial scales and are variable in the impact they have on tropical forests. The spatial scale of disturbances ranges from branch-falls and small gaps to landscape level blowdowns due to microbursts that can cover thousands of hectares (Nelson *et al.* 1994). Tree mortality in tropical forest plots ranges from 0.001 to 0.07 y⁻¹ (Carey 1994, Phillips and Gentry 1994). Disturbance in tropical forests includes individual tree processes, landscape level processes, and regional and climate influences.

Tree mortality in tropical forests is driven on the individual tree level by competition, primarily for water, nutrients and light (Prance 1985, Martinez- Ramos *et al.* 1998, Lieberman *et al.* 1989). As a tree dies and falls to the forest floor a gap in the canopy is created (Denslow 1987). These gaps are important in an ecological sense because they are involved with tree regeneration dynamics and species diversity and distribution (Schemske and Browkaw 1981, Denslow 1987, and Vitousek and Denslow 1986). Gaps increase light levels in understory, enhance nutrient mineralization, and create structural habitat for some species of flora, fauna, and fungi (Schemske and Browkaw 1981, Denslow 1987, and Vitousek and Denslow 1986, Dickinson *et al.* 2000, Svenning 2000).

Blackburn *et al.* (1996) examined gap generation and progressive enlargement of gaps as natural disturbances instead of catastrophic events. Young and Hubbell (1991) also found that trees were more likely to fall into gaps and suggested that gaps may be more persistent in tropical forests than previously thought. The persistence of gaps also predicts the locations where necromass is likely to collect. This spatial coincidence has not been tested.

Mortality of trees in the tropics is also influenced by fungi, insects and other animals, and the trees themselves (Denslow 1987). Branch fall as a source of necromass has rarely been quantified although, it has been recognized as is a major disturbance for seedlings growing in the understory (Lang and Knight 1983, Aide 1987, Clark and Clark 1991, van der Meer and Bongers 1996, Scariot 2000). The diversity of trees in the mosaic that is a tropical forest landscape makes it rare for a single insect infestation to create denuded canopies and cause the death of many trees (Janzen 1985). Vines entangling adjacent crowns may cause the death of a single tree to result in tree falls that involve several neighboring trees (personal observation). Some species of *Ficus*, strangler figs, have constricting vines that eventually kill the host tree (Windsor *et al.* 1989). Epiphytic vegetation load has also been tied to tree mortality (Prance 1985). Trees can also die as a result of genetic programming as is the case for monocarpic trees such as *Tachigalia versicolor* (Kitajima and Augspurger, 1989).

On non-degraded moist and wet forests, fires are rare events that do not propagate easily (Prance 1985). However, this belief is being challenged with studies of forest drying during El Niño events (Nepstad *et al.* 2002). Fire has also been shown to be an influential disturbance on white-sand forests in the Amazon (Anderson 1981). Fire in the Amazon is strongly influenced by people. Lightning may also cause fires and localized mortality in tropical forests (Magnusson *et al.* 1996).

Disturbances are also influenced by weather and topography (Bellingham and Tanner 2000). Topography was found to be influential on disturbances and thus was reflected in the local species distributions (Gale 2000). Tropical trees tend to have shallow root mass for nutrient exploitation and buttresses for structural support and have been shown to topple easily (Prance 1985). In the tropics, disturbances also include larger scale processes such as microbursts, blowdowns, volcanoes, and landslides (Nelson *et al.* 1994, Sanford *et al.* 1986, Lawton and Putz 1988, Garwood *et al.* 1979). Hurricanes have been shown to have an influence on tropical forests in the Caribbean and elsewhere (Lugo and Scatena 1996, Walker *et al.* 1996). Spatial patterns and recent trends in tree mortality have been attributed to ENSO events (Condit *et al.* 1995, Malhi *et al.* 2004).

Approximately half of the studies we reviewed compared undisturbed forests with forests experiencing disturbance due to anthropogenic factors, such as selective logging. Selective logging is a practice that fells a few trees per hectare (Peireira *et al.* 2002). This type of logging has been shown to affect substantial areas in the Brazilian Amazon and in tropical Asia (Asner *et al.* 2005; Curran *et al.* 2004). Other human influenced

disturbances in the literature of tropical necromass included fire, agriculture, conversion to pasture through deforestation, and repeated disturbances due to a combination of fire and agricultural practices (Table 5.1). The number of sites in our literature review was evenly distributed among undisturbed and disturbed forests. We excluded a study by Feldpausch *et al.* (2005) because that study measured the amount of necromass created by selective logging, but did not measure total coarse necromass stocks in either logged or undisturbed forests.

Few studies have measured the production of necromass in tropical forests. Approaches to the estimation of necromass production include allocating a portion of Net Primary Productivity (NPP), a portion of existing biomass (Palace *et al.* in press), or mortality estimates of trees (Rice *et al.* 2004). Flaws associated with these methods include the lack of variation over time, lack of spatial influence, lack of size class estimates, and a lack of knowledge of the proportion of necromass that remains standing.

Necromass production has been directly measured using repeated surveys on the same plots by marking necromass or removing it at each survey period (Harmon *et al.* 1986, Clark *et al.* 2002). All but three necromass production studies examined had only one repeated survey (Palace *et al.* to be submitted, Clark *et al.* 2002, Eaton and Lawrence 2006). This lack of repeated sampling limits the understanding of longer term influences of weather patterns such as El Niño or ability to assess if the forest is at steady state or if it is recovering from a larger scale disturbance (e.g. Saleska *et al.* 2003).

Rare events such as blowdowns or even large tree falls complicate sampling design and interpretation of coarse necromass data. For example, a tree fall of diameter 150 cm DBH drastically altered the measured flux of coarse necromass in one sampling interval from a study at the Tapajos National Forest in Brazil (Palace *et al.* to be submitted). Trees of this size occur with a frequency of only about 0.079 per ha at Tapajos (Keller *et al.* 2001). Assuming adequate sampling of 100 ha blocks, there are only 7.9 trees of this size class per block. If these trees have a 1.7 % annual mortality rate (Rice *et al.* 2004) then the chance of seeing a fall of this size is $(1-0.983^{7.9})$ or 12.7% per year. In the study of Palace *et al.*, a much larger sample area would have been required to record a large tree death annually. Larger but less frequent disturbances such as blowdowns (Nelson *et al.* 1994) require even more extensive sampling designs.

A compilation of studies that directly measured coarse necromass production is present in Table 5.3. Of the 39 papers reviewed here only 38 % measured coarse necromass production. Eaton and Lawrence (2006) measured coarse production in several disturbed sites and in one undisturbed site in dry tropical forest in southern Mexico. They removed and measured new coarse necromass four times over a two year period for an undisturbed forest and estimated a coarse necromass production of $0.91 \text{ Mg ha}^{-1} \text{ yr}^{-1}$. Tanner (1980) estimated coarse necromass production in a Jamaican forest to be $2.0 \text{ Mg ha}^{-1} \text{ yr}^{-1}$ using repeated samples over four years. Other estimates in dry tropical studies include 0.1 and $0.97 \text{ Mg ha}^{-1} \text{ yr}^{-1}$ conducted by Buxton (1981) and Collins (1981) respectively. Kira (1978) directly measured coarse necromass production of $3.3 \text{ Mg ha}^{-1} \text{ yr}^{-1}$ in Pasoh Forest in western Malaysia. Clark *et al.* (2002) measured influx of coarse necromass to be 4.8

Mg ha⁻¹ yr⁻¹ using a repeated survey in Costa Rica. In a 4.5 year study in the Brazilian Amazon, Palace *et al.* (to be submitted), measured coarse necromass production to be 6.7 Mg ha⁻¹ yr⁻¹. Large size class CWD (>10 cm DBH) production was 4.7 Mg ha⁻¹ yr⁻¹. The production of small size class CWD (2-5 cm) was 0.8 Mg ha⁻¹ yr⁻¹ and medium size class CWD (5-10 cm) was 1.2 Mg ha⁻¹ yr⁻¹. Interestingly, Rice *et al.* (2004) estimated coarse necromass production based on mortality of trees > 10 cm DBH at 4.8 Mg ha⁻¹ yr⁻¹ for a nearby forest area. This suggests that mortality based approaches potentially underestimate coarse necromass production.

Decomposition of Necromass

Decomposition of wood is generally a slow process that involves biological, chemical, and physical processes. The sequence that these processes act on dead wood varies over time due to changes in physical climate and the chemical and physical makeup of the wood over its decay life. Each piece of CWD has a unique chemical and physical makeup (Kaarik 1974). The difference in chemical and physical composition starts with differences in live trees. Differences among trees depend on tree species (wood characteristics), nutrient composition of soil, climate, tree health (including infections by insects, microbes, and fungus), and how the tree died (Harmon *et al.* 1986, Martius 1997). Differences within an individual tree may also be important due to internal variation in wood density (Nogueira *et al.* 2005).

Temperature and moisture have been tied to microbial activity and decomposition processes in necromass (Kaarik 1974, Harmon *et al.* 1986). Moisture levels and

temperature are not directly measurements of the decomposition process, their correlation with decomposition have been used to develop regression and model necromass decay (Harmon *et al.* 1986, Chambers *et al.* 2000). Too much moisture can create low levels of oxygen inhibiting decomposition and lack of water slows or halts decomposition (Harmon *et al.* 1986). An exponential relationship has been shown between microbial activity and temperature, until temperature is so high that proteins are damaged and enzymes denature (Mackensen *et al.* 2003).

Wood decay organism can be grouped into three categories, bacteria, fungi, and macroorganisms (Dickinson and Pugh 1974). The presence of fauna and their own growth efficiencies, nutrient requirements, and temperature and moisture requirements control the overall decomposition. Each of these categories of organisms acts on wood differently and are important at different time in the temporal sequence of wood decay (Kaarik 1974). In the tropics, wood fragmentation is primarily caused by termites (Buxton 1981). This fragmentation occurs on highly decayed logs or parts of logs. In addition, termites remove the wood to other places (Collins 1981).

The placement of the wood on the ground can influence the rate of its decay. Logs on hills tend to accumulate more soil on the uphill side, creating a wetter microclimate beneficial for many decomposing soil organisms (Harmon *et al.* 1986). In the Brazilian *varzea* forest, (a flooded forest type), the season that the wood falls is influential on its immediate and longer term decomposition rate (Martius 1997). Decomposition of smaller litter occurs rapidly, often less than one year, while larger coarse necromass can

have a turnover time close to a century (Harmon *et al.* 1986, Mackensen *et al.* 2003).

Estimation of coarse necromass decomposition rates uses two major approaches, chronosequences and time series (Harmon and Sexton 1996). In a time series, individual pieces of wood are followed over time (Harmon and Sexton 1996). In chronosequence studies, varying ages of coarse necromass are examined at a single point in time (Harmon *et al.* 1999). Dates of coarse necromass production have been made using disturbance records, living stumps, seedlings, dendrochronology, fall scars, and bent trees (Harmon *et al.* 1999). Some researchers have conducted a combination of chronosequences and time series (Harmon and Sexton 1996, Chambers *et al.* 2000).

Within sample chronosequences or time series, decomposition may be studied by mass loss, density change, uniform substrate decomposition, radioisotopes, respiration rates, mineralization, enzyme activity, and selective inhibition experiments (Swift *et al.* 1979, Harmon and Sexton 1996, Harmon *et al.* 1999). The majority of studies in the tropics have used mass loss, density change, or chamber systems to measure respiration.

Measurement of decomposition through mass loss requires multiple measurements of coarse necromass over time (Buxton 1981, Harmon *et al.* 1999, Chambers *et al.* 2000). This can only be done accurately if moisture content can be measured accurately and non-destructively. Alternatively, changes in density can be used as a surrogate for mass loss. It is important for density measurements to account for void spaces. Void spaces in logs must be accounted for in density measurements either by using large pieces of

necromass (e.g., Chambers *et al.*, 2000, Clark *et al.*, 2002) or by separately quantifying void space (Keller *et al.*, 2004a, Palace *et al.* in press). Direct measurements have also been made in the laboratory with coarse necromass removed from the field (Richards 1962, Chambers 2000).

Respiration studies have been conducted on coarse necromass in a number of ways. Essentially all methods depend upon isolating sections, full pieces, or extracted samples of coarse necromass in a chamber. Chambers may be attached to the surface of coarse necromass or pieces may be inserted into chambers. The chambers are sealed and the rise in CO₂ concentration is measured directly by infra-red detection (Chambers *et al.* 2001) or, in older studies, CO₂ emitted is absorbed in alkali (Swift *et al.* 1979; Marra and Edmonds 1994). Respiration will underestimate coarse necromass loss because it does not account for dissolution and fragmentation. However, there are indications that for tropical moist forests, respiration is the major pathway for CO₂ loss. Chambers *et al.* (2004) estimated that 80% of mass loss in CWD resulted for respiration. This was done by using the ratio from a respiration study and a mass loss study (Chambers *et al.* 2000, 2001)

Two methods mentioned here but not used in tropical forest necromass decomposition are substrate decomposition and radioisotopes. Substrate decomposition studies have also been conducted (Harmon *et al.* 1999). In this method, uniform substrates such as Popsicle sticks or wooden dowels are placed in the field and measured over time. These studies provide information on the temporal variability of decomposition and also

provide a standard for comparison of decomposition rates across sites. These results only provide relative rates that may lack the complexity of decomposition of larger logs or interaction of decay organisms. Radioisotopes have been used as tagging agents for materials to estimate leaching and soil organic matter formation (Wedin *et al.* 1995, Carvalho *et al.* 2003). Studies have been done by injecting isotopes into litter, but for coarse necromass this is difficult (Harmon *et al.* 1999).

A compilation of field measured decay rates and estimated decay rates based on a mortality estimate of 0.02 yr^{-1} are presented in Table 5.2. Of the 39 papers we reviewed only 33 % made measurement of necromass decomposition. Estimates of CWD decomposition rates in the Brazilian Amazon include only three studies. Chambers *et al.* (2001 and 2000) used two different methods (closed chamber using an infra-red analyzer and measured mass loss) for estimates of 0.13 y^{-1} and 0.17 y^{-1} for each method. Rice *et al.* (2004) estimated decomposition of coarse necromass using stock measurements and the decomposition model developed in Chambers *et al.* (2000). Palace *et al.* (to be submitted) estimated decomposition rates using a steady state model. Their estimates of decay rates is 0.17 y^{-1} for large ($>10 \text{ cm}$ diameter), 0.21 y^{-1} for medium ($5\text{-}10 \text{ cm}$ diameter), and 0.47 y^{-1} for small size ($2\text{-}5 \text{ cm}$ diameter) class coarse necromass. No other study that we know of has data for these smaller size classes and their production decomposition rates for tropical forests. Other tropical forest necromass decomposition rates range from 0.03 y^{-1} (Delaney *et al.* 1998) to 0.51 yr^{-1} (Collins 1981). An extremely high decay rate of 2.0 y^{-1} was estimated in a tropical mangrove forest by Robertson and Daniel (1989). We found only two studies that estimated decomposition rates for

standing dead with estimates being 0.461 y^{-1} (Lang and Knight 1979) and 0.115 y^{-1} (Odum 1971). Palace *et al.* (to be submitted) estimated the movement of standing dead through the pool to be 0.24 y^{-1} .

A Simple Model to Expand and Compare Literature Results

We used a simple model that is a first order differential equation to examine coarse necromass dynamics.

$$dM/dt = -kM + F$$

where M is the necromass pool (Mg ha^{-1}), F is the rate of necromass production ($\text{Mg ha}^{-1} \text{ y}^{-1}$), and k is the instantaneous decay rate (y^{-1}). By definition at steady state dM/dt is zero. The residence time for necromass is M/F .

We solved this differential equation using a series of values ranging from 0.1 to 8 $\text{Mg ha}^{-1} \text{ y}^{-1}$ for necromass production and 0.01 to 0.5 for decomposition rate (y^{-1}). Our result is a conceptual model comparing stocks, decomposition rates, and production rates for steady state systems is shown in Figure 5.1.

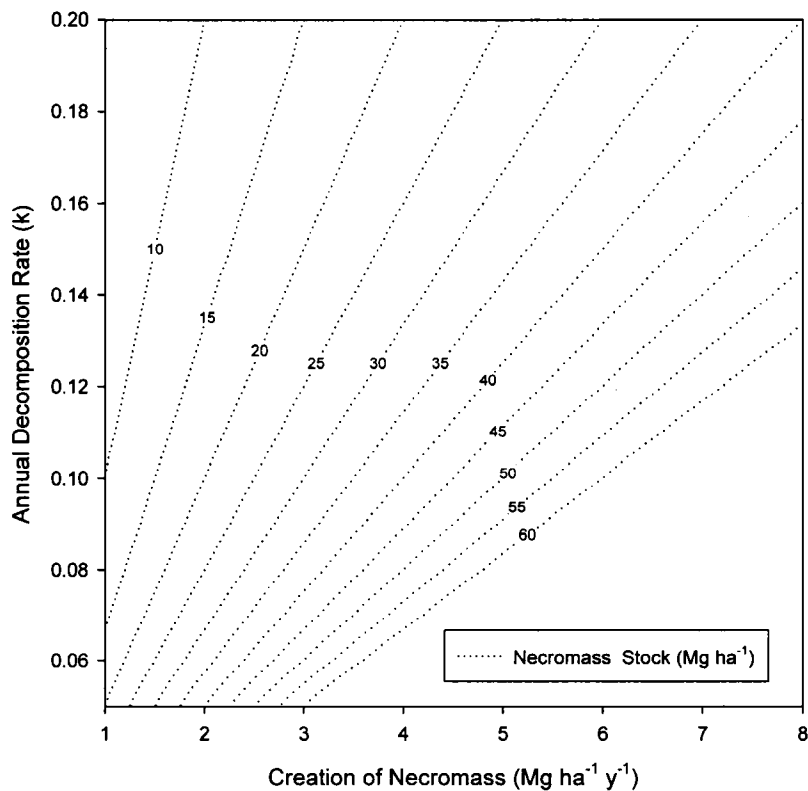


Figure 5.1. A simple model solved for many values in parameters.

When production or decomposition rates were lacking in the literature that we reviewed, estimates were generated using the following methods and rationale. A production estimate of necromass was generated using the biomass value and a mortality rate of 0.02 y^{-1} . We used a mortality rate at the upper end of the range for old-growth tropical forests (Philips and Gentry, 1994) but feel that this is a reasonable estimate, since most biomass studies do not include smaller diameter trees and lianas. In addition, mortality rates we used to estimate necromass production often underestimate necromass production because branch fall is not included (Palace *et al.* in press).

Using the production estimate divided by the stock measured values we calculated decomposition rates. If no biomass estimate was available, we estimated necromass production to be 0.15 y^{-1} of the total necromass stock. Though these estimates of decay and production amounts are prone to error and hypothetical in nature, they allow us to attempt to compare sites and biomes in tropical forests (Table 5.3). Comparison of field data and model estimates also allow us to evaluate the assumption of steady state for a variety of sites.

Discussion

Methodology

Methodology was comparable among sites with similarity in decay classes and size classes used (Table 5.3, Table 5.4). Although there are some discrepancies among papers, stock estimates are broadly comparable between studies. Biomass estimates were not done at all sites and we suggest that biomass be measured whenever necromass is examined. Production and decomposition measurements were both lacking at many sites and existing measurements lacked consistency. We suggest longer temporal studies that would allow for a better understanding of the dynamics of these fluxes and their relation to meteorological parameters. We would also like to see decomposition studies conducted at one site use multiple methods to allow for comparison between such methodologies.

Different methods for fallen necromass quantification may be used depending upon the question being asked by the researcher, such as fuel load amount (Uhl and Kauffman

1990) or biometry and respiration estimates (Chambers *et al.* 2000, Keller *et al.* 2004a). In concert with previous evaluations for other regions, we find that line intercept sampling is generally easier to adapt to field conditions where sufficient area is available for sampling. For example, Grove (2001) switched from plot based work to line intercept sampling when confronted with dense understory (Grove 2001). We conducted line intercept sampling at the same site as Rice *et al.* (2004) and had similar estimates with similar uncertainties. Our line intercept sampling was six times as efficient; it took about one third the amount of time and with half the field crew. Plot estimates require more movement than line intercept sampling and become especially difficult in logged sites or in sites with dense under-story.

Fallen coarse necromass stock was measured almost two times more frequently than standing dead. This is likely due to difficulty measuring the height of standing dead in a complex and dense forest canopies common in many tropical sites. Although standing dead stock is more difficult to measure than fallen coarse necromass stocks, stock estimates tend to be the easiest and most accurate coarse necromass component to measure when compared to decomposition and production rates, which require multiple samples over time.

Methodology for decay classes was similar among studies. Much of the recent literature cites Harmon *et al.* (1995) in regard to decay classification. It is likely that this paper has set the standard for decay classes terminology used. Implementation of the decay classification may vary across sites in necromass studies. We do not know of tests for

field classification differences across sites in tropical forests other than Palace *et al.* (in press). A number of studies we examined had similar decay class definitions (Harmon *et al.* 1995, Eaton and Lawrence 2006, Keller *et al.* 2004a, and Palace *et al.* in press). In addition, some studies had similar decay class density measurements (Table 5.4).

Decomposition and production estimates of dead wood both have unique difficulties. Decomposition is a complex process; however estimates for decomposition rates based on a variety of methods often give similar results (Palace *et al.* in press, Chambers *et al.* 2001). Production estimates need to cover a large enough area to capture the rare episodic tree fall events. While trading space for time is helpful for quantifying coarse necromass production, long term studies that could link necromass to weather changes and other aspects of interannual variability would help us understand interannual variability in carbon dynamics.

Tropical forests contain a large number of tree species and this creates difficulty when measuring decomposition rates (Chambers *et al.* 2000). Decomposition rate measurements maybe be misleading when only a few species of trees or a few trees are only examined for a short period of time. Chambers *et al.* (2000) developed a regression for decay that incorporates temperature, moisture, and necromass diameter.

Many of the studies (42%) only examined one component of coarse necromass dynamics. A combination of methods and components measured is preferable, allowing for the comparison of production and decomposition rates with stock estimates at the beginning

and end of the study. Comparison to other measurable ecological parameters, such as NPP, woody increment, and mortality rates proves helpful in better understanding necromass dynamics. Necromass and biomass estimates should be done in conjunction at research sites. Finally, similar studies using the same methodology are beneficial to coarse necromass research (Palace *et al.* in press). Studies that examined more than three coarse necromass components are Rice *et al.* (2004), Chambers *et al.* (2000), Harmon *et al.* (1995), Nascimento and Laurence (2002), Clark *et al.*, (2002), Collins (1981), Roberston and Daniel (1989), Palace *et al.* (to be submitted), Delaney *et al.*, (1998), Eaton and Laurence (2006).

Comparison among sites

Necromass studies in tropical forests are few in number and concentrated in Central American dry forests and areas of the Eastern Amazon, especially in the State of Pará, Brazil. Many of the sites were highly disturbed due to logging activity, agriculture, fire, and in one case elephants (Buxton 1981, Uhl *et al.* 1988, Eaton and Lawrence 2006). We estimated production and decay estimates for these areas, but admit that our steady state approach is ill-suited to these sites.

The proportion of coarse necromass to biomass is highly variable among sites (Figure 5.2) ranging from 0.01 in an undisturbed site in the Ivory Coast (Bernhard-Reversat *et al.*, 1978) to 3.04 (Gerwing, 2002) in a heavy logged and burned site in Paragominas, Brazil. In undisturbed forests there appears to be a peak in the coarse necromass with middle values of the biomass distribution (Figure 5.2b). Beyond that peak as biomass increases

the proportion of necromass decreases. The highest biomass sites may have been undisturbed for long periods resulting in low necromass. We drew a hypothetical limit to illustrate such a relationship. High biomass and low necromass sites were often from studies that used small plots that do not reflect the landscape spatial distribution of biomass and necromass. Small plots may be chosen with the “majestic forest bias” that tends toward high biomass and little recent disturbance (Keller *et al.* 2001, Chave *et al.* 2001).

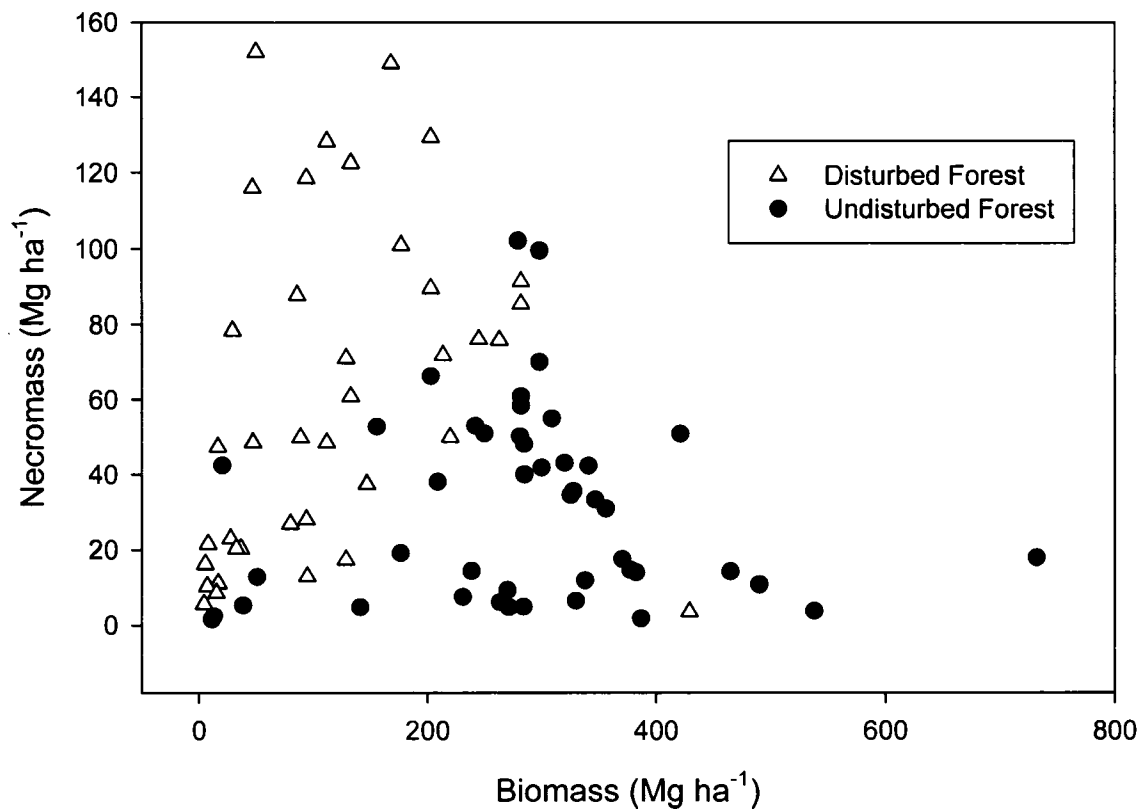


Figure 5.2a. Biomass and Necromass field measured values in undisturbed and disturbed tropical forests.

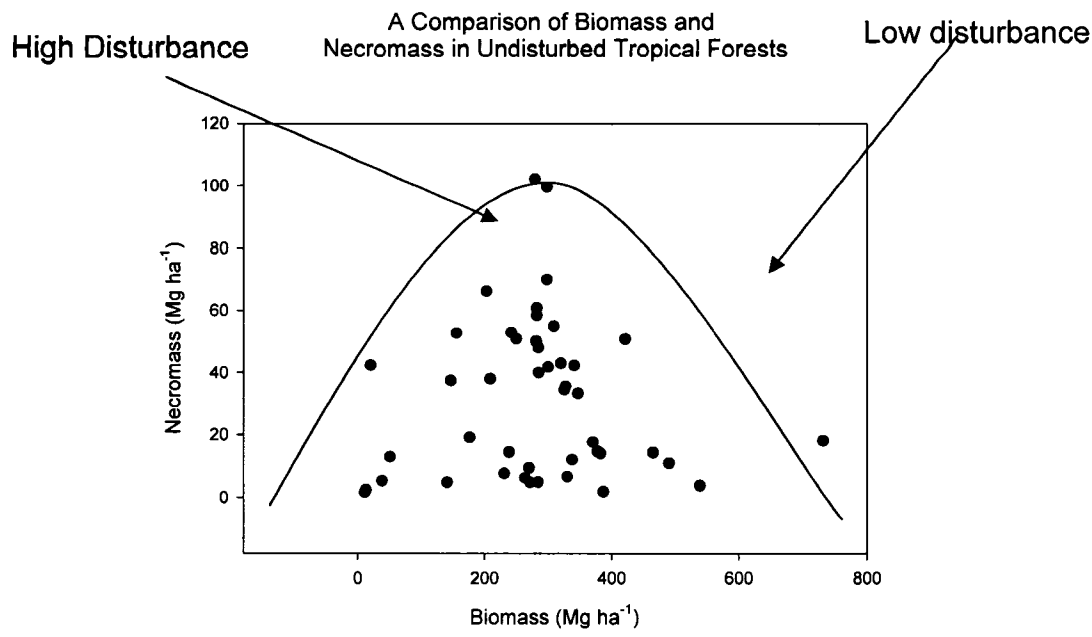


Figure 5.2b. Biomass and Necromass field measured values in undisturbed tropical forests showing areas of high and low disturbance. Line is not a limit or regression, but draw to show the upper bound of data.

Standing dead and fallen coarse necromass have been found to be proportionally related, even at disturbed sites (Palace *et al.* in press; Figure 5.3). However, the proportional relation found at two sites using the same methodology did not hold when compared across tropical sites and studies (Figure 5.4). A regression comparing just undisturbed sites had a higher r^2 value (0.06) than when disturbed sites were included in the analysis (0.00007) (Figure 5.4). Nonetheless, standing necromass accounts for a large proportion of the total coarse necromass stock, up to 66% in an undisturbed forest and 98% at a heavily disturbed site, and should be included in future field estimates (Palace *et al.* in press, Harmon *et al.* 1995).

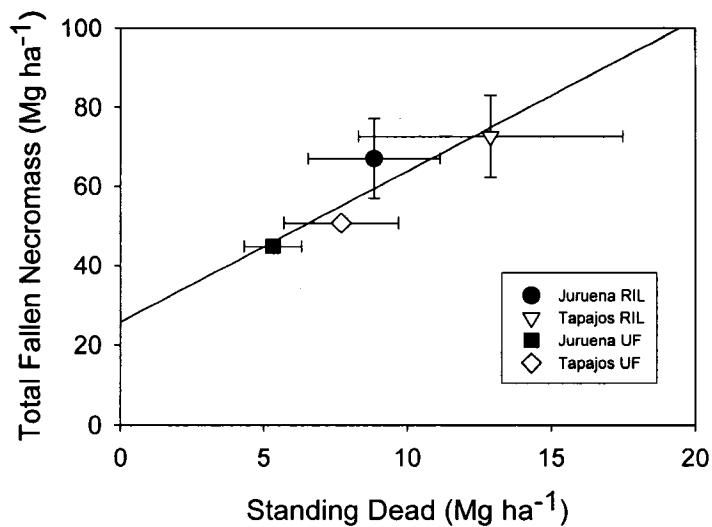


Figure 5.3. Fallen vs. standing necromass for sites and treatments. Error bars represent standard errors (from Palace *et al.* in press)

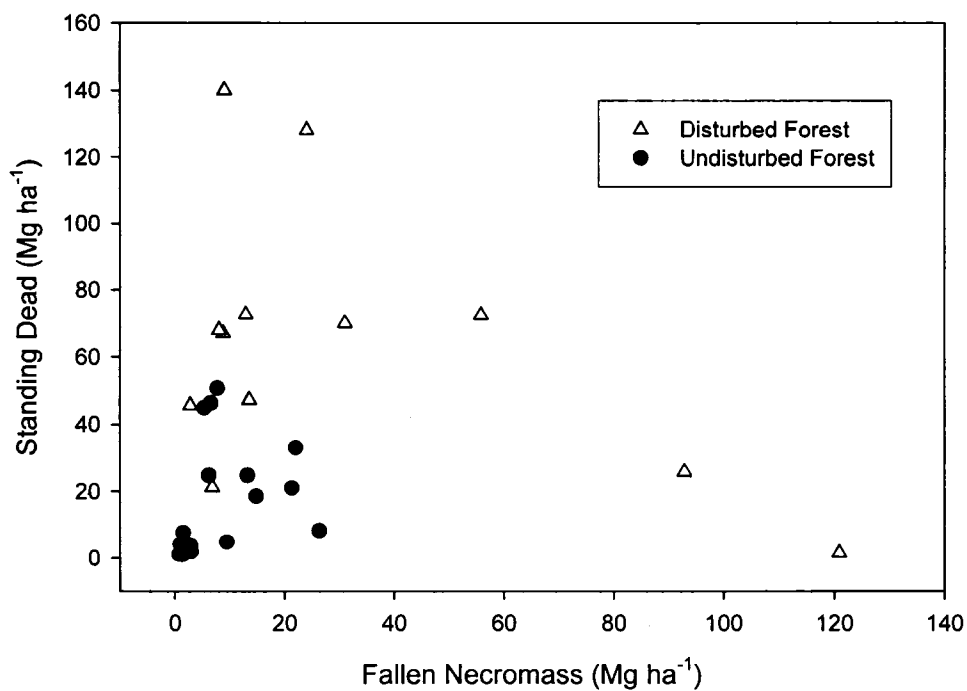


Figure 5.4. Fallen necromass and standing dead field measured values in undisturbed and disturbed tropical forests.

We did not make comparisons of size classes among sites because few studies separated data by size class. In addition, comparisons among studies for necromass size classes are difficult because of differences in the limits for size classes themselves (Table 5.3). Still some studies indicate that smaller size classes (generally less than 10 cm diameter) contribute up to 21% of the total coarse necromass stock (Uhl and Kauffman 1990, Palace *et al.* in press) and we suggest that smaller size classes be included in field measurements. Smaller size classes decay more quickly and may contribute more to the overall site respiration budget (Harmon *et al.* 1986, Palace *et al.* to be submitted). Chambers *et al.* (2000), showed a relation with decomposition rates and necromass diameter. Palace *et al.* (to be submitted) using production and stock estimates grouped by size classes were able to estimate decomposition rates for the size classes using a simple model.

Trees lose branches through several processes that do not lead to whole tree mortality. For example, shaded lower branches may be shed and physical damage may result from crown interactions or animal activity. Mortality estimates used to determine coarse necromass may underestimate production due to branch fall that is not associated with the death of a tree. Determination of the source of coarse necromass would aid in quantifying branchfall. These small and medium classes are likely to include a substantial component from branchfall. Chambers *et al.* (2001) estimated branch-fall to be $0.9 \text{ Mg ha}^{-1} \text{ y}^{-1}$ based upon a comparison of field measured allometries and an optimized model tree structure based on the hydraulic constraints to tree architecture. Palace *et al.* (to be submitted) examined the source of necromass by field classification of

coarse necromass as either branch, trunk, or unidentifiable. Coarse necromass derived from tree trunks dominated the large size class in both necromass production and in pools (Table 5.3). The other size classes were more evenly distributed among sources. They found significant differences between logged and undisturbed forest treatments for the proportions of trunk, branch, and unidentified material within both the production and pool of coarse necromass (χ^2 , $p < 0.0001$). Proportions between groups (production and pool estimates) and within a treatment were also found to be significantly different (χ^2 , $p < 0.0001$).

We used measured coarse necromass stock and either an estimated production (biomass * 0.02) or decomposition rate (coarse necromass * 0.15) to generate production and decay rates when they were missing from the literature. Using these rates and stocks, we examined if sites were at steady state. No sites were found to be at steady state. Either these sites were not at steady state or the generalized assumptions of production and decomposition rates may not accurately reflect real world values. It is not reasonable to expect all sites to be at steady state. Plots were often too small to represent landscape coarse necromass dynamics.

We found that measured decomposition rates and those estimated by our simple model were similar (Figure 5.5). Higher decomposition rates associated with lower coarse necromass stocks suggests that decomposition rates are an important control. We caution that this conclusion depends upon our model estimates using necromass production equal to a fixed proportion of biomass (0.02 y^{-1}). Higher decomposition rates may be

associated with forests that experience higher disturbance rates as hypothesized by Baker *et al.* (2004) and Mahli *et al.* (2004) based upon a comparison between western and eastern Amazon forests. Baker *et al.* (2004) discussed the variation in wood density and how this determines the biomass in Amazonian forests. Wood density variation is attributed to nutrient cycling influences on species assemblages. The syndrome suggested by these two studies is that high-turnover forests have low density wood that in turn decomposes faster.

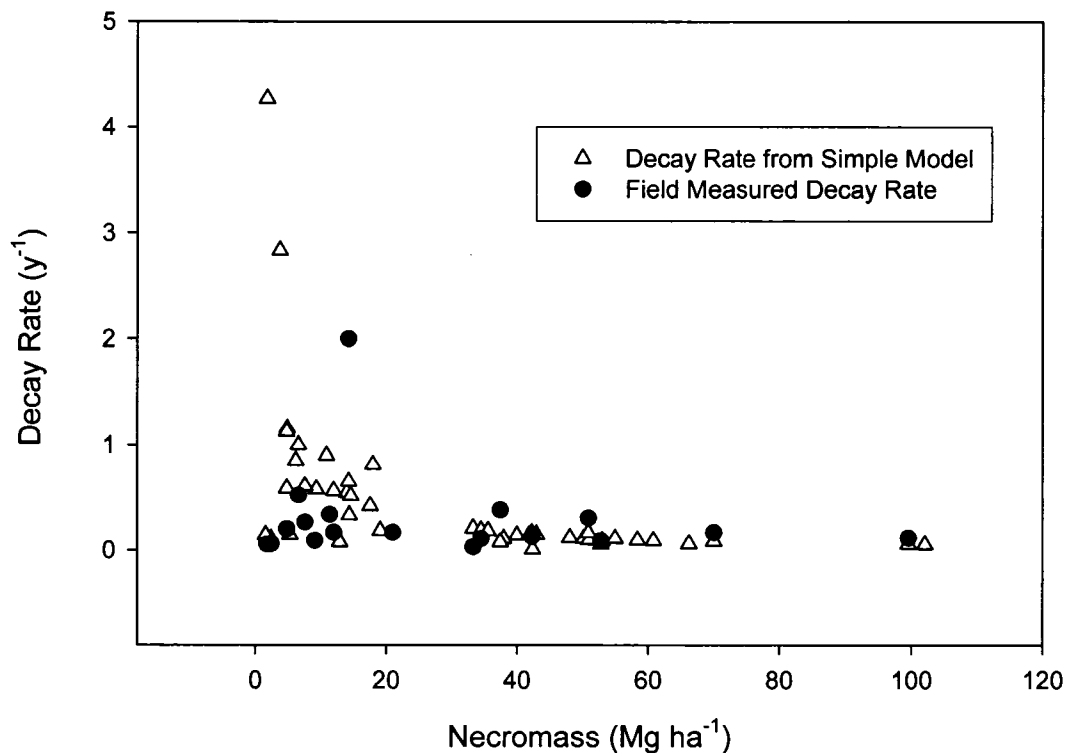


Figure 5.5. A comparison of estimated decay rates ((biomass * 0.2 y⁻¹) / necromass stock) and field measured decay rates versus CWD stocks.

Conclusions

We compiled data from existing studies and compared pools and fluxes of coarse necromass among tropical forest sites. General relationships among necromass components were explored such as coarse necromass to biomass proportions and fallen to standing dead coarse necromass. Methodology was comparable across the literature for coarse necromass production and stock estimates. Fallen stock was almost two times more frequently measured than standing dead. We calculated production and decomposition rate estimates through the use of a simple model when these values are not available. General relations and proportions between coarse necromass components were explored and were found to vary greatly. No definitive relations were found among coarse necromass components across sites. In undisturbed forests there appears to be a peak in the coarse necromass with middle values of the biomass distribution. Beyond that peak as biomass increases the proportion of coarse necromass decreases. The ratio of coarse necromass to biomass ranged from 0.4 % in an undisturbed forest to 304% in a disturbed forest. Standing dead necromass accounts for a large proportion of the total CWD stock, up to 66% in an undisturbed forest and 98% at a heavily disturbed site, and should be included in further field estimates. We found that localized variability is high and complicates or hinders the development of general relationships of coarse necromass components across the tropics. Many of the studies (42%) only examined only one component of necromass dynamics. We stress the importance of measuring multiple coarse necromass components and ideally conducting these measurements over years or even decades in order to improve our knowledge of coarse necromass dynamics in tropical forests.

REFERENCES

- Aide, T.M., 1987. Limbfalls: A major cause of sapling mortality for tropical forest plants. *Biotropica* 19(3), 284-285.
- Anderson, A. 1981. White-sand vegetation of Brazilian Amazonia. *Biotropica* 13(3), 199-210.
- Apolinário, F.B.E., Martius, C., 2004. Ecological role of termites (Insecta, Isoptera) in tree trunks in central Amazonian rain forests. *Forest Ecology and Management* 194(1-3), 23-28.
- Asner, G.P., Keller, M., Pereria, R., Zweede, J.C., Silva, J.N.M., 2004. Canopy damage and recovery after selective logging in Amazonia: field and satellite studies. *Ecological Applications* 14 (4), s280-s298.
- Asner, G. P., Palace, M., Keller, M., Pereira R., Silva, J. N. M., Zweede, C., 2002. Estimation canopy structure in an Amazon forest from laser range finder and IKONOS satellite observations. *Biotropica* 34, 483-492.
- Asner, G.P., Knapp, D.E., Broadbent, E.N., Oliveira, P.J.C., Keller, M., Silva, J.N., 2005. Selective logging in the Brazilian Amazon. *Science* 310, 480-482.
- Asner, G.P., E.N. Broadbent, P.J.C. Oliveira, D.E. Knapp, M. Keller, and J.N. Silva. 2006. Condition and fate of logged forests in the Brazilian Amazon. *Proceedings of the National Academy of Sciences*. 103(34):12947-12950.

- Baker, T.R., Phillips, O.L., Malhi, Y., Almeida, S., Arroyo, L., Di Fiore, A., Erwin, T., Killeen, T.J., Laurance, S.G., Laurance, W.F., Lewis, S.L., Lloyd, J., Monteagudo, A., Neill, D.A., Patino, S., Pitman, N.C.A., Silva, N.M., Martinez, R.V., 2004. Variation in wood density determines spatial patterns in Amazonian forest biomass. *Global Change Biology* 10, 545-562.
- Bernhard-Reversat, F., C. Huttel, and G. Lemée. 1978. Structure and functioning of evergreen rain forest ecosystems of the Ivory Coast. Pages 557-574 in *Tropical Forest Ecosystems: A State-of-the-Knowledge Report*. UNESCO, Paris.
- Blackburn, G. A., Milton, E.J. 1996. Filling the Gaps: Remote Sensing Meets Woodland Ecology. *Global Ecology and Biogeography Letters*, 5, No. 4/5, Remote Sensing and GIS in the Service of Ecology and Biogeography: A Series of Case Studies. pp. 175-191.
- Bolduc, P., Lowell, K., Edwards, G., 1999. Automated estimation of localized forest volume from large-scale aerial photographs and ancillary cartographic information in a boreal forest. *International Journal of Remote Sensing* 2018, 3611- 3624.
- Brandtberg, T., Walter, F., 1998. Automated delineation of individual tree crowns in high spatial resolution aerial images by multiple-scale analysis. *Machine Vision and Applications* 11, 64–73.
- Brokaw, N.L. 1985. Gap-phase regeneration in a tropical forest. *Ecology* 6630, 682-687.
- Brokaw, N.L. 1987. Gap-phase regeneration of three pioneer tree species in a tropical forest. *Journal of Ecology* 75, 9-19.
- Brown, I.F., Martinelli, L. A., Thomas, W. W., Moreira, M.Z., Ferreira, C.A.C., Victoria, R.A., 1995. Uncertainty in the biomass of Amazonian forests: an example from Rondonia, Brazil. *Forest Ecology and Management* 75, 175-189.
- Brown, J.K., 1974. Handbook for inventorying downed woody material. USDA Forest Service, Ogden, Utah, 1-24.

- Brown, S., 1997. Estimating biomass and biomass change of tropical forests: A primer. United Nations Food and Agriculture Organization.
- Brown, S., Pearson, D. Slaymaker, S. Ambagis, N. Moore, D. Novelo, Sabido, W., 2005. Creating a virtual tropical forest from three-dimensional aerial imagery: Application for Estimating Carbon Stocks. *Ecological Applications* 15, 1083-1095.
- Buxton, R. D. 1981. Termites and the turnover of dead wood in an arid environment. *Oecologia* 51, 379-384.
- Carey, E.V., Brown, S., Gillespie, A.J.R., Lugo, A.E., 1994. Tree Mortality in Mature Lowland Tropical Moist and Tropical Lower Montane Moist Forests of Venezuela. *Biotropica*, 26(3), 225-265.
- Chambers, J.Q., Higuchi, N., Schimel, J.P., Ferreira L.V., Melack, J.M., 2000. Decomposition and carbon cycling of dead trees in tropical forests of the central Amazon. *Oecologia* 122, 380-388.
- Chambers, J.Q., Schimel, J.P., Nobre, A.D., 2001a. Respiration from coarse wood litter in central Amazon forests. *Biogeochemistry* 52, 115-131.
- Chambers, J.Q., Dos Santos, J., Ribeiro, R.J., Higuchi, N., 2001b. Tree damage, allometric relationships, and above-ground net primary production in central Amazon forest. *Forest Ecology and Management* 152, 73-84.
- Chambers, J. Q., Tribuzy, E.S., Toledo, L.C., Crispim, B.F., Higuchi, N., Dos Santos, J., Araújo, A.C., Kruijt, B., Nobre, A.D., Trumbore, S.E., 2004. Tropical Forest Ecosystem Respiration. *Ecological Applications* 14(4), s72-s88.
- Chave, J., Riera, B., Dubois, M. A., 2001. Estimation of biomass in a neotropical forest of French Guiana: spatial and temporal variability. *Journal of Tropical Ecology*. 17: 79-96.

- Chave, J., Condit, R., Lao, S., Caspersen, J.P., Foster, R.B., Hubbell, S.P. 2003. Spatial and temporal variation of biomass in a tropical forest: results from a large census plot in Panama. *Journal of Ecology* 91, 240–252.
- Clark, D.A., Brown, S., Kicklighter, D.W., Chambers, J.Q., Thomlinson, J.R., Nif, J., 2001a. Measuring Net Primary Production in Forests: Concepts and Field Methods. *Ecological Applications* 11(2), 356–370.
- Clark, D.A., Brown, S., Kicklighter, D.W., Chambers, J.Q., Thomlinson, J.R., Nif, J., 2001b. Net Primary Production in Tropical Forests: An Evaluation and Synthesis of Existing Field Data. *Ecological Applications* 11(2), 371–384.
- Clark, D.B., Clark, D.A., 1991. The Impact of Physical Damage on Canopy Tree Regeneration in Tropical Rain Forest. *The Journal of Ecology*, 79(2) 447-457.
- Clark, D.B., Clark, D.A., Brown, S., Oberbauer, S.F., Veldkamp, E., 2002. Stocks and flows of coarse woody debris across a tropical rain forest nutrient and topography gradient. *Forest Ecology and Management* 164, 237-248.
- Clark, D.B., Castro, C.S., Alvarado, L.D.A., Read, J.M., 2004. Quantifying mortality of tropical rain forest trees using high-spatial-resolution satellite data. *Ecology Letters* 7, 52-59.
- Cochrane, M. A., Alencar, A., Schulze, M. D., Souza, C. M., Nepstad, D. C., Lefebvre, P. & Davidson, E. 1999. Positive feedbacks in the fire dynamics of closed canopy tropical forests. *Science* 284,1832–1835.
- Collins, N.M., 1981. The role of termites in the decomposition of wood and leaf litter in the southern Guinea savanna of Nigeria. *Oecologia* 51, 389-399.
- Condit, R., Hubbell, S. P., Foster, R. B., 1995, Mortality Rates of 205 Neotropical Tree Species and the Responses to a Severe Drought, *Ecol. Monogr.* 65, 419–439.
- Culvenor, D.S., 2002. TIDA: an algorithm for the delineation of tree crowns in high spatial resolution remotely sensed imagery. *Computers and Geosciences* 28(1), 33-44.

- Curran, L. M., Trigg, S.N., McDonald, A.K., Astiani, D., Hardiono, Y.M. Siregar, P., Caniago, I., Kasischke, E., 2004, Lowland Forest Loss in Protected Areas of Indonesian Borneo. *Science* 303, 1000-1002.
- Dar A. R., Keller, M., and Soares, J. V., 2003. Studies of land-cover, land-use, and biophysical properties of vegetation in the Large Scale Biosphere Atmosphere experiment in Amazônia. *87* (4), 377-388.
- Dawkins, H.C. 1962. Crown diameters: their relation to bole diameter in tropical forest trees. *Commonwealth Forestry Review* 26, 318–333.
- Davidson, EA., Artaxo, P., 2004. Globally significant changes in biological processes of the Amazon Basin: results of the Large-scale Biosphere-Atmosphere Experiment. *Global Change Biology* 10(5), 519
- Delaney, M., Brown, S., Lugo, A.E. , Torres-Lezama, A., Quintero, N.B., 1998. The quantity and turnover of dead wood in permanent forest plots in six life zones of Venezuela. *Biotropica* 30(1), 2-11.
- Denslow, J.S., 1987. Tropical rainforest gaps and tree species diversity. *Annual. Review Ecology and Systematics* 18, 431-451.
- Denslow, J.S., 1980. Gap partitioning among tropical rainforest trees. *Tropical Succession* 12: 47-77.
- De Vries, P.G., 1986. Sampling theory for forest inventory. A teach-yourself course. Springer-Verlag Berlin Heidelberg, Wageningen, 399 pp.
- Dickinson, C.H., Pugh, G.J.F., 1974. *Biology of Plant Litter Decomposition*. Academic Press, NYC. Vol 1 and 2.
- Eaton, J. M., Lawrence, D., 2006. Woody debris stocks and fluxes during succession in a dry tropical forest. *Forest Ecology and Management* 232, 46-55.

- Edwards, P.J., Grubb, P.J., 1977. Studies of mineral cycling in mountain rainforest in New Guinea, I. The distribution of organic matter in the vegetation and soil. *Journal of Ecology*, 65, 943-969.
- Feldpausch, T.R., Jirka, S., Passos, C.A.M., Jasper, F., Riha, S.J., 2005. When big trees fall: damage and carbon export by reduced impact logging in southern Amazonia. *Forest Ecology and Management* 219, 199-215.
- Fensham, R.J., Fairfax, R.J., Holman, J.E., Whitehead, P.J., 2002. Quantitative assessment of vegetation structural attributes from aerial photography. *International Journal of Remote Sensing* 23(11), 2293-2317.
- Frey, S.D., Sixb, J., Elliott, E.T., 2003. Reciprocal transfer of carbon and nitrogen by decomposer fungi at the soil-litter interface. *Soil Biology and Biochemistry* 35, 1001-1004.
- Gale, N., 2000. The relationship between canopy gaps and topography in a western Ecuadorian rain forest. *Biotropica* 32(4a):653-661.
- Garwood, N., Janos, D.P., Brokaw, N., 1979. Earthquake-caused landslides: a major disturbance to tropical forests. *Science* 205, 997-999.
- Garwood, N., 1985. Earthquake-caused landslides in Panama: Recovery of vegetation, *Nat. Geogr. Soc. Res. Reports* 21, 181-183.
- Gerwing, J.J., 2002. Degradation of forests through logging and fire in the eastern Brazilian Amazon. *Forest Ecology and Management* 157, 131-141.
- Golley, F.B., McGinnis, J.T., Clements, R.G., Child, G.I., Duever, M.J., 1969. The structure of tropical forests in Panama and Colombia. *BioScience*, 19 (8), 693-696.

- Golley, F.B., McGinnis, J.T., Clements, R.J., 2004 La biomasa y la estructura mineral de algunos bosques de Darien, Panama. *Turrialba*, 21, 189-196.
- Goulden, M.L., Miller, S.D., da Rocha, H.R., Menton, M.C., de Freitas, H.C., Figueira, A.M.E.S., de Sousa, C.A.D., Diel and seasonal patterns of tropical forest CO₂ exchange. *Ecological Applications* 14 (4), S42-S54.
- Gove, J.H., Ducey, M.J., Valentine, H.T., 2002. Multistage point relascope and randomized branch sampling for downed coarse woody debris estimation. *Forest Ecology and Management* 155, 153–162.
- Greenland, D.J., Kowal, J.M.L., 1960. Nutrient content of the moist tropical forest of Ghana. *Plant and Soil*, 12, 154-174.
- Grove, S.J., 2001. Extent and composition of dead wood in Australian lowland tropical rainforest with different management histories. *Forest Ecology and Management* 154, 35-53.
- Harmon, M.E., Franklin, J.F., Swanson, F.J., Sollins, P., Gregory, S.V., Lattin, J.D., Anderson, N.H., Cline, S.P., Aumen, N.G., Sedell, J.R., Lienkaemper, G.W., Cromack, K., Cummins, K.W., 1986. Ecology of coarse woody debris in temperate ecosystems. *Advances in Ecological Research* 15, 133-302.
- Harmon, M. E., Franklin, J. F., 1989. Tree seedlings on logs in *Picea-Tsuga* forests of Oregon and Washington. *Ecology* 70, 48-59.
- Harmon, M.E., Whigham, D.F., Sexton, J., Olmsted, I., 1995. Decomposition and mass of woody detritus in the dry tropical forests of the northeastern Yucatan peninsula, Mexico. *Biotropica* 27(3), 305-316.
- Harmon, M.E., Sexton, J., 1996. Guidelines for Measurements of Woody Debris in Forest Ecosystems. Publication No. 20. U.S. LTER Network Office:University of Washington, Seattle, WA, USA. 73 pp.
- Higuchi, N. and Biot, Y, 1995. Convênio INPA/ODA: BIONTE. Biomassa florestal e nutrientes. Relatório semestral (Janeiro a junho 1995), Volume 2. Unpublished report, Instituto Nacional de Pesquisas da Amazônia (INPA), Manaus.

- Houghton, R.A., Lawrence, K.T., Hackler, J.L. Brown, S., 2001. The spatial distribution of forest biomass in the Brazilian Amazon: a comparison of estimates. *Global Change Biology* 7, 731-746.
- Houghton, R.A., Skole, D.L., Nobre, C.A., Hackler, J.L., Lawrence, K.T., Chomentowski, W.H., 2000. Annual fluxes of carbon from the deforestation and regrowth in the Brazilian Amazon. *Nature* 403, 301-304.
- Hurt, G., Xiao, X.M., Keller, M., Palace, M., Asner, G.P., Braswell, R., Brondizio, E.S., Cardoso, M., Carvalho, C.J.R., Fearon, M.G., Guild, L., Hagen, S., Hetrick, S., Moore, B., Nobre, C., Read, J.M., Sa, T., Schloss, A., Vourlitis, G., Wickel, J.A., 2003. IKONOS imagery for the large scale biosphere atmosphere experiment in Amazonia LBA. *Remote Sensing of the Environment* 88(1-2), 111-127.
- Kaarik, A.A. 1974. Decomposition of wood. In Dickinson, C.H., Pugh, G.J.F., 1974. *Biology of Plant Litter Decomposition*. Academic Press, NYC.
- Kitajima, K., Augspurger, C.K., 1989. Seed and Seedling Ecology of a Monocarpic Tropical Tree, *Tachigalia Versicolor*. *Ecology*, 70, (4) 1102-1114.
- Kauffman, J.B., Uhl, C., Cummings, D.H., 1988. Fire in the Venezuelan Amazon 1: Fuel biomass and fire chemistry in the evergreen rainforest of Venezuela. *Oikos* 53, 167-175.
- Kauffman, J.B., Uhl, C., 1990. Deforestation, Fire Susceptibility, and Potential Tree Responses to Fire in the Eastern Amazon. *Ecology*, 71(2) 437-449.
- Kauffman, J.B., Cummings, D.L., Ward, D.E., Babbitt, R., 1993. Fire in the Brazilian Amazon: 1. Biomass, nutrient pools, and losses in slashed primary forests. *Oecologia*, 104(4), 397-408.
- Keller, M., Palace, M., Hurt, G., 2001. Biomass estimation in the Tapajos National Forest, Brazil: examination of sampling and allometric uncertainties. *Forest Ecology and Management* 154, 371-382.

- Keller, M., Palace, M., Asner, G.P., Pereira, R., Silva, J.N.M., 2004a. Coarse woody debris in undisturbed and logged forests in the eastern Brazilian Amazon. *Global Change Biology* 10(5), 784-795.
- Keller, M., Alencar, A., Asner, G.P., Braswell, B., Bustamante, M., Davidson, E., Feldpausch, T., Fernandes, E., Goulden, M., Kabat, P., Kruijt, B., Luizão, F., Miller, S., Markewitz, D., Nobre, A.D., Nobre, C.A., Filho, N.P., Rocha, H., Dias, P.S., von Randow, C., Vourlitis, G.L., 2004b. Ecological Research in the Large Scale Biosphere Atmosphere Experiment in Amazônia (LBA): Early Results. *Ecological Applications* 14(4) Supplement., S3-S16.
- Kira, T. 1978. Community architecture and organic matter dynamics in tropical lowland rain forests of Southeast Asia with special reference to Pasoh Forest, West Malaysia. Pages 561-590 in *Tropical Trees as Living Systems*. P.B. Tomlinson and M.H. Zimmerman, editors. Cambridge: Cambridge University Press.
- Klinge, H., 1973. Biomassa y materia orgánica del suelo in el ecosistema de la pluviselva centro-amazonica. *Acta Cientifica Venezolana* 24, 174-181.
- Lang, G.E., Knight, D.H., 1983. Tree growth, mortality, recruitment, and canopy gap formation during a 10-year period in a tropical moist forest. *Ecology* 64, 1075-1080.
- Lawton, RO., Putz, FE., 1988. Natural disturbance and gap-phase regeneration in a wind-exposed tropical cloud forest. *Ecology*, 69(3), 764-777.
- Leckie, D.G., Gougeon, F.A., Walsworth, N., Paradine, D., 2003. Stand delineation and composition estimation using semi-automated individual tree crown analysis. *Remote Sensing of Environment* 85: 355–369.
- Lieberman, M., Lieberman, D., Peralta, R.. 1989. Forests are not just swiss cheese: canopy stereogeometry of non-gaps in tropical forests. *Ecology* 70(3), 550-552.
- Lugo, AE., Scatena, FN., 1996. Background and catastrophic tree mortality in tropical moist, wet, and rain forests. *Biotropica* 28(4a), 585-599.

- Mackensen, J., Bauhus, J., Webber, E., 2003. Decomposition rates of coarse woody debris – A review with particular emphasis on Australian tree species. *Australian Journal of Botany* 51, 27-37.
- MacNally, R., Parkinson, A., Horrocks, G., Conole, L., Tzaros, C., 2001. Relationships between terrestrial vertebrate diversity, abundance and availability of coarse woody debris on south-eastern Australian floodplains. *Biological Conservation* 99, 191-205.
- Magnusson, W.E., Lima, A.P., Lima, O.P., 1996. Group lightning mortality of trees in a neotropical forest. *Journal of Tropical Ecology* 12, 899-903.
- Malhi, Y., *et al.* 2004. The above-ground coarse woody productivity of 104 neotropical forest plots. *Global Change Biology* 10(5), 563.
- Markewitz, D., Nobre, A.D., Nobre, C.A., Filho, N.P., Rocha, H., Dias, P.S., von Randow, C., Vourlitis, G.L., 2004a. Ecological Research in the Large Scale Biosphere Atmosphere Experiment in Amazônia (LBA): Early Results. *Ecological Applications* 14(4) Supplement, S3-S16.
- Marra, J.L., Edmonds, R.L., 1994. Coarse woody debris and forest floor respiration in an old-growth coniferous forest on the Olympic Peninsula, Washington, USA. *Can. J. For. Res.* 24, 1811-1817.
- Martinez-Ramos, M., Alvarez-Buylla, E., Sarukhan, J., Pinero, D., 1988. Treefall age determination and gap dynamics in a tropical forest. *Journal of Ecology* 76, 700-716.
- Martius, C., 1997. Decomposition of wood. In Junk, Wolfgang J., 1997. *Ecological Studies* 126. The Central Amazon Floodplain. Ecology of a Pulsing System. Springer, NYC.
- Martius, C., Bandeira, A.G., 1988. Wood litter stocks in tropical moist forest in central Amazonia. *Ecotropica* 4, 115-118.

- Melillo, J.M., McGuire, A.D., Kicklighter, D.W., Moore, B., Vorosmarty, C.J., Schloss, A.L., 1993. Global climate change and terrestrial net primary production. *Nature* 363, 234 – 240.
- Miller, S.D., Goulden, M.L., Menton, M.C., da Rocha, H.R., de Freitas, H.C., Figueira, A.M., and Dias de Sousa, C.A., 2004. Biometric and micrometeorological measurements of tropical carbon balance. *Ecological Applications* 14(4), s114-s126.
- Moran, E.F., Brondizio, E., Mausel, P., Wu, Y., 1994. Integrating Amazonian vegetation, land-use, and satellite data. *Bioscience* 44, 329-338.
- Nascimento, H.E.M., Laurance, W.F., 2002. Total aboveground biomass in central Amazonia rainforests: a landscape-scale study. *Forest Ecology and Management*, 168, 311-321.
- Nelson, B.W., Kapos, V., Adams, J.B., Oliveria, W.J., Braun, O.P.G., Doamaral, I.L., 1994. Forest disturbance by large blowdowns in the Brazilian Amazon. *Ecology* 75(3), 853-858.
- Nepstad, D.C., Decarvalho, C.R., Davidson, E.A., Jipp, P.H., Lefebvre, P.A., Negreiros, G.H., Da Silva, E.D., Stone, T.A., Trumbore, S.E., Vieira, S. 2002. The role of deep roots in the hydrological and carbon cycles of Amazonian forests and pastures. *Nature*, 372, 666 – 669.
- Nobre, C., Sellers, P., Shukla, J., 1991. Amazonian deforestation and regional climate change. *Journal of Climate* 4, 957-988.
- Nogueira, E.M., Nelson, B.W., Fearnside, P.M., 2005. Wood density in dense forest in central Amazonia, Brazil. *Forest Ecology and Management* 208, 261–286
- Nordén, B., Paltto, H., 2001. Wood-decay fungi in hazel wood: species richness correlated to stand age and dead wood features. *Biological Conservation* 101, 1-8.

- Odum, H.T., 1970, A tropical rain forest: a study of irradiation and ecology at El Verde, Puerto Rico, US. A. E. C., National Technical Information Service, Springfield, Virginia.
- Ometto, J.P.H.B., Nobre, A.D., Rocha, H.R., Artaxo, P Martinelli, L.A., 2005. Amazonia and the modern carbon cycle: lessons learned. *Oecologia* 143 (4), 483-500.
- Ozanne, C.M.P., Anhof, D., Boulter, S. L., Keller, M., Kitching, R.L., Korner, C., Meinzer, F. C., Mitchell, A.W., Nakashizuma, T., Dias, P.L.S., Stork, N.E., Wright, S.J., Yoshimura, M.. 2003. Biodiversity meets the atmosphere: A global view of forests canopies. *Science* 301, 183-186.
- Palace, M., Keller, M., Asner, G.P., Jose Natalino M. Silva, J.N.M and Passos, C. In press. Necromass in Undisturbed and Logged Forests in the Brazilian Amazon. *Forest Ecology and Management*.
- Palace, M, Keller, M, Silva, H. (submitted to *Ecological Application*). Necromass Production in an Amazon Forest: Examination of Undisturbed and Logged Forest Sites.
- Pereira, R., Zweede, J.C., Asner, G.P., Keller, M.M., 2002. Forest canopy damage and recovery in reduced impact and conventional logging in eastern Para, Brazil. *Forest Ecology and Management* 168, 77-89.
- Phillips, O.L., Gentry, A.H., 1994. Increasing turnover through time in tropical forests. *Science* 263, 954-958.
- Pouliot, D.A., King, D.J., Bell, F.W., And D.G. Pitt. 2002. Automated tree crown detection and delineation in high-resolution digital camera imagery of coniferous forest regeneration. *Remote Sensing of Environment*. 82: 322–334.
- Prance, Ghilleen T., Lovejoy, Thomas E., 1985. *Key Environments Amazonia*. Pergamon Press, NYC.

- Read, J.M., Clark, D.B., Venticinque, E.M., Moreira, M.P., 2003. Application of merged 1-m and 4-m resolution satellite data to research and management in tropical forests. *Journal of Applied Ecology* 40, 592-600.
- Rice, A.H., Pyle, E.H., Saleska, S.R., Hutyra, L., Camargo, P.B., Portilho, K., Marques, D.F., Palace, M., Keller, M., Wofsy, S.C., 2004. Carbon balance and vegetation dynamics in an old-growth Amazonian forest. *Ecological Applications* 14(4), s55-s71.
- Richards, P.W., 1952. *The Tropical Rain Forest: An Ecological Study*. Cambridge University Press, Cambridge, UK.
- Ringvall A., Stahl, G., 1999. Field aspects of line intersect sampling for assessing coarse woody debris. *Forest Ecology and Management* 119, 163-170.
- Roberts, D.A., Keller, M., Soares, J.V., 2003. Studies of land-cover, land-use, and biophysical properties of vegetation in the Large Scale Biosphere Atmosphere experiment in Amazonia. *Remote Sensing Of Environment* 87(4), 377-388.
- Robertson, A.I., Daniel, P.A., 1989. Decomposition and the annual flux of detritus from fallen timber in tropical mangrove forests. *Limnol. Oceanogr.* 34(3), 640-646.
- Roughgarden, J., Running, S., Matson, P., 1991. What does remote sensing do for ecology? *Ecology* 726, 1918-1922.
- Salati, E., Vose, P.B., 1984. Amazon basin: a system in equilibrium. *Science* 225, 129-138.
- Saleska, S.R., Miller, S.D., Matross, D.M., Goulden, M.L., Wofsy, S.C., da Rocha, H.R., de Camargo, P.B., Crill, P., Daube, B.C., de Freitas, H.C., Hutyra, L., Keller, M., Kirchhoff, V., Menton, M., Munger, J.W., Pyle, E.H., Rice, A.H., Silva, H. 2003. Carbon in Amazon forests: Unexpected seasonal fluxes and disturbance-induced losses. *Science* 302 (5650), 1554-1557.
- Sanford, R.L., Braker, H.E., Hartshorn, G.S., 1986. Canopy openings in a primary neotropical lowland forest. *Journal of Tropical Ecology* 2, 277-282.

- Schemske, D.W., Brokaw, N., 1981. Treefalls and the Distribution of Understory Birds in a Tropical Forest. *Ecology* 62(4), 938-945.
- Schwarzkoft, L., Rylands, A.B., 1989. Primate species richness in relation to habitat structure in Amazonian rainforests fragments. *Biological Conservation* 48, 1-12.
- Scarth, P., Phinn, S., 2000. Determining forest structural attributes using an inverted geometric-optical model in mixed eucalypt forests, Southeast Queensland, Australia. *Remote Sensing of Environment* 71, 141-157.
- Scott, D.A., Proctor, J., Thompson, J., 1992. Ecological studies on a lowland evergreen rain forest on Maracá Island, Roraima, Brazil. II. Litter and nutrient cycling. *Journal of Ecology* 80, 705-717.
- Schulze, M., Zweede, J., 2006. Canopy dynamics in unlogged and logged forest stands in the eastern Amazon. *Forest Ecology and Management* 236(1), 56-64.
- Scott, D.A., Proctor, J., and Thompson, J., 1992. Ecological studies on a lowland evergreen rain forest on Maracá Island, Roraima, Brazil. II. Litter and nutrient cycling. *Journal of Ecology* 80, 705-717.
- Shugart, H.H., Bourgeau-Chavez, L., Kasischke, E.S., 2001. Determination of stand properties in boreal and temperate forests using high-resolution imagery. *Forest Science* 46, 478-486.
- Silva, H., 2005. Carbon dioxide fluxes from coarse woody debris in undisturbed and logged areas at the Tapajos National Forest in Brazil, University of New Hampshire, M.S. Thesis.
- Silva, J.N.M., Carvalho, J.P.O., de Lopes, J.C.A., 1995. Growth and yield of a tropical rainforest 13 years after logging. *Forest Ecology and Management* 71, 267-274.

- Silver, W.L., J. Neff, E. Veldkamp, M. McGroddy, M. Keller, Cosme, R., 2000. The effects of soil texture on belowground carbon and nutrient storage in a lowland Amazonian forest ecosystem. *Ecosystems* 3, 193-209.
- Skole, D., Tucker, C., 1993. Tropical deforestation and habitat fragmentation in the Amazon: Satellite data from 1978 to 1988. *Science* 260, 1905-1910.
- Sokal, R.R., Rohlf, F.J., 1995. *Biometry: The Principles And Practice Of Statistics In Biological Research*. 3rd edition, W. H. Freeman and Co., New York.
- Souza, C., Firestone, L., Silva, L.M., Roberts, D., 2003. Mapping forest degradation in the Eastern Amazon from SPOT 4 through spectral mixture models. *Remote Sensing of Environment* 87(4), 494-506.
- Spies, T.A., 1998. Forest Structure: A key to the ecosystem. Pages 34-39 in J.A. Trofymow and A. MacKinnon, editors. *Proceedings of a workshop on Structure, Process, and Diversity in Successional Forests of Coastal British Columbia*, February 17-19, 1998, Victoria, British Columbia. *Northwest Science*, Vol. 72 (special issue No. 2).
- Steininger, M., 1996. Tropical secondary forest regrowth in the Amazon: Age, area, and change estimation with Thematic Mapper. *International Journal of Remote Sensing* 17(1), 9-27.
- Summers, P. M., 1998. Estoque, decomposicao, e nutrientes da liteira grossa em floresta de terra firme, na Amazonia Central. Pages 118. *Ciencias de Florestas Tropicais*. Instituto Nacional de Pesquisas da Amazonia, Manaus, Brazil.
- Svenning, J.C., 2000. Small canopy gaps influence plant distributions in the rain forest understory. *Biotropica* 32(2), 252-261.
- Swift, M.J., Heal, O.W., Anderson, J.M., 1979. *Decomposition in Terrestrial Ecosystems*. University of California Press, Berkeley.
- Tan, C. Y., Iglewicz, B., 1999. Measurement Methods Comparisons and Linear Statistical Relationship. *Technometrics* 41, 192-201.

- Tanner, E.V.J., 1980. Studies on the biomass and productivity in a series of Montane rain forests in Jamaica. *The Journal of Ecology* 68(2), 573-588.
- Tansley, A.G., 1935. The use and abuse of vegetational concepts and terms, *Ecology* 16, 284-307
- Telles E. C. C., P. B. Camargo, L. A. Martinelli, S. E. Trumbore, E. S. Costa, J. Santos, N. Higuchi, R. C. Oliveira Jr., Influence of soil texture on carbon dynamics and storage potential in tropical forest soils of Amazonia, *Global Biogeochem. Cycles*, 17 (2), 1040, doi:10.1029/2002GB001953, 2003.
- Terborgh, J., 1992. Maintenance of diversity in tropical forests. *Biotropica* 24, 283-292.
- Terborgh, J., Foster, R. B., Nunez, P., 1996. Tropical tree communities: a test of the nonequilibrium hypothesis. *Ecology* 77, 561-567.
- van der Meer, P.J., Bongers, F., 1996. Patterns of Tree-Fall and Branch-Fall in a Tropical Rain Forest in French Guiana. *The Journal of Ecology*, 84(1) 19-29.
- Veríssimo, A., P. Barreto, M. Mattos, R. Tarifa, Uhl, C., 1992. Logging impacts and prospects for sustainable forest management in an old Amazonian frontier: the case of Paragominas. *Forest Ecology and Management* 55,169-199.
- Vieira, S., Barbosa de Camargo, P., Selhorst, D., da Silva, R., Hutyrá, L., Chambers, J.Q., Brown, I.F., Higuchi, N., dos Santos, J., Wofsy, S.C., Trumbore, S.E., Martinelli, L.A. 2004. Forest structure and carbon dynamics in Amazonian tropical rain forests. *Oecologia* 140, 468–479
- Uhl, C., Buschbacher, R., Serrão, E.A.S., 1988. Abandoned pastures in eastern Amazonia. *Journal of Ecology* 76, 663-681.
- Uhl, C., Kauffman, J.B., 1990. Deforestation, Fire Susceptibility, and Potential Tree Responses to Fire in the Eastern Amazon. *Ecology*, 71(2), 437-449.

- Vitousek, P.M., Denslow, J.S., 1986. Nitrogen and Phosphorus Availability in Treefall Gaps of a Lowland Tropical Rainforest. *The Journal of Ecology*, 74(4) 1167-1178.
- Walker, L.R., Zarin, D.J., Fetcher, N., Myster, R.W., Johnson, A.H., 1996. Ecosystem development and plant succession on landslides in the Caribbean. *Biotropica* 28, 566-576.
- Watts, A.S. 1947. Pattern and Process in the Plant Community. *Journal of Ecology*. 35:1-22.
- Wedin, D.A., Tieszen, L.L., Dewey, B., Pastor, J., 1995. Carbon Isotope Dynamics During Grass Decomposition and Soil Organic Matter Formation. *Ecology* 76(5), 1383-1392.
- Werth, D., Avissar, R., 2002. The local and global effects of Amazon deforestation, *J. Geophys. Res.* 107, doi:10.1029/2001JD000717.
- Wessman, C.A., 1992. Spatial scales and global change: Bridging the gap from plots to GCM grid cells. *Ann. Rev. Ecol. Syst.* 23, 175–200.
- West, D.C., Shugart, H.H., Botkin, D.B., 1981. *Forest Succession. Concepts and Application.* Springer-Verlag, New York.
- Whitmore, T.C. 1982. On Pattern and Process in Forests. In *The Plant Community as a Working Mechanism.*, E.I. Newman editor. 45-59.
- Wilcke, W., Hess, T., Bengel, C., Homeier, J., Valarezo, C., Zech W., 2005. Coarse woody debris in a montane forest in Ecuador: mass, C and nutrient stock, and turnover. *Forest Ecology and Management* 205, 139–147.
- Windsor, D.M., Morrison, D.W., Estribi, M.A., de Leon, B., 1988. Phenology of fruit and leaf production by “strangler” figs on Barro Colorado Island, Panama. *Experientia*. 45, 647-653.

- Wulder, M., Niemann, K.O., Goodenough, D.G., 2000. Local maximum filtering for the extraction of tree locations and basal area from high spatial resolution imagery. *Remote Sensing of Environment* 73, 103– 114.
- Yoda, K., Kira, T., 1982. Accumulation of organic matter, carbon, nitrogen, and other nutrient elements in the soils of a lowland rainforest at Pasoh, Peninsular Malaysia. *Japan Journal of Ecology* 32, 275-291.
- Young, T.P., Hubbell, S.P., 1991. Crown Asymmetry, Treefalls, and Repeat Disturbance of Broad-Leaved Forest Gaps. *Ecology*, 72(4) 1464-1471.